The development of an ISFET-based heparin sensor

Joost van Kerkhof

THE DEVELOPMENT OF AN ISFET-BASED HEPARIN SENSOR

This work has been supported by the Netherlands Organization of Applied Scientific Research TNO.

CIP-GEGEVENS KONINKLIJKE BIBLIOTHEEK, DEN HAAG

Kerkhof, Johannes Cornelis van

The development of an ISFET-based heparin sensor /
Johannes Cornelis van Kerkhof ; [ill. van de auteur]. -
[S.l. : s.n.]. - Ill.
Proefschrift Enschede. - Met lit. opg.
ISBN 90-9007514-3
Trefw.: biosensoren

THE DEVELOPMENT OF AN ISFET-BASED HEPARIN SENSOR

Proefschrift

ter verkrijging van
de graad van doctor aan de Universiteit Twente,
op gezag van de rector magnificus,
prof.dr. Th.J.A. Popma,
volgens besluit van het College voor Promoties
in het openbaar te verdedigen
op vrijdag 7 oktober 1994 te 15.00 uur

door

Johannes Cornelis van Kerkhof

geboren op 10 augustus 1965
te Wijk bij Duurstede

Dit proefschrift is goedgekeurd door de promotor:

Prof.dr.ir. P. Bergveld

Neen, neen, één weten bleef in ons bezit,
en nimmer kan het door den vloed dier golven
van droom en van vergeten
worden bedolven;
en het is dit:

A. Roland Holst
(uit: Mensch en Paradijs)

Voor Ulberthe
en mijn ouders

Contents

Introduction 1

1.1 Chemical sensors and biosensors

A chemical sensor can be defined as a device which converts the concentration of a chemical species into an electrical signal. As other sensors, chemical sensors usually consist of a selective detecting system and a transducing element. A biosensor is a special type of chemical sensor and can be defined as a sensor that makes use of biological material for its selective detecting system.

The prospects for the use of chemical sensors and biosensors is very promising according to the prognosis of the market for these devices [1]. The impressive figures mentioned, which are also regularly presented at scientific conferences, apparently provide the motivation for a lot of companies and research institutes, to develop different kinds of chemical- and biosensors. However, the present number of commercially available chemical sensors is much lower then was expected about ten years ago. This is probably the result of a combination of commercial and technical factors. Apparently, the market was (or maybe still is) not ready yet for the large scale introduction of chemical- and biosensors, replacing well known standard equipment and sampling procedures. On the other hand, also the technical aspects can be a delaying factor. The successful development of chemical sensors asks for very specific chemical expertise, as well as specific expertise on the transducing element. The interdisciplinary character of this type of research makes it, in the authors opinion, very difficult and time consuming.

For chemical sensors in general the detecting systems can vary from acid-base equilibria at inorganic oxides to synthetic ionophores which specifically capture an ion. For biosensors, the detecting systems vary from enzymatic- and immunoreactions to specific interactions with whole cells. The transducing elements in chemical- and biosensors can vary from acoustic wave devices and resonating microstructures to ion-sensitive transistors and optical waveguides and fibres.

The heparin sensor which is described in this thesis, uses the electrostatic interaction between heparin and a specific protein (or a synthetic molecule), as the selective detecting system and an ion-sensitive field effect transistor (ISFET) as the transducing element. In this chapter the ISFET will be introduced and a brief review of the possibilities and limitations of the ISFET as a transducing element for chemical sensors will be given.

1.2 The ion sensitive field effect transistor (ISFET)

The ISFET was first described by Bergveld in 1970 [2], and is today a well-known transducing element for the development of chemical- and biosensors. The transducing principle of an ISFET is based on the dependence of the drain current of the transistor on the surface charge of the inorganic gate insulator which is in contact with an aqueous solution. The surface charge is determined by the pH of the solution in which the ISFET is immersed. The corresponding drain current is electronically converted to an output voltage of an amplifier [3].

The ISFET is deduced from the MOSFET, which is a well known electronic device. Cross sections of the MOSFET and the ISFET are shown in fig.1.1. A MOSFET consists of a p-type silicon substrate in which two n-type diffusions are realized, which are called the source and the drain. The structure is covered with an insulating layer (usually SiO_2) and a metal gate electrode is deposited over the area between the source the and drain.

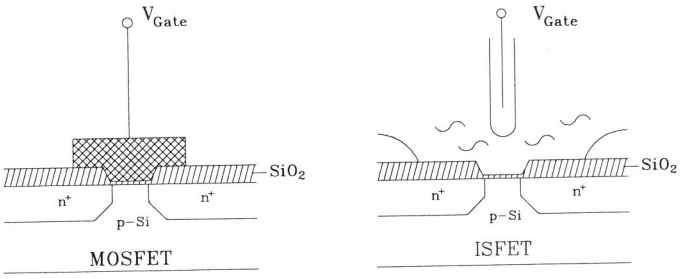

Fig.1.1 Cross sections of a MOSFET and an ISFET

In normal operation, the drain is maintained at a voltage V_D with respect to the source, which is normally at 0 V. When a positive voltage V_G is applied to the gate with respect to the substrate (which is also normally at 0 V), and this voltage exceeds the so-called threshold voltage V_T, electrons (the minority carriers in the substrate) are attracted to the surface and create a conducting channel between the source and the drain. The current I_D, which consequently flows between source and drain, is determined by the electrical resistance of the conducting channel (determined by V_G) and the magnitude of V_D. For the condition that $V_D<(V_G - V_T)$, the drain current is given by:

$$I_D = \frac{C_{ox}\mu W}{L}\left(V_G - \frac{1}{2}V_D - V_T\right)V_D \qquad (1.1)$$

where C_{ox} is the gate insulator capacitance per unit area, μ the electron mobility in the channel and W/L the width to length ratio of the channel.

The expression for the drain current is also valid for the ISFET which in fact is a MOSFET without a metal gate, immersed in an aqueous solution. The reference electrode, which defines the potential of the solution in which the ISFET is immersed, has the same function as the metal gate of a MOSFET. However, the threshold voltage V_T of a MOSFET is constant, whereas the threshold voltage of an ISFET is influenced by the surface potential ψ_0 which exists at the oxide surface-solution interface. The acid-base equilibria at the oxide surface makes the surface potential ψ_0 a function of the pH of the solution [4]. This will be described in more detail in chapter 3.

If an ISFET is connected to a so-called source-drain follower, a change in the threshold potential V_T, resulting from a change in the surface potential ψ_0 (which is caused by a pH change), is compensated by an equal change of the gate-source voltage which is the output of the source-drain follower. The final result is an output voltage V_{GS} which has a Nernstian dependence on the pH of the solution (see also chapter 3):

$$V_{GS} = \alpha \frac{RT}{F} \ln a_{H^+} + \text{constant} \qquad (1.2)$$

where a_{H^+} represents the activity of the protons in the solution and α the sensitivity factor of the ISFET ($0<\alpha\leq1$), which is 1 for maximum Nernstian behaviour. The constant reflects, among other constants, the reference electrode potential.

1.3 The ISFET as transducing element in chemical sensors

The transducing principle of an ISFET makes it an interesting device for the development of chemical sensors. Several chemical sensors have already been developed with the use of an ISFET as transducing element.

pH-sensitive ISFETs

The most direct application is of course the direct use of the ISFET as a pH sensor. As described in the previous section, the surface potential at the interface between the gate oxide and the solution, is determined by the acid-base equilibria of the OH-groups and is therefore a function of the pH. In chapter 3, the operational mechanism will be described in more detail. For the development of pH-sensitive ISFETs, several gate oxides have been investigated including Si_3N_4, Al_2O_3

and Ta_2O_5 [3]. These oxides were believed to have better properties then SiO_2, which was initially used, and were deposited on top of the initial SiO_2 layer. It appears that Ta_2O_5 has the best properties resulting in a pH sensitivity factor α of almost 1 and thus resulting in a pH sensitivity of 59 mV/pH at 25°C [5]. Today, several pH-meters, based on a pH-sensitive ISFET, are commercially available. Most of them use Al_2O_3 or Si_3N_4 as gate oxide.

EnzymeFETs (ENFETs)

ISFETs are also used as transducing element in so-called ENFETs (enzyme FETs). An enzyme is immobilized in a membrane deposited on the ISFET, and if a reaction with the specific substrate from the solution results in a change in the pH in the membrane, this is measured by the ISFET [6]. To avoid problems with the pH-dependent activity of the enzymes, Van der Schoot developed the pH-static enzyme sensor by integrating a coulometric H^+-actuator, which is incorporated in a feed-back loop together with the ISFET. This actuator is used to keep the pH in the membrane at a constant predetermined value. The current which is needed to achieve this constant pH, linearly depends on the substrate concentration [7].

CHEMFETs

Another successful application of ISFETs as transducing element, is the development of so-called CHEMFETs, which are modified ISFETs with a selectivity for ions other than H^+ [8]. The ISFETs are modified by applying a two layer membrane. The first layer is a hydrogel in which the pH is kept constant thus ensuring a constant surface potential at the gate oxide of the ISFET. The second layer is a membrane containing ionophores for the specific entrapment of ions. Across this membrane a potential is established, which is a function of the concentration of the specific ion and measured by the underlying ISFET. In this case the ISFET is purely used as a potential sensor because its pH response is suppressed by the buffering hydrogel. CHEMFETs have been developed for the measurement of K^+ [9], Na^+ [10], heavy metal ions [11] and various anions [12].

ImmunoFETs (IMFETs)

The understanding that an ISFET is in fact a device which is able to measure surface charges, was the reason that several research projects were started to investigate the possibility to detect proteins deposited in a layer on the ISFET surface. It was expected that the protein charge could be measured with an ISFET. In 1976, Schenck proposed to use an ISFET to detect an immunological reaction [13]. He suggested to immobilize a layer of antibody on the gate oxide, and after reaction of this antibody with its specific antigen, the altered charge of the protein

layer should affect the drain current of the transistor. Many research groups have tried to realize this concept but experimental results with this type of devices have been very disappointing, mainly due to a poor understanding of the operational mechanism.

In 1990 Schasfoort et al. reviewed the different exertions to determine proteins by measuring the protein charge, and described the possibilities and limitations of the ISFET as a direct protein charge measuring device [14]. In 1991, Bergveld published a critical review on direct electrical protein detection methods [15]. In the following, a brief description will be given of the ISFET as possible protein sensor.

If an ISFET is considered with a monolayer of protein on top of the gate, the layer must fit into the electrical double layer at the oxide-solution interface to be able to directly modulate the drain current. Outside the double layer, the protein charges are screened by counter ions which are always present in the solution. This means that the dimensions of the proteins must be smaller than the Debye length which is determined by the ionic strength of the solution. In a physiological salt solution, the Debye length is about 0.8 nm which is much smaller than the dimensions of an average protein (5-10 nm). Consequently, for direct detection of protein charges, the ionic strength of the solution must be much lower then 0.15. However, even at low ionic strength it remains questionable if an immunological reaction can be detected because interaction between immobilized antibodies and antigens results in at least two layers of protein which then both have to fit within the thickness of the electrical double layer.

If the proteins are immobilized in a membrane matrix, which is deposited on an ISFET, a different theoretical approach for describing the effects of the protein charges on the ISFET must be applied. Schasfoort et al. used the theory first presented by Donnan, which describes the potential and ion distribution in a membrane with a fixed charge density [14]. A brief review will be given here.

Consider a membrane containing a constant concentration of charged groups, for instance immobilized proteins in the membrane matrix, which is deposited on the ISFET surface. The ISFET is immersed in a solution which only contains KCl. The potassium and chloride ions can diffuse freely through the solution as well as through the membrane whereas the protein charges are immobilized in the membrane. As a result of the fixed protein charges in the membrane, there is a difference between the ion concentrations in the membrane and in the solution. At equilibrium the ion concentrations must fulfil the equality of electrochemical potentials:

$$\mu_{0,K^+} + RT\ln a_{K^+,e} + F\phi_e = \mu_{0,K^+} + RT\ln a_{K^+,m} + F\phi_m \qquad (1.3)$$

$$\mu_{0,Cl^-} + RT\ln a_{Cl^-,e} - F\phi_e = \mu_{0,Cl^-} + RT\ln a_{Cl^-,m} - F\phi_m \quad (1.4)$$

where μ_{0,K^+} and μ_{0,Cl^-} are the electrochemical standard potentials of K^+ and Cl^- respectively, $a_{K^+,e}$ and $a_{Cl^-,e}$ the activities of the potassium and chloride ions in the solution (electrolyte), $a_{K^+,m}$ and $a_{Cl^-,m}$ the activities of the potassium and chloride ions in the membrane, ϕ_e and ϕ_m the electrical potentials in the solution and the membrane. R,T and F have their usual meaning.
If equations 1.3 and 1.4 are written as an electrical potential difference, it results in:

$$\phi_m - \phi_e = \frac{RT}{F}\ln\frac{a_{K^+,e}}{a_{K^+,m}} \quad (1.5)$$

$$\phi_m - \phi_e = \frac{RT}{F}\ln\frac{a_{Cl^-,m}}{a_{Cl^-,e}} \quad (1.6)$$

The ratio between the activities of the ions in the solution and in the membrane is called the Donnan ratio (r_D) and is given by:

$$r_D = \frac{a_{K^+,e}}{a_{K^+,m}} = \frac{a_{Cl^-,m}}{a_{Cl^-,e}} \quad (1.7)$$

The H^+ and OH^- ions must also fulfil the equality of electrochemical potential and are therefore also distributed according to the Donnan ratio. This means that the pH in the membrane will be different from the pH in the solution. The difference in pH is given by:

$$pH_m - pH_e = \log r_D \quad (1.8)$$

As a total result of the redistribution of the ions, a membrane potential is established as well as a change in the pH inside the membrane. Both effects will affect the gate-source voltage V_{GS} of the ISFET connected to a source-drain follower circuit. The gate-source potential V_{GS} of an ISFET with a protein-loaded membrane is therefore given by (using eq.1.1):

$$\begin{aligned} V_{GS} &= \text{constant} + \alpha\frac{RT}{F}\ln a_{H^+,m} + \phi_D \\ &= \text{constant} + \alpha\frac{RT}{F}\ln a_{H^+,m} + \frac{RT}{F}\ln\frac{a_{H^+,e}}{a_{H^+,m}} \end{aligned} \quad (1.9)$$

Rearranging this equation results in:

$$V_{GS} = \text{constant} + \alpha \frac{RT}{F} \ln a_{H^+,e} + (1-\alpha) \frac{RT}{F} \ln \frac{a_{H^+,e}}{a_{H^+,m}}$$
$$= \text{constant} + \alpha \frac{RT}{F} \ln a_{H^+,e} + (1-\alpha)\phi_D \qquad (1.10)$$

If $\alpha=1$, the gate-source voltage V_{GS} is only determined by the pH of the bulk solution and the protein-loaded membrane has no influence. The effect of the Donnan potential is fully compensated by the membrane pH. This means that it is impossible to measure the effect of a protein-loaded membrane with an ISFET in this way. Only when an ISFET with a reduced sensitivity is used ($\alpha<1$), the static measurement of the Donnan potential seems feasible.

Kruise investigated the feasibility of static measurement of partly compensated Donnan potentials with ISFETs with a reduced pH-sensitivity ($\alpha<1$) [16][17]. He used ISFETs with SiO_2 as a gate oxide ($\alpha\approx0.8$, for 4<pH<8) and ISFETs with Ta_2O_5 as a gate oxide which was covered with a thin layer of epoxy ($\alpha\approx0.08$, for 4<pH<8). Although these ISFETs also showed a response to other ions than H^+, Kruise concluded that in theory it should be possible to detect the partly compensated Donnan potential with both the SiO_2 and epoxy-covered Ta_2O_5-ISFETs. However, he was unable to prove this experimentally. The explanation was found in the existence of a so-called interlayer between the ISFET and the protein membrane. If this interlayer has the same composition as the bulk solution, which is reasonable to assume, the Donnan potential will be present at both sides of the protein membrane. In this case the potential between the ISFET surface and the reference electrode in the bulk solution is not influenced by the protein membrane.

1.4 The ion-step measuring method

The understanding that it would be difficult to measure a Donnan potential across a protein membrane with an ISFET, brought Schasfoort to a total new approach [18]. The essential aspect of this approach is that the measurement is not carried out during thermodynamical equilibrium, but rather the effect of a disturbance of this equilibrium is measured. The ISFET with protein membrane is incorporated in a flow-through system and thermodynamical equilibrium is established in a 10 mM KCl solution at a certain pH. The equilibrium is then disturbed by a sudden increase of the electrolyte concentration to (for instance) 40 mM KCl at constant pH. The response of the ISFET to this 'ion-step' is a transient potential which eventually returns to the same value as before the ion-

step. The amplitude of this potential peak is a measure of the charge density in the protein membrane.

Schasfoort claimed that the origin of the ISFET response is a transient diffusion potential across the membrane which is created due to the difference in the mobility of cations and anions inside the charged protein membrane [19]. However, later it became clear that the response is a combination of a changing Donnan potential and a temporary pH-change in the membrane due to the release or uptake of protons by the protein molecules in the membrane [20]. The release or uptake of protons by protein molecules is caused by the fact that the titration curves of proteins are a function of the ionic strength of the solution. If the ionic strength is changed, as occurs during an ion-step, the amount of bound protons per protein molecule also changes. A detailed description of the mechanism of the ion-step response is given in chapter 3.

By using the ion-step method, Schasfoort showed the possibility to measure lysozyme and HSA concentrations in buffer solutions and to measure the HSA-αHSA immuno-reaction [18]. Moreover, the ion-step method was used to detect an immuno-reaction involving the non-charged antigen progesterone by using competitive binding of progesterone and a charged progesterone lysozyme conjugate [21].

1.5 The background of the research project described in this thesis

In September 1989 a research project was started in the Biosensors group (project of J.C.T. Eijkel) to continue the development of the ion-step measuring method as initiated by R.B.M. Schasfoort [22]. This project has resulted in a profound theoretical description of the different mechanisms behind the ion-step measuring method, endorsed with an impressive numerical simulation model [23].

In July 1990 the project of which the results are described in this thesis was started. The aim of the project has been the development of a sensor system, based on the ion-step measuring method, focusing on a specific application. As a first practical application, the anticoagulant drug heparin has been chosen, which is used to delay the clotting process of blood, thereby preventing the formation of bloodclots. There are two main reasons for choosing heparin as the first specific application. The first reason is the fact that heparin molecules are highly charged which is favourable for detection with the ion-step measuring method. The other main reason is the presumption that there is a need and a significant clinical market for a simple sensor system determining heparin concentrations in blood.

Because the insight in the mechanisms behind the ion-step measuring method evolved during the project, a substantial part of the research effort has been focused on the measuring method itself, rather than on the specific application. However, heparin has always served as the 'model' analyte to be determined.

1.6 Outline of this thesis

In this chapter an introduction is given on the ISFET as a transducing element in chemical- and biosensors. Moreover, the ion-step measuring method is briefly introduced, which is used for the development of the sensor system as described in the following chapters.

In chapter 2 the backgrounds of the clinical use of heparin as an anticoagulant are described. From this chapter it is concluded that a simple sensor system determining the heparin concentration in blood plasma, might be useful for the monitoring of heparin treatments.

Chapter 3 deals with the theoretical background of the ion-step measuring method. The mechanism behind the response to an ion-step is described in more detail and the role of the ISFET as transducing element is contemplated in more perspective.

In chapter 4 results are presented of experiments with ISFETs provided with membranes of polystyrene beads in which protamine has been immobilized as an affinity ligand for heparin. Different types of polystyrene beads and different procedures for the immobilization of protamine are used.

A new approach to the ion-step measuring method, where the receptor molecules are not immobilized in a membrane but directly at the ISFET surface, is presented in chapters 5 and 6. In chapter 5 surface modification of Ta_2O_5-ISFETs is described. An amino-functionalized silane is used to modify the oxide surface acting directly as an affinity ligand for coupling heparin to the modified surface. In chapter 6, ISFETs with an immobilized layer of protamine at the surface are described. Results are presented of measurements in buffer solutions as well as in blood plasma. Moreover, the sensor is used in plasma samples from the clinical practice and the results are compared with the results of a standard clinical assay.

This thesis ends with chapter 7 in which the main conclusions are summarized and the future developments are outlined. Also some suggestions are given for further research on the ion-step measuring method in general and the heparin sensor in particular. These suggestions include some alternatives for the

reaction between protamine and heparin to be able to determine other parameters of importance for the monitoring of heparin treatments. As an aspect of the future developments, a pre-prototype of a simple measurement system is described which is developed to replace the flow-system by a more simple, cheap and easy to use sensor system.

References

[1] E.A.H. Hall, Biosensors, Open University Press, Buckingham, UK (1990)

[2] P. Bergveld, Development of an ion-sensitive solid-state device for neurophysiological measurements, IEEE Trans. Biomed. Eng., 17 (1970), p.70

[3] P. Bergveld, A. Sibbald, Analytical and biomedical applications of ion-selective field-effect transistors, in: Comprehensive analytical chemistry, Vol. XXIII, ed. G. Svehla, Elsevier, Amsterdam (1988)

[4] L.B. Bousse, N.F. de Rooij, P. Bergveld, Operation of chemically sensitive field-effect sensors as a function of the insulator-electrolyte interface, IEEE Transactions on Electron Devices, 30 (1983), p.1263

[5] Unpublished results

[6] B.H. van der Schoot, P. Bergveld, ISFET based enzyme sensors, Biosensors, 2 (1988), p.161

[7] B.H. van der Schoot, P. Bergveld, Evaluation of the sensor properties of the pH-static enzyme sensor, Anal. Chim. Acta, 233 (1990), p.49

[8] A. van den Berg, Ion sensors based on ISFETs with synthetic ionophores, Thesis University of Twente, Enschede, the Netherlands, ISBN 90-9001782-8 (1988)

[9] P.D. van der Wal, The development of a durable potassium sensor based on FET-technology, Thesis University of Twente, Enschede, the Netherlands, ISBN 90-9004577-5 (1991)

[10] J.A.J. Brunink, Sodium-selective CHEMFETs, Thesis University of Twente, Enschede, the Netherlands, ISBN 90-9006565-2 (1993)

[11] P.L.H.M. Cobben, Sensors for heavy metal ions based on ISFETs, Thesis University of Twente, Enschede, the Netherlands, ISBN 90-9005294-1 (1992)

[12] W.P.R.V. Stauthamer, Anion sensitive CHEMFETs, Thesis University of Twente, Enschede, the Netherlands, ISBN 90-9007033-8 (1994)

[13] J.F. Schenck, Field effect transistor for detection of biological reactions, United States Patent nr. 4,238,757 (1980) (Filed 1976)

[14] R.B.M. Schasfoort, P. Bergveld, R.P.H. Kooyman, J. Greve, Possibilities and limitations of direct detection of protein charges by means of an immunological field-effect transistor, An. Chim. Acta, 238 (1990), p.323

[15] P.Bergveld, A critical evaluation of direct electrical protein detection methods, Bios. Bioelectron. 6 (1991), p.55

[16] J. Kruise, J.A. Voorthuyzen, P. Bergveld, F.J.B. Kremer, D.A.J. Starmans, E.J.R. Südholter, J. Feijen, D.N. Reinhoudt, Protein-covered ISFETs, theory and measurements, Proc. 3rd Int. Meeting Chem. Sensors, Cleveland, USA, Sept. 24-26 (1990), p.264

[17] J. Kruise, Perspectives of glucose sensing based on a charge-modulating competition reaction, Thesis University of Twente, Enschede, the Netherlands, ISBN 90-9005754-4 (1993)

[18] R.B.M. Schasfoort, R.P.H. Kooyman, P. Bergveld, J. Greve, A new approach to ImmunoFET operation, Bios. Bioelectron., 5 (1990), p.103

[19] R.B.M. Schasfoort, P. Bergveld, R.P.H. Kooyman, J. Greve, The ion-step-induced response of membrane-coated ISFETs: theoretical description and experimental verification, Bios. Bioelectron., 6 (1991), p.477

[20] J.C.T. Eijkel, W. Olthuis, P. Bergveld, J. Greve, Interpretation of transient potentials in protein loaded membranes. Book of abstracts of Eurosensors VI, October 1992, San Sebastian, Spain, p.336

[21] R.B.M. Schasfoort, C.E.J.M. Keldermans, R.P.H.Kooyman, P. Bergveld, J. Greve, Competitive immunological detection of progesterone by means of the ion-step induced response of an ImmunoFET, Sensors & Actuators B1 (1990), p.368

[22] R.B.M. Schasfoort, A new approach to ImmunoFET operation, Thesis University of Twente, Enschede, the Netherlands, ISBN 90-9003145-6 (1989)

[23] J.C.T. Eijkel, Thesis University of Twente, the Netherlands, in preparation

The clinical use of heparin as an anticoagulant 2

2.1 Introduction

2.1.1 Heparin

Heparin was discovered in 1916 by J. McLean [1,2] who, as a medical student, worked in the laboratory of W.H. Howell. In the course of studying another problem, McLean extracted a substance from dog liver which delayed the coagulation of blood. The new anticoagulant was named 'heparin' by Howell and Holt in 1918 [3]. Heparin was initially thought to be a phospholipid because it had been isolated by a procedure designed for such compounds and because the early preparations contained substantial amounts of phosphorous. In 1925 Howell discovered that heparin contained carbohydrate [4] and further analysis in 1928 indicated that glucuronic acid was present [5]. Due to further intensive investigations by many researchers and the refinement of methods for purification and structural analysis of polysaccharides, the chemical definition of heparin has changed several times over the years [6].

Present-day heparin is defined as a family of polysaccharide species, consisting of chains of alternating, 1-4-linked and variously sulphated residues of a uronic acid and D-glucosamine. The uronic acid residues are either L-iduronic acid or D-glucuronic acid, and the D-glucosamine residues are either N-sulphated or N-acetylated [7]. At physiological pH values, the three functional groups in heparin are fully dissociated to yield OSO_3^-, $NHSO_3^-$ and COO^- groups thus resulting in a highly negatively charged heparin molecule. The heparin fragments have molecular weights of 5,000 to 30,000 (corresponding with x to y saccharide residues) with an average of 12,000 to 15,000. The polysaccharide chains are structurally heterogeneous because of the incomplete biosynthetic modifications of the heparin's precursors [8]. Recently, so-called low molecular weight heparins have been developed, which have mean molecular weights that vary between 4,000 to 6,500.

Since Howell's work during the 1920s, there have been drastic changes and improvements in the isolation procedure of heparin. Dog liver, used for the first commercial production of heparin was obviously not suitable for large scale production, and other tissue sources had to be sought. During the early 1930s

Charles and Scott [9-11] developed large scale procedures which were particularly applied to beef liver, and soon to beef lung. In the 1960s a gradual shift to the use of porcine intestinal mucus and mucosa took place. Today, approximately 5 kg of heparin is manufactured from 20.000 kg of pig intestinal slimes [6].

Heparin does have a number of pharmacological properties [12], but the property of heparin which has attracted most attention and resulted in its widespread clinical use, is its ability to prolong the clotting time of blood. In this chapter, this property of heparin is described in further detail.

2.1.2 Haemostasis and thrombosis

Because of the vital interest of the blood circulation, there exists an effective mechanism to prevent blood loss and repair a possible leakage in the vascular system: *haemostasis*. This mechanism consists of three components which efficiently cooperate: the wall of the blood vessel, platelets and a number of coagulation proteins which are called coagulation factors. If a blood vessel is damaged, platelets will adhere to the damaged wall of the vessel and to each other. In this way, a plug is formed which provisionally closes the hole. At the same time the blood clotting (or coagulation) process starts and the plug is stabilized by a fibrin matrix. This clot will later be degraded by an enzymatic process which is called the fibrinolytic process or fibrinolysis.

Blood which normally flows through the vessels, will not spontaneously clot due to a sophisticated equilibrium between coagulation factors and anti-coagulant factors. If, however, this equilibrium is disturbed, for instance by a tiny aggregate of platelets, a clot (or thrombus) is formed. Upon growth and extension in the blood stream, thrombi may plug up vessels which stop or diminish the supply of blood to tissues or organs. The development of clots in blood vessels is called *thrombosis*.

In haemostasis and thrombosis, a number of processes are involved which also have many interactions with each other [13]. In this chapter we will only focus on the coagulation process and the effect of heparin on blood clotting.

2.2 The coagulation process

2.2.1 The coagulation enzymes

In the blood coagulation process, more than 10 different proteins are involved which are called coagulation (or clotting) factors, each of them is given a roman number. Most of these proteins are (pro-)enzymes which subsequently activate each other in a cascade reaction. A schematic representation of the coagulation cascade

is shown in fig. 2.1. The result of this chain reaction is the formation of the enzyme thrombin. This enzyme plays a crucial role in the clotting process. Thrombin converts soluble protein fibrinogen into insoluble fibrin which forms the basis of a blood clot. Thrombin also has important regulatory functions in the clotting system. It activates cofactors factor V and factor VIII, thereby greatly increasing the rate of coagulation. Moreover, when bound to an endothelial cell-surface receptor (thrombomodulin), thrombin activates an anticoagulant protein, protein C, which then inactivates the cofactors V and VIII and retards blood clotting. Accurate regulation of the level of active thrombin is therefore critically important in haemostasis and thrombosis (see section 2.3.1).

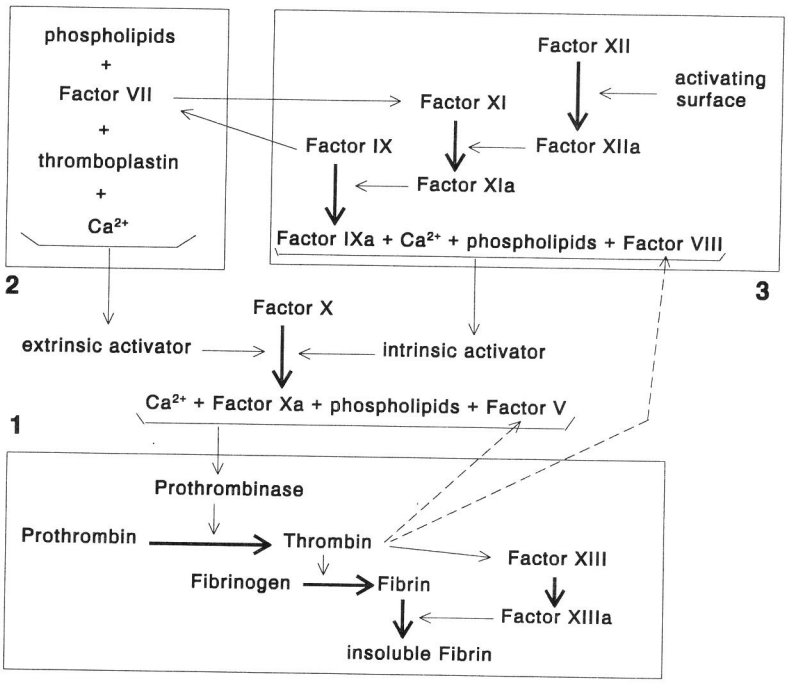

Fig.2.1 Schematic representation of the coagulation process [14].

In fig. 2.1 the most important interactions between the different coagulation factors are shown. The thin arrows indicate enzymatic interactions, whereas the thick arrows indicate conversion from a proenzyme into an active enzyme. The two dashed arrows from thrombin to factor V and VIII indicate activation of these factors following the interaction with thrombin through limited proteolysis instead of a conversion from a non-active pro-enzyme into an active enzyme. Factor V and

VIII are called cofactors because they don't have an enzymatic function.

The schematic figure consists of three blocks. Block 1 describes the formation of thrombin and how this leads to the formation of insoluble fibrin. To convert prothrombin into thrombin, factor X has to be activated to factor Xa. There are two possible pathways for this activation, the so-called extrinsic and the intrinsic path. Block 2 of the scheme shows the formation of the extrinsic activator and block 3 shows the formation of the intrinsic activator of factor X. The different interactions between the coagulation factors will now be discussed in more detail.

The formation of insoluble fibrin

Fibrinogen is a large protein (MW 340.000) which circulates in plasma in the dimer form. Dimeric fibrinogen consists of a pair of α, β and γ-polypeptide chains linked together by disulphide bonds. Thrombin acts on dimeric fibrinogen by removing four fibrinopeptides. The removal of these small fibrinopeptides results in the appearance of polymerization sites through which the formed fibrin monomers interact with each other. In the final coagulation step, fibrin polymer is stabilized by a crosslinking reaction in which initially formed hydrogen bonds are replaced by covalent bonds. The crosslinks are formed during a condensation reaction of glutamine and lysine residues on different chains. Factor XIIIa, which is formed during the conversion of factor XIII by thrombin in the presence of Ca^{2+} ions, plays an important role in this crosslinking reaction.

The conversion of prothrombin to thrombin

Prothrombin (factor II) is the pro-enzyme of thrombin (factor IIa), which plays a key role in the coagulation process. Thrombin is one of the so-called serine proteases, with a serine residue as the active site. Besides the conversion of fibrinogen into fibrin, thrombin is responsible for the activation of factor XIII and for the activation of the cofactors factor V and factor VIII.

Under normal physiological conditions, the conversion of prothrombin to thrombin is the result of the activity of four components: the protease factor Xa, Ca^{2+} ions, phospholipids and factor V. This complex is also called prothrombinase. The conversion of prothrombin to thrombin is schematically shown in fig.2.2.

Prothrombin is a single chain protein which consists of 582 amino acids. Factor Xa can break the linkage between the amino acids 274 and 275 and subsequently the link between 318 and 319. The two chains 275-318 and 319-582 are connected by a disulphide linkage and form the thrombin molecule. The first part (1-274), which is called fragment 1-2, has no enzymatic function.

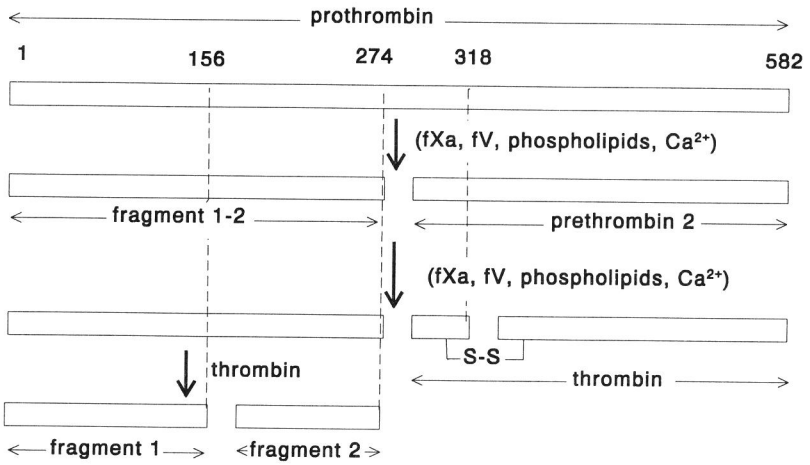

Fig.2.2 The conversion of prothrombin to thrombin, the numbers indicate the sequence of amino acids and fXa and fV are abbreviations for factor Xa and factor V [14].

As factor Xa has a preference to cleave the link between an arginine (Arg) and a isoleucine (Ile), factor Xa cuts the prothrombin molecule after the amino acids 274 and 318. However, there are 14 other Arg-Ile links in the prothrombin molecule which are not cleaved by factor Xa. This is the result of several mechanisms. Because factor Xa 'recognizes' more of the cleavage site than just the Arg-Ile linkage, the surrounding amino acids also play a role. Moreover, some of the Arg-Ile residues, which are located at the 'inner' side of the folded prothrombin molecule are not attainable for factor Xa. Another important aspect is the spatial orientation of prothrombin and factor Xa. The two molecules are orientated in a specific way with respect to each other because the reaction does not take place in solution but only at a phospholipid surface provided by platelets or damaged endothelial cells. Prothrombin and factor Xa both bind to the phospholipid surface through Ca^{2+} bonds which reduces the freedom of movement with respect to each other. Furthermore, both molecules also bind to coagulation cofactor factor V, which reacts with the apolar part of phospholipids. In this way, prothrombin and factor Xa are orientated in the proper way to interact. The prothrombinase complex is schematically shown in fig.2.3.

The interaction of prothrombin and factor Xa with phospholipids is a direct consequence of the vitamin K dependent modification of factor II (prothrombin), factor VII, factor IX and factor X which takes place in the liver. These coagulation factors are made from so-called PIVKAs (Protein Induced in Vitamin K Absence).

These PIVKAs are converted to coagulation factors by the enzyme carboxylase. Extra carboxyl groups are added to glutamic acid residues (Glu), which leads to the formation of γ-carboxyglutamic acid residues. The negatively charged carboxyl groups of these residues are responsible for the binding via Ca^{2+} ions to the negatively charged groups at the phospholipid surface.

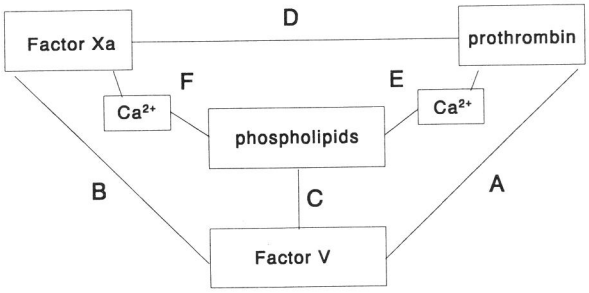

Fig.2.3 Schematic representation of the prothrombinase complex, A-E indicate the different interactions. A: Binding of a part (156-274) of prothrombin to factor V. B: Binding of factor Xa to factor V. C: Binding of factor V to the apolar part of the phospholipid surface. D: Enzymatic interaction of factor Xa with prothrombin (cleavage at 274 and 318). E: Binding of a part (1-156) of prothrombin via a calcium bond to negatively charged groups at the phospholipid surface. F: Binding of the light chain of factor Xa via a calcium bond to the phospholipid surface.

The first part of prothrombin (1-256, fragment 1) contains 10 γ-carboxylglutamic acid residues which are responsible for the Ca^{2+} binding to the phospholipid surface. The second part (157-274, fragment 2) contains no γ-carboxylglutamic acid residues but has specific binding sites for factor V. After being separated from prothrombin, the complete fragment 1-2 can be cleaved into fragment 1 and fragment 2 by thrombin molecules which are already formed.

Thrombin can also break the same link between fragment 1 and 2 before prothrombin is cleaved at the linkage between 156 and 157. This results in fragment 1 and a part called prethrombin 1 (157-582). Prethrombin 1 contains the complete thrombin structure but can only be activated very slowly because it cannot bind anymore to a phospholipid surface (fragment 1 is not present).

Activation of factor X

Factor X (MW ±55.000) consists of two chains, a heavy and a light chain which are connected through a disulphide linkage. When factor X is activated, a peptide (about 50 residues) is released from the heavy chain. The remaining chain

is now the heavy chain of factor Xa (MW 40.000) which contains the active serine centre, responsible for the proteolytic activity of factor Xa. After activation, the light chain (MW 15.000) remains unchanged and contains 12 γ-carboxylglutamic acid residues which are used for the Ca^{2+} binding to the phospholipid surface.

Two different mechanisms of activation of factor X are distinguished, activation by an extrinsic activator (block 2 in fig.2.1) and activation by an intrinsic activator (block 3 in fig.2.1). The extrinsic activator is formed after tissue damage (for instance an injury) when the damaged tissue cells release specific proteins and phospholipids which are called tissue thromboplastin (or tissue factor). This tissue thromboplastin forms a complex with factor VII and factor X is activated through interaction with Ca^{2+}-ions and phospholipids.

The result of the intrinsic path of the coagulation process is a complex of factor VIII (a cofactor, activated by thrombin in the same way as factor V), factor IXa, Ca^{2+}-ions and phospholipids. The Ca^{2+}-ions are responsible for the binding of factor IXa to the phospholipids. Coagulation via the intrinsic path is only possible if first a small amount of thrombin is formed (for the activation of factor VIII), possibly by the extrinsic system.

Factor IX is being activated through factor XIa. Activation of factor XI can be established both by interaction with factor XIIa and by the interaction with platelets in the presence of collagen (tissue). When factor XI is activated by the interaction with platelets, factor XII does not contribute to coagulation.

The activation of factor XII by activating surfaces is called the contact activation and the two plasma proteins prekallikrein and high molecular weight kininogen (HMWK) play an important role in the contact activation of factor XII, which is schematically shown in fig.2.4. When plasma makes contact with a foreign material surface, factor XII binds to the surface. This causes a conformational change in the molecule and results in a surface bound factor XIIa molecule. Prekallikrein and factor XI circulate in plasma in a complex with HMW kininogen which is responsible for the binding of prekallikrein and factor XI to the activating surface. Factor XIIa can activate prekallikrein to kallikrein and factor XI to factor XIa. This newly formed kallikrein activates more factor XII to factor XIIa which intensifies the activation of prekallikrein. Kallikrein is released from the surface while factor XIa remains immobilized. Kallikrein also plays an important role in the kinin system because kallikrein may generate bradykinin and so-called fragment 1.2 from HMW kininogen. In this way the kinin system is activated, which attributes to the inflammatory reaction by mediating the contraction of smooth muscle cells, increasing vascular permeability, dilating small blood vessels and by migration of white cells and pain generation [15-17].

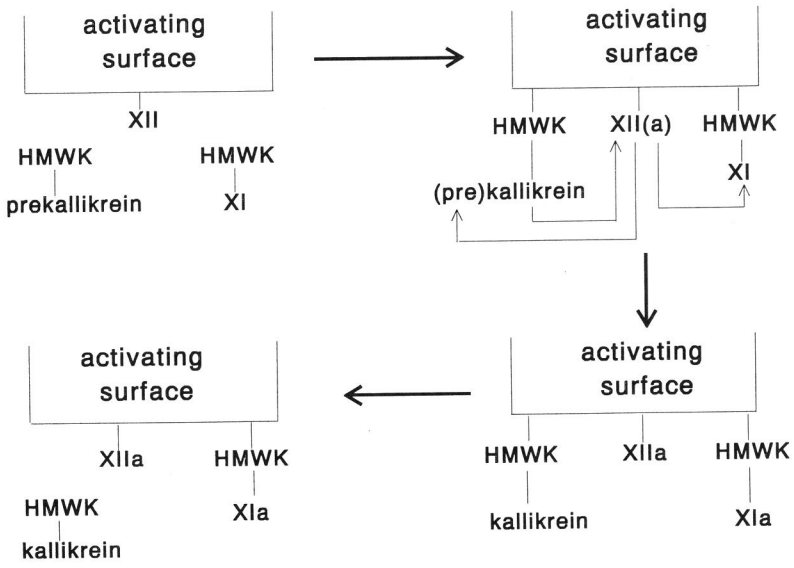

Fig.2.4 Contact activation; activation of factor XII by an activating surface [18].

Not only the intrinsic coagulation and the kinin system but also fibrinolysis can be activated through contact activation (see section 2.2.2).

2.2.2 The fibrinolytic process

The fibrinolytic process or fibrinolysis is the enzymatic process that degrades a formed blood clot. Activation of the fibrinolytic process results in the conversion of plasminogen into the proteolytic enzyme plasmin. Plasmin is a non-specific proteolytic enzyme which is able to degrade fibrin and fibrinogen but also to hydrolyse other plasma proteins. Under normal circumstances, a large excess of plasmin inhibitors is present which results in fibrinolytic activity only at the site of thrombi.

Activation of plasminogen can be established by three different activators which have been identified in plasma. The first two are tissue plasminogen activator and urokinase and will not be considered in further detail. The third possible path is initiated through contact activation (factor XII, prekallikrein, HMW kininogen and factor XI) and is called the factor XII dependent fibrinolytic pathway. After contact activation of factor XII, factor XIIa converts plasminogen proactivators to plasminogen activators. The proactivators are factor XI and prekallikrein and the

corresponding activators are factor XIa and kallikrein respectively. The plasminogen activators convert plasminogen into plasmin. Since plasmin is able to activate factor XII and factor XI, it provides a positive feedback mechanism for its own generation.

2.2.3 The role of blood cells (notably platelets)

The inner side of the membrane of red cells is very suited as phospholipid surface for the formation of activating complexes such as the extrinsic activator of factor X and the prothrombinase complex. White blood cells contain active tissue factor.

Platelets play an essential role in haemostasis and thrombosis. However, within the scope of the studies described in this thesis, it is not useful to give a detailed description of the role of the platelets; instead, only a brief description will be presented and for further details ref [13] is recommended.

The formation of a haemostatic plug is the result of a combination of several processes; the adhesion of platelets to the damaged vessel wall, the secretion of platelet granules, the aggregation of the platelets and the formation of thrombin [19].

adhesion

When a bloodvessel is damaged, blood may make contact with subendothelial tissue which consists (among other components) of collagen fibres of different lengths. Collagen consists of three polypeptide chains with several sugar residues which are important in the reaction with platelets. Different types of collagen are defined which can be distinguished by the number of sugar residues. Type 1 collagen, which contains few sugar residues, causes a relative strong adhesion to platelets. Type 4 collagen contains many sugar residues and is therefore less reactive with platelets. Skin and muscle tissue contains type 1 collagen, cartilage mainly type 2, vessel walls type 3 and vessel membranes type 4.

When the vascular damage is relatively small, blood is only in contact with collagen type 4 of the vessel membrane and there is only a limited reaction between platelets and collagen. When the damage is more serious and blood and collagen type 2 or 1, are in contact, the adherence of the platelets is stronger. Coagulation factor VIII (von Willebrand factor) also plays a role in the adherence of platelets to collagen.

secretion

As a result of the adherence of platelets to collagen, the dense- and α-granules are secreted. These secretion granules release substances (such as ADP and Ca^{2+}-ions) which are responsible for the continuation of platelet aggregation which

results in the haemostatic plug. In the haemostatic plug also thrombin is formed which is a very strong activator of the platelet secretion process.

aggregation

ADP released from platelets is the initiator for the aggregation of platelets. Under the influence of ADP the shape of platelets changes from a disc shape into an irregular sphere with pseudopods. Platelets become glutinous and aggregate, first where pseudopods from adjacent platelets meet, followed by more intense contact. Fibrinogen and Ca^{2+}-ions also play a role in the aggregation of platelets.

formation of thrombin

During the formation of the haemostatic plug, different mechanisms may result in thrombin formation. After interaction with collagen and ADP the platelet surface changes which result in the activation of different coagulation factors. Platelets also contain activated factor V. Probably the most important contribution of platelets to the coagulation process is the formation of a phospholipid surface after 'activation' of platelets. These phospholipid surfaces form a substrate for several interactions between coagulation factors, as described in the previous section, which finally result in the formation of thrombin and subsequently fibrin.

Thrombin amplifies the aggregation and the secretion of platelets while fibrin stabilizes the fragile plug of aggregated platelets. The formation of a haemostatic plug can thus be regarded as two separate processes; the formation of a plug of platelets and the coagulation inside this agglomerate.

2.3 The anticoagulant effect of heparin

2.3.1 The regulation of the coagulation process

Once the clotting cascade reaction is initiated, thrombin will be formed at a relatively high reaction rate. Because an excess of thrombin is as fatal as a deficiency, it is not very surprising that there exists an efficient control mechanism which restrains the free concentration of thrombin. There are many positive and negative feedback mechanisms in the coagulation process itself (e.g. the role of thrombin) and between the coagulation process and for instance the fibrinolytic process. However, one of the major systems for controlling coagulation, fibrinolysis and the kallikrein/kinin system, is the existence of inhibitory proteins that are components of normal blood. These inhibitors can inactivate some of the proteases involved in coagulation, fibrinolysis and kallikrein/kinin formation.

At least ten different proteins in plasma have been characterized as inhibitors

of serine proteases [20]. These inhibitors are present in blood in relatively high concentrations, thereby suggesting their physiological importance. They constitute approximately 10% of the plasma proteins. Eight of these inhibitors have been found to inhibit proteases involved in coagulation, fibrinolysis and kinin formation. Table 2.1 shows the most important interactions between these inhibitors and the proteases involved.

Table 2.1 Proteases which are involved in coagulation, fibrinolysis and kinin formation and their inhibitors. AT, antithrombin III; α_2PI, α_2-plasmin inhibitor; C1-INH, C1-inhibitor; α_1AT, α_1-antitrypsin; α_2M, α_2-macroglobulin; HCII, heparin cofactor II; APCI, activated protein C inhibitor; PAI, plasminogen activator inhibitor. + indicates a inhibitory effect, - indicates no effect.

PROTEASES	INHIBITORS							
	AT	α_2PI	C1-INH	α_1AT	α_2M	HCII	APCI	PAI
kallikrein	+	+	+	+	+	-	-	-
plasmin	+	+	+	+	+	-	-	-
factor XIIa	+	+	+	-	-	-	-	+
thrombin	+	+	-	+	+	+	+	-
factor XIa	+	+	+	+	-	-	-	-
factor Xa	+	+	-	+	+	-	+	-
factor IXa	+	-	-	-	-	-	-	-
protein C	-	-	-	-	-	-	+	-

Once the coagulation process is activated, other processes which restrict the process to one place, repair any damages to the vessel and restore the bloodflow through the vessel are initiated almost simultaneously. One of these processes is the fibrinolytic process which degrades blood clots. Some inhibitors inactivate clotting factors and thereby localize the clotting process and other inhibitors localize the fibrinolytic process to the place where clots were formed.

The anticoagulant activity of heparin is based on its ability to increase the inhibitory effect of some of the inhibitors mentioned in table 2.1. Only the interactions between the different inhibitors and the proteases which are influenced by heparin will be mentioned here. Antithrombin III is considered as the most important inhibitor of the coagulation process. Its activity towards the proteases (table 2.1) is greatly increased by heparin. This is thought to be the major aspect of

the anticoagulant activity of heparin and therefore, the interaction between antithrombin III and heparin is discussed in more detail in section 2.3.2.

Although other interactions between heparin and plasma (inhibitory) proteins are obviously of less importance, some of these interactions will be mentioned very briefly (as recently reviewed by J. Hirsh [21]) to indicate that there are many possible interactions between heparin and plasma components.

Heparin is able to increase the activity of heparin cofactor II which is the second thrombin inhibitor besides antithrombin III [22,23]. Thrombin is the only protease which is inhibited by heparin cofactor II, whereas antithrombin III has an inhibitory effect to all mentioned proteases except protein C (table 2.1).

Activated protein C (APC) plays an important role in the regulation of blood coagulation through its ability to degrade coagulation cofactors V and VIII. An inhibitor of APC has been isolated and characterized [24,25]. Heparin is able to accelerate by 30-fold the rate of inhibition of APC by the APC-inhibitor [26].

Heparin also interacts with fibrinolysis. It enhances the conversion of plasminogen to plasmin [27], impairs the activation of plasminogen by tissue plasminogen activator on a fibrin surface [28,29], and it accelerates the inactivation of plasmin by antithrombin III [30,31].

The anticoagulant effect of heparin is modified by platelets, fibrin, vascular surfaces and plasma proteins. Platelets inhibit the anticoagulant effect of heparin by binding factor Xa and protecting it from inactivation by the heparin-antithrombin III complex [32,33] and by secreting the heparin-neutralizing protein platelet factor 4 [34]. Fibrin binds thrombin and protects it from inactivation by the heparin-antithrombin III complex [35,36]. Thrombin bound to subendothelial surfaces is also protected from inactivation by heparin [37], possibly through mechanisms similar to those that protect fibrin-bound thrombin.

Heparin binds to many proteins, of which three (histidine-rich glycoprotein [38], platelet factor 4 [34] and vitronectin [39]) also neutralize its anticoagulant activity.

2.3.2 The heparin-antithrombin III interaction

Antithrombin III (AtIII) consists of a single polypeptide chain with 432 amino acid residues and has a molecular weight of 58.000 [40]. The isoelectric point is 5.11 and the concentration of AtIII in human plasma is about 150 µg/ml [41]. The complete primary structure of AtIII has been reported by Petersen et al. [42].

As indicated in table 2.1, antithrombin III not only inhibits thrombin, as its name indicates, but also other coagulation factors (IXa, Xa, XIa and XIIa) [43-48]. Thrombin and factor Xa are the most sensitive to inactivation; of these, thrombin

is the most sensitive (by about one order of magnitude) [49,50].

The mechanism by which thrombin is inhibited by antithrombin III was first described by Rosenberg and Damus [40] and later reviewed in detail by Björk [51]. AtIII and thrombin initially form a weak complex which is very rapidly converted to a stable 1:1 complex with very tight binding via interaction between the reactive arginine site of AtIII and the active serine centre of thrombin. The bimolecular rate constant at 37 °C has been reported as $1.4x10^4$ $M^{-1}s^{-1}$, giving a theoretical plasma half-life for thrombin of 20 seconds [52]; the actual half-life is approximately 40 seconds, probably caused by the presence of fibrinogen and other thrombin substrates in plasma. It has been shown by several investigators [43-48] that the inhibition by AtIII of the factors IXa, Xa, XIa and XIIa occurs in a manner similar to that outlined for thrombin.

Heparin is able to dramatically accelerate each of these coagulation factor-AtIII interactions and these effects are already demonstrable at plasma heparin concentrations as low as 0.01 U/ml[1)], which correspond with a concentration in the order of 1 nM, i.e. some 2000-3000 times less than the plasma concentration of AtIII. At therapeutic heparin concentrations of over 1 U/ml, the reaction between thrombin and AtIII is accelerated over 2000-fold, and the half-life time of thrombin is reduced from 40 seconds to less than 0.01 second. The ability of heparin to act at low concentrations and the fact that it is not 'consumed' during the reaction, indicates that heparin acts as a catalyst.

The most frequently suggested mechanism by which heparin enhances the inhibition ability of AtIII is as follows [49,51]. First, heparin forms a 1:1 complex with AtIII which increases the affinity of AtIII to inhibit the different coagulation factors. Then a ternary complex is formed, in which the interaction between the active site of the coagulation factor and the reactive site of AtIII is established [53]. After this interaction is established, heparin is released from the ternary complex and is available to bind to a new free AtIII molecule because the binding of heparin to the coagulation factor-AtIII complex is 100 to 1000-fold weaker than the interaction of heparin with free AtIII [54].

The mechanism by which the intermediate ternary complex is assembled, depends on the coagulation factor which is involved [51,54-58]. For thrombin, factor IXa and probably factor XIa, the complex is assembled by the initial binding of AtIII to the heparin molecule and subsequently binding of the coagulation enzyme to the same heparin molecule. This mechanism is schematically shown in fig.2.5a for thrombin (the same mechanism is applicable for factor IXa and XIa). Binding

---

[1)] The concentration of heparin is usually given in International Units per ml (U/ml). See section 2.4.1

of AtIII to the heparin molecule before thrombin may also direct thrombin to a specific site on the heparin molecule adjacent to the AtIII binding region. After both AtIII and thrombin are bound to the heparin molecule, the interaction between thrombin and AtIII takes place and subsequently, heparin is released from the stable AtIII-thrombin complex. This mechanism is called 'approximation' because both AtIII and thrombin are bound to the heparin surface. The three coagulation enzymes (thrombin, factor IXa and factor XIa) which are inhibited by this mechanism are sometimes referred to as the 'thrombin group'.

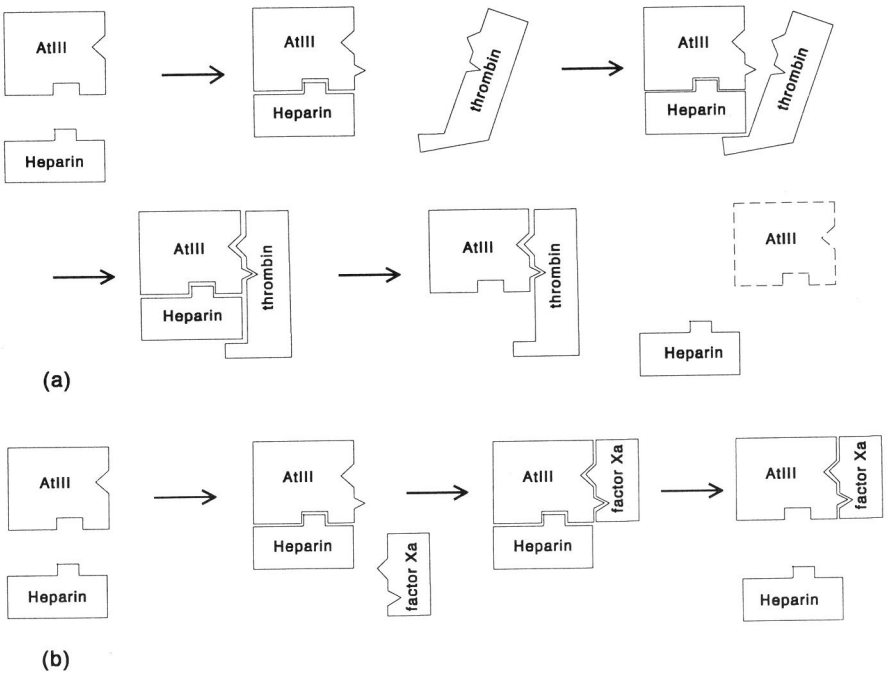

Fig.2.5 Formation of the ternary complex and the subsequent release of heparin. (a): interaction between heparin, AtIII and thrombin. (b): Interaction between heparin, AtIII and factor Xa.

In the case of factor Xa, and possibly also factor XIIa and plasma kallikrein, a ternary complex is presumably formed by an initial binding of AtIII to heparin followed by the binding of factor Xa (or factor XIIa or kallikrein) directly to AtIII but not to heparin. This mechanism is schematically shown in fig.2.5b for factor Xa. The three enzymes which are inhibited by this mechanism (factor Xa, factor XIIa and kallikrein) are sometimes referred to as the 'factor Xa group'.

For all reactions of coagulation enzymes and AtIII, the binding of heparin to AtIII induces a favourable conformational change of AtIII, which enhances its affinity for the different enzymes. This is schematically shown in the first step of figs.2.5 a and b. For the reaction of AtIII with the 'thrombin group', it is still unclear if this conformational change of AtIII or the earlier described approximation mechanism (the binding of both the enzyme and AtIII to heparin) is primarily responsible for the accelerating effect of heparin [51]. In case of the 'factor Xa group' the conformational change is mainly responsible for the accelerating effect of heparin.

2.3.3 The molecular weight dependence of the anticoagulant activity of heparin

In 1976 three research groups independently demonstrated that only 30-50 % of the molecules in normal heparin preparations are able to bind to AtIII and thereby induce anticoagulant activity [59-61]. Pure AtIII, bound to an insoluble matrix, can be used to separate heparin into two distinct fractions: one with high affinity and one with low affinity for AtIII. The high-affinity fraction is responsible for virtually all the anticoagulant activity and the low-affinity fraction is almost inactive. The molecules which bind with high affinity to AtIII all contain a unique pentasaccharide unit which is found to be the binding site for AtIII [62,7]. The structure of this pentasaccharide has been confirmed by chemical synthesis and is as follows: (N-sulphate-6-O-sulphate-α-D-glucosamine)1-4(β-D-glucuronic acid)1-4(N-sulphated-3,6-di-O-sulphate-α-D-glucosamine)1-4(2-O-sulphate-α-L-iduronic acid)1-4(N-sulphate-6-O-sulphate-D-glucosamine) [63,64].

After the binding site for AtIII became known to be only a pentasaccharide, interest in the anticoagulant activity of fractionated heparin started to grow. Heparin can be separated by, for example, gel-filtration techniques into fractions with different average molecular weights and with relatively narrow molecular weight distributions. Studies of such fractions have shown that the anticoagulant activity of each of them is highly dependent on the molecular weight. However, a discrepancy was found between the molecular weight dependences when the results of an anti-coagulant test based on inhibition of thrombin were compared to the results of a test based on inhibition of factor Xa.

For the 'thrombin group' it has been found that heparin chains at a minimum of approximately 18 monosaccharide residues are required to produce a detectable enhanced rate of inhibition by AtIII [58,56,65,66]. This finding has been interpreted as a confirmation of the approximation mechanism according to which heparin chains must be large enough to accommodate both AtIII and the coagulation enzyme to enhance these reactions (see also fig.2.5a).

For the 'factor Xa group', heparin chains containing less than 18 monosaccharides, even as small as the specific pentasaccharide fragment, provide large acceleration of enzyme inhibition by AtIII. This acceleration is comparable to or only a little lower than that seen with larger heparin chains [63,65-70]. This observation confirmed that binding of these coagulation enzymes with heparin is not important to enhance the rate of inactivation of these enzymes by AtIII (see also fig.2.5.b).

Low Molecular Weight Heparin

The understanding of the different mechanisms opened a new area of research and the practical result has been the development of the so called 'low molecular weight heparins' (LMWHs). Commercially developed LMWHs have different mean molecular weights that vary from 4,000 to 6,500 [71-73]. The ability of LMWHs to catalyze the inactivation of thrombin (which is dependent on the molecular size) is reduced relative to their ability to inhibit factor Xa. Compared with unfractionated heparin, which by definition has an anti-factor Xa to anti-thrombin ratio of 1:1, the various commercial LMWHs have anti-factor Xa to anti-thrombin ratios varying between 4:1 and 2:1 [74]. These ratios are based on assays performed in vitro using platelet-poor plasma and may not reflect the anticoagulant profiles of LMWHs in whole blood in vivo, because the effect of platelets on unfractionated heparin is larger than on LMWHs. As distinct from unfractionated heparin, LMWHs are not neutralized by platelet factor 4 and LMWHs are able to inhibit factor Xa which is bound to platelet membranes. These properties can make LMWHs a more effective anticoagulant in whole blood than unfractionated heparin.

2.3.4 The overall effect of heparin on thrombin generation

It may be clear that the intended aim of heparin is to reduce, delay or prevent the generation of thrombin. We have seen that most of the inhibitory actions of heparin on the different coagulation enzymes are fairly well characterised. However, because of the complexity of the coagulation system, including the different feedback mechanisms, it is very difficult to predict which reactions are most important for inhibition of thrombin generation. Since the coagulation process is a cascade reaction, it might be thought that thrombin generation could be most efficiently prevented by inhibition of the enzymes at the beginning of the cascade. This is however an oversimplification. Especially the existence of the thrombin feedback loops (activation of the cofactors V and VIII, see fig.2.1) can result in an enormous increase in the rate and amount of thrombin subsequently generated.

Recent studies claim that the inhibition of thrombin induced activation of

factor V and VIII is the most important effect of heparin while the anti factor Xa activity is less important [75-80]. This is also claimed for the LMWHs, which is an unexpected conclusion because of their relatively low anti-thrombin activity. However, the unambiguously shown therapeutic effect of LMWHs indicates that the anti-factor Xa activity of LMWHs might become more important under in vivo conditions [73].

2.4 Monitoring heparin treatment

2.4.1 Heparin standards

Heparin is one of a variety of drugs extracted from natural sources, whose activity cannot be adequately described or predicted by chemical and physical methods. In spite of the enormous advances made in recent years of the knowledge of the chemical basis for heparin's anticoagulant activity, the assessment of heparin for quality control purposes by manufacturers, and for dosage by clinicians, is still made in units of biological activity which can be a source of indistinctness. It may be clear that for such a widely used drug as heparin, it is of crucial importance to ensure that measurements of biological activity are properly standardized.

The first definition of the unit of biological activity of heparin was made by Howell, who defined the unit as the amount of heparin which prevented the clotting of 1 ml of cat's blood for 24 hours at 0 °C [81]. This was a very reasonable definition at the time, but it suffers from the basic drawback of all such definitions which is the difficulty of reproducing the same assay conditions in different laboratories. This problem can be overcome by establishing one batch of the substance as a reference material with a defined potency which may be defined by its activity in a certain assay system, and the potency of unknown samples may then be measured by comparative assay against the reference material. This system of comparative bioassay against a reference material was first suggested for insulin in 1925 and has since been applied successfully to almost every category of biological substance. The great advantage is that the variability of the different test systems is the same for both the reference and test materials. However, a very important condition for standardization is that the reference and test preparations have to behave similarly in the assay system which is used. In other words, 'like' has to be compared with 'like'. This means that the sensitivity of the assay to concentrations of the test material must be the same as the sensitivity of the assay to concentrations of the reference material (only a constant offset is allowed). These assays are sometimes called 'parallel line' assays because all test samples will give a line parallel to the line of the reference material. If the lines intersect, the assay cannot

be used to compare a test material with a reference material [82].

The 1st international standard of heparin was established by the World Health Organization (WHO) in 1947. The potency of this standard was defined as 130 international units per mg (IU/mg). The second international standard was established in 1957 when stocks of the 1st international standard were almost exhausted. This new standard, the sodium salt of a commercial bovine lung heparin, had the same potency as the 1st international standard (130 IU/mg). During the 1960s, a major change occurred in the raw material used for the manufacture of heparin. Bovine lung was replaced as the main tissue source by intestinal mucosa from pigs, sheep and oxen. This gave some discrepancies between different assay methods when determining the potency of new (mucosa) heparin preparations in comparison with the international standard which was a lung heparin. The 3rd international standard was therefore a porcine mucosal heparin and was established in 1973. The potency was 1370 IU/ampoule and was based on the overall mean of all assays by all assay methods. The present international standard is the 4th international standard which has the same potency as the 3th standard and was established in 1984 after the stocks of the 3th standard were exhausted.

As mentioned in the previous section, in the 1980s different low-molecular-weight heparins (LMWHs) became commercially available. Because the anti-thrombin and anti-factor Xa activity of LMWH is substantially different from unfractionated heparin, difficulties arose when these LMWH preparations were assayed against the 4th international standard for unfractionated heparin. The assays gave lines which were not parallel to the line of the standard material. Apparently, 'like' was not being compared with 'like' anymore. A collaborative study resulted in significant interlaboratory variability when the LMWHs were compared with the standard for unfractionated heparin [83]. Another, more extensive collaborative study resulted in a possible candidate for a new special standard for LMWH which was established by the WHO in 1986 [84]. This standard has a potency of 1680 IU/ampoule by anti-factor Xa assay and 665 IU/ampoule by anti-thrombin assay (see next section).

2.4.2 The modern assay methods

The heparin preparations which were made in the 1920s in the laboratory of professor Howell, were assessed for anticoagulant activity by their ability to prevent or delay the clotting of fresh cat blood at 0 °C [81]. As the availability and clinical use of heparin became more widespread over the next decades, an increasing number of variations on this basic method was introduced. A feature of all early assays was the long time required for blood to clot in the presence of heparin which

resulted in very long incubation periods (1-24 h). This is the reason why accelerators of the coagulation were introduced. In the presence of initiators of the intrinsic or extrinsic pathway (i.e. surface activators or tissue factor) coagulation is greatly accelerated and anticoagulant activity can then be measured by the delay of appearance of a clot, with clotting times of the order of minutes rather than of hours. Also the use of additional thrombin was introduced in the heparin assays. The evolution in the heparin assays is described in more detail by Barrowcliffe [82]. In this paragraph, only the modern assay methods which are presently in use, will be described.

All the assays which will be described, use cell- and platelet-free plasma, because cells and platelets can interfere with the tests. When taking blood samples from patients, blood is directly mixed with citrate, oxalate or EDTA (ethylene-diamine-tetra-acetic-acid) which all bind the Ca^{2+}-ions to prevent the blood from coagulation. The blood is then centrifuged for about 15 min. at 2000-4000 g to remove cells and platelets. In coagulation tests, calcium ions are again added to initiate coagulation.

Activated partial thromboplastin time (APTT)

The APTT is the most widely used clinical laboratory test for heparin monitoring. It is an accelerated clotting test in which the time for the formation of clots is measured. For normal plasma, a typical APTT is of the order of 40-50 seconds. A surface activator (e.g. kaolin) is added to citrated plasma, to accelerate activation of factor XII. After incubation, phospholipids are added, also to accelerate coagulation and again after an incubation period, some $CaCl_2$ is added which finally initiates the coagulation process. After the addition of $CaCl_2$, the time needed to form a clot is recorded.

The two most widespread methods to detect clots are the optical method and the electromechanical method. The optical method is based on changes in optical density of a beam directed through plasma. The electromechanical method consists of two electrodes of which one is moved in and out the plasma about every second. If the electrode is in the upper position (outside the plasma), the electrical impedance between the two electrodes is measured. As long as no clot is formed, this impedance will be infinitely high. However, if a clot is formed, the moving electrode, which is shaped like a hook, will pull up one or more fibrin threads which will lower the electrical impedance.

In different laboratories there are wide differences between reagents and methodology for performing APTT assays. For the surface activation substances such as kaolin, celite or soluble activators (e.g. ellagic acid) are used in commercial APTT reagents. There is also a large variety of phospholipids available which differ

considerably in their sensitivity to heparin. Although all these differences may have important clinical consequences, they are less critical for heparin assays, when standard and test are compared under the same conditions. But it does mean that the response of the particular APTT reagent which is used, must be known. In practice, this means that a calibration curve must be made in which the APTT is plotted as a function of the (known) heparin concentration in normal plasma. Variation in pretreatment or 'baseline' APTT (i.e. the APTT of the patient's plasma before heparin is injected) is another source of relative poor correlation between heparin concentration and APTT. In one study [85] a mean baseline APTT of 35.9 sec was found with a standard deviation of 6.8 sec. in 20 normal volunteers. Another study [86] reports that 77 out of 933 consecutive plasma samples (8.2 %) from hospital patients not receiving heparin, had APTT values above 1.6 times the mean of normal baseline. Unfortunately, pretreatment values often are not available. Based on experimental animal data and clinical studies, a therapeutic range of 1.5-2.5 times the mean of the normal reference range is often recommended. By translating this APTT range to heparin concentration ranges, the latter have been defined as 0.2-0.7 U/ml [87] or more precisely as 0.3-0.5 U/ml [88].

Thrombin clotting time (TCT)

The thrombin clotting time is one of the oldest heparin assays still in use. In this test, thrombin is added to the heparinized plasma sample, and subsequently the clotting time is measured. It is one of the simplest methods, but the precise measurement of the clotting time is very sensitive to variations in pH, temperature and ionic strength. The presence of additional calcium ions in the thrombin clotting test minimizes the effect of pH changes and shortens the heparin thrombin clotting time which improves the reproducibility of the assay. Therefore, it has been claimed that the so-called calcium thrombin time (with additional calcium ions) is superior to the thrombin clotting time for clinical use [89]. Other variables in the assay are the species and concentration of thrombin [90-92]. Teien found that the heparin response of the calcium thrombin clotting time shows less variation than the APTT [93].

Polybrene or protamine titration

Polybrene and protamine are both basic (alkaline) compounds which neutralize the effect of acidic heparin stoichiometrically. Polybrene is a poly-quaternary ammonium salt species and protamine is a small highly basic (alkaline) protein (MW ±4000). The anticoagulant activity of heparin is determined by measuring the thrombin clotting time with various concentrations of polybrene or protamine [94,95]. In this way, the concentration of active heparin molecules can be

accurately determined. Despite some simplifications, the method is nevertheless often regarded too complex for clinical use, because the range of protamine concentrations at which heparin is neutralized is quite narrow.

Anti-Xa clotting tests

In 1973, two new heparin assays were introduced which both determine the ability of heparin to accelerate the inhibition of factor Xa [96,97]. The principle of the two methods is the same but they differ in technical detail. In both methods, a fixed quantity of bovine factor Xa is added to the heparinized plasma sample. After a certain incubation time, residual factor Xa is determined by adding some of the plasma to a well defined clotting mixture (subsampling) and recording the clotting time. It is claimed that this method can detect heparin concentrations as low as 0.01 Units/ml in clinical samples. Because the range of linearity with this method is relatively small (between 0 and 0.2 U/ml) it is necessary to dilute each heparin sample to the appropriate range.

In 1985, Yin introduced a new variant of the anti-Xa clotting assay: the so-called Heptest [98]. In this modification of the earlier assay, factor Xa is incubated for 2 minutes with citrated plasma containing the heparin test. Instead of subsampling to determine the residual factor Xa, the remaining Xa activity is determined simply by addition of phospholipid and $CaCl_2$ to the plasma and recording the clotting time. Preliminary data in an international collaborative study [99] indicate that the Heptest gives comparable results to the other anti-Xa clotting assays.

Chromogenic substrates

With the use of specific peptide substrates for factor Xa and thrombin, a more accurate estimate of the activity of these enzymes can be made. Several substrates are commercially available for factor Xa and thrombin and also for other coagulation enzymes. The principle of these assays is the same as for the anti-Xa clotting assays: determination of residual enzyme activity after incubation of factor Xa or thrombin (or another enzyme) with heparinized plasma or purified antithrombin III. Residual factor Xa or thrombin is determined either by addition of peptide substrate to the mixture or subsampling a sample from the reaction mixture into the substrate solution. All the commercially available substrates use p-nitroanaline as a chromophore which is released as a result of the reaction with factor Xa or thrombin. This release is measured either by monitoring the change in optical density (at 405 nm) per minute or by termination of the enzyme-substrate reaction after a fixed time with acetic acid and determination of the stable value of the optical density. Also with the use of chromogenic substrates many variations

have been introduced for the control of heparin therapy in clinical laboratories [82,100]. In the chromogenic substrate assays, the endpoint is electronically determined by an instrument, often by automated procedures and the precision is higher than for clotting assays.

Since the recovery of known amounts of heparin added to normal plasma samples is very near to 100%, the assay methods based on the use of chromogenic substrates are often called 'specific'. If the test plasma is the only source of antithrombin, the result is influenced by the antithrombin III concentration, which can be different from patient to patient, and a combined heparin/antithrombin activity is measured [101,93]. If antithrombin III is added as a reagent to the test, variations in the plasma antithrombin III concentration of the test sample will have minimal influence on the result [102]. For pharmacokinetic studies, assays which are not influenced by antithrombin must be preferred. In the clinical situation, both types of assay have their specific advantages.

2.4.3 Comparison of the different heparin assays

Since it is impossible to predict the in vivo behaviour of heparin by physico-chemical means only, none of the assay methods can claim a unique relationship with the in vivo therapeutic efficacy of heparin. However, the assays can be used to determine and compare the in vitro activities of various products.

Activity versus concentration

The various assays determine different parameters and some determine a combination of parameters. The APTT assay determines a clotting time which is dependent on the amount of active heparin but also on the concentration of AtIII and other coagulation factors. The thrombin clotting time assay is influenced by the concentration of AtIII in the plasma sample but not by the concentration of other coagulation factors. The anti-Xa clotting tests determine the clotting time of a well defined mixture after subsampling of residual factor Xa. In this case, the AtIII concentration does not influence the assay. The chromogenic substrates which use additional AtIII are also not influenced by the plasma AtIII concentration.

An assay can be called 'specific' when it determines just one specific parameter. In case of a 'specific' heparin assay, the concentration of the biological active heparin molecules (the molecules with high affinity for AtIII) is determined. A chromogenic substrate which uses additional AtIII can be called specific and the correlation to the concentration of biological active heparin (molecules with AtIII affinity) is high [103,87]. When, in the context of heparin assays, the concentration of the anticoagulant is mentioned, the concentration of active heparin molecules

(with AtIII affinity) is usually meant. Specific assays which measure quantities which correlate with the active heparin concentration are often called 'concentration type' assays and assays which are influenced by the plasma concentration of AtIII and/or other coagulation factors are often referred to as 'activity type' assays (e.g. APTT).

Table 2.2 Modern heparin assays: influence of some components in test plasma relevant to monitoring [100]

Assay	Influence of coagulation factor concentrations	Influence of AtIII concentration	Correlation to active heparin concentration
APTT	+	(+)	+
TCT	0	+	+(+)
Calcium TCT	0	+	++
P/P titration	0	0	+++
CS and related	0	+	++
CS with added AtIII	0	0	+++

TCT=thrombin clotting time, CS=chromogenic substrate, P/P=polybrene or protamine titration

Several authors have compared the in vitro sensitivity and specificity of the various heparin assays [87,102-104]. Table 2.2 shows the different heparin assays and the influence of some plasma components relevant to monitoring [100]. The specificity, in terms of response to an added amount of heparin, was found to increase in the following order: APTT < thrombin clotting time < anti-factor Xa clotting assay < chromogenic substrate assays. The correlation to the antithrombotic effect was found to be higher for the specific assays, and probably best for assays reflecting both the active heparin concentration and antithrombin concentration. With respect to the detection of unacceptable bleeding risk, all current assays are useful, but the specific assays with high correlation to the active heparin concentration are the most informative because this is the most important variable in this case [100].

If a 'concentration type' assay is used (i.e. a chromogenic substrate with AtIII as reagent), patients with low plasma AtIII concentration may still have low anticoagulant activity, even if the active heparin concentration is well within what

is usually considered as the 'therapeutic range'. On the other hand, if an activity assay is used for patients with low plasma AtIII concentration, a defined therapeutic range may lead to excessive heparin dosage and undue risk of bleeding. Moreover, it is found that the plasma AtIII concentration regularly decreases during heparin treatment [105]. Holm et al. suggested therefore the use of a concentration type assay in combination with plasma AtIII monitoring in patients receiving heparin for the treatment of deep vein thrombosis (DVT) [106].

Despite the fact that the specific assays show a higher correlation to the antithrombotic effect of heparin, the simplicity of the APTT assay makes this assay the most widely used laboratory test for heparin monitoring. However, when using the APTT, it is necessary to have a calibration curve of the heparin sensitivity of the reagent. The patient's pretreatment (or baseline) APTT value can also be very useful.

For monitoring LMWHs, anti-factor Xa methods should be used because of the low activity of LMWH in overall clotting tests. The mostly used method in clinical trials for monitoring LMWHs, is a chromogenic substrate for factor Xa.

Determination of absolute amounts of heparin

Several authors have found that the anticoagulant activity of heparin may change after injection into the circulation. The antithrombin activity of a heparin sample was determined after the heparin was injected and again separated from plasma, and subsequently this was compared with the antithrombin activity of the same heparin before injection. It appeared that the antithrombin activity of heparin after injection was greater than before injection [107-109]. This observation is the source of discrepancies between the measurement of absolute concentrations of heparin (the concentration of all molecules), and 'the amount of heparin' as determined by in vitro coagulation tests. Even if a specific test is used, with high correlation to the concentration of active heparin, the in vivo generation of anticoagulant activity cannot be observed.

This is the reason why Jaques et al. have claimed that it is essential to determine the total absolute amount of heparin in plasma [110]. They developed a method to determine microgram quantities by adsorption of heparin on an affinity column followed by elution in a buffer solution and determination of the heparin content by electrophoresis.

Gitel et al. developed a heparin immunoassay to determine absolute amounts of heparin. They used antiheparin antibodies obtained by immunizing rabbits with a methylated bovine serum albumin-heparin precipitate [111]. The immunoassay is able to determine heparin concentrations as low as 25 ng/ml in plasma without pretreatment of plasma. This sensitivity is equivalent to that of an assay based on the inhibition of binding of ^{125}I-heparin to protamine sulphate- or polybrene-

sepharose, which was developed by Dawes et al. [112].

2.4.4. Towards a new heparin sensor

From the previous concerning modern assay methods, it may be concluded that different assays determine different parameters and that there is a variation in specificity. Within the scope of the studies described in this thesis, we will not discuss the question which assay, or combination of assays, is the best way to monitor heparin treatment.

One of the limitations of all current assays is that they use additional reagents and require specific equipment and therefore can only be performed in clinical laboratories. This is why a simple sensor which determines the (active) heparin concentration may be a useful device for heparin monitoring. A sensor can be used for very small samples (in the order of microliters) and, if necessary, bloodcells and platelets can be directly removed by using a filter membrane. Because no sample pre-treatment is necessary, and no additional reagents are used, a simple heparin sensor system might be used at the 'bedside' and therefore safe time and money. In this perspective, it is interesting to note that approximately 500 million doses of heparin are used worldwide each year [113]. However, a sensor, measuring the heparin concentration in plasma, might also be used as an additional laboratory instrument in heparin monitoring together with for instance an APTT-assay.

In this thesis, the development of a heparin concentration sensor is described and in the last chapter, some alternatives for determining other parameters related to the biological activity of heparin are outlined.

To the knowledge of the author, only one research group has reported about the development of a heparin concentration sensor [114-117]. Ma and coworkers developed an ion-selective electrode with a polymer membrane in which TDMAC (tridodecylmethyl-ammonium chloride) is used as an affinity ligand for heparin. The sensor measures absolute amounts of heparin because TDMAC does not distinguish active from non-active heparin molecules. The concentration range which can be determined is reported as 1.0 to 9.8 U/ml with a slope of 28.2 mV per decade. This sensor can therefore be used in certain procedures such as cardio-vascular surgery, where doses of 2-8 U/ml are commonly used. However, in the usual heparin treatment (for instance for the prevention of deep vein thrombosis) the therapeutic concentration range is in between 0.2 and 0.7 U/ml [87,88]. This means that this sensor cannot be used as an alternative for the assay methods as described in the previous sections.

References

[1] J. McLean, The thromboplastic action of cephalin, American Journal of Physiology, 41 (1916), p.250

[2] J. McLean, The discovery of heparin, Circulation, 19 (1959), p.75

[3] W.H. Howell, E. Holt, Two new factors in blood coagulation - heparin and pro-antithrombin, American Journal of Physiology, 47 (1918), p.328

[4] W.H. Howell, The purification of heparin and its presence in blood, American Journal of Physiology, 71 (1925), p.553

[5] W.H. Howell, The purification of heparin and its chemical and physiological reactions, Bulletin of the John Hopkins Hospital, 42 (1928), p.199

[6] L. Roden, Highlights in the history of heparin, in: Heparin, chemical and biological properties, clinical applications, D.A. Lane and U. Lindahl (eds.), Edward Arnold, London, UK, (1989)

[7] B. Casu, Methods of structural analysis, in: Heparin, chemical and biological properties, clinical applications, D.A. Lane and U. Lindahl (eds.), Edward Arnold, London, UK, (1989)

[8] U. Lindahl, Biosynthesis of heparin and related polysaccharides, in: Heparin, chemical and biological properties, clinical applications, D.A. Lane and U. Lindahl (eds.), Edward Arnold, London, UK, (1989)

[9] A.F. Charles, D.A. Scott, Studies on heparin II. Heparin in various tissues, Journal of Biological Chemistry, 102 (1933), p.431

[10] A.F. Charles, D.A. Scott, Studies on heparin I. The preparation of heparin, Journal of Biological Chemistry, 102 (1933), p.425

[11] A.F. Charles, D.A. Scott, Studies on heparin III. The purification of heparin, Journal of Biological Chemistry, 102 (1933), p.437

[12] H.B. Nader, C.P. Dietrich, Natural occurrence and possible biological role of heparin, in: Heparin, chemical and biological properties, clinical applications, D.A. Lane and U. Lindahl (eds.), Edward Arnold, London, UK, (1989)

[13] R.W. Colman, J. Hirsh, V.J. Marder, E.W. Salzman (eds.) Hemostasis and thrombosis, basic principles and clinical practice, Third Edition, J.B. Lippincott Company, Philadelphia (1994).

[14] H.C. Hemker, De bloedstolling, het reactie mechanisme, in: De bloedstolling, thrombose, artherosclerose en het hartinfarct, special edition of: Natuur en Techniek, August 1979

[15] F. van der Graaf, J.A. Koedam, B. Bouma, Inactivation of kallikrein in human plasma, J.Clin. Invest., 71 (1983), p.149

[16] R.J. Ulevitch, C.G. Cochrane, A.R. Johnston, Rabbit prekallikrein, purification, biochemical characterization, and mechanism of activation, Inflamm., 4 (1980), p.9

[17] J.F. Davidson, Recent advances in fibrinolysis, In: Recent advances in blood coagulation 2, p. 91-122, L. Poller (ed.), Churchill Livingstone, London, UK, (1977)

[18] Platenatlas Hemostase, Boehringer Ingelheim, 1979

[19] J.J. Sixma, De bloedstelping, bloedplaatjes en de vorming van de hemostatische prop, in: De bloedstolling, thrombose, artherosclerose en het hartinfarct, special edition of: Natuur en Techniek, August 1979

[20] P.C. Harpel, Blood proteolytic enzyme inhibitors: their role in modulating blood coagulation and fibrinolytic enzyme pathways. In: Haemostasis and Thrombosis, Basic Principles and clinical practice,, R.W. Colman, J. Hirsh, V.J. Marder and E.W. Salzman (eds.), J.B. Lippincott Company, Philadelphia, (1987)

[21] J. Hirsh, Heparin, The new england journal of medicine, 324 (1991), p.1565

[22] G.F. Birginshaw, J.N. Shanberge, Identification of two distinct heparin cofactors in human plasma: I. Separation and partial purification, Arch. Biochem. Biopphys., 161 (1974), p.683

[23] G.F. Birginshaw, J.N. Shanberge, Identification of two distinct heparin cofactors in human plasma: II. Inhibition of thrombin and activated factor X, Thrombosis Research, 4 (1974), p.463

[24] K. Suzuki, J. Nishioka, S. Hashimoto, Protein C inhibitor: purification from human plasma and characterization, Journal of Biological Chemistry, 258 (1983), p.163

[25] K. Suzuki, Activated protein C inhibitor, Semin Thromb Hemost, 10 (1984), p.154

[26] K. Suzuki, J. Nishioka, H. Kusumoto, S. Hashimoto, Mechanism of inhibition of activated protein C by protein C inhibitor, Journal of Biochemistry, 95 (1984), p.187

[27] J.M. Edelberg, S.V. Pizzo, Kinetic analysis of the effects of heparin and lippoproteins on tissue plasminogen activator mediated plasminogen activation, Biochemistry, 29 (1990), p.5906

[28] P. Andrade-Gordon, S. Strickland, Interaction of heparin with plasminogen activators in plasminogen: effects on the activation of plasminogen, Biochemistry, 25 (1986), p.4033

[29] E.P. Paques, H.A. Stohr, N. Heimbeurger, Study on the mechanism of action of heparin and related substances on the fibrinolytic system: relationship between plasminogen activators and heparin, Thrombosis Research, 42 (1986), p.797

[30] Highsmith, R.F.; Rosenberg, R.D., The inhibition of human plasmin by human antithrombin-heparin cofactor, J. Biol. Chem., 249 (1974), p.4335

[31] R. Machovich, P.I. Bauer, P. Aranyi, E. Kecskes, K.G. Buki, I. Horvath, Kinetic analysis of the heparin enhanced plasmin antithrombin III reaction, Biochem. J., 199 (1981), p.521

[32] E. Marciniak, Factor Xa inactivation by antithrombin. 3. Evidence for biological stabilization of factor Xa by factor V-phospholipid complex., Br. J. Haemmatol., 24 (1973), p.391

[33] F.J. Walker, C.T. Esmon, The effects of phospholipid and factor Va on the inhibition of factor Xa by antithrombin III, Biochem. Biophys. Res. Commun., 90 (1979), p.641

[34] J.C. Holt, S. Niewiarowski, Biochemistry of alpha-granule proteins, Semin. Hematol., 22 (1985), p.151

[35] J.I. Weitz, M. Hudoba, D. Massel, J. Maraganore, J. Hirsch, Clot-bound thrombin is protected from inhibition by heparin-antithrombin III but is susceptible to inactivation by antithrombin III-independent inhibitors, J. Clin. Invest., 86 (1990), p.385

[36] P.J. Hogg, C.M. Jackson, Fibrin monomer protects thrombin inactivation by heparin-antithrombin III: implications for heparin efficacy, Proc. Natl. Acad. Sci. USA, 86 (1989), p.3619

[37] R. Bar-Shavit, A. Eldor, I. Vlodavsky, Binding of thrombin to subendothelial extracellular matrix: protection and expression of functional properties, J. Clin. Invest., 84 (1989), p.1096

[38] H.R. Lijnen, M. Hoylaerts, D. Collen, Heparin binding properties of human histidine rich glycoprotein: mechanism and role in the neutralization of heparin in plasma, J. Biol. Chem., 258 (1983), p.3803

[39] K.T. Preissner, G. Muller-Berghaus, Neutralization and binding of heparin by S-protein/vitronectin in the inhibition of factor Xa by antithrombin III, J. Biol. Chem., 262 (1987), p.2247

[40] Rosenberg, R.D.; Damus, P.S., The purification and mechanism of action of human anti-thrombin-heparin cofactor., J. Biol. Chem., 248 (1973), p.6490

[41] Murano, G.; Williams, L.; Milier-Andersson M.; Aronson, D.; King, C., Some properties of antithrombin III and its concentration in human plasma., Thromb. Res., 18 (1980), p.259

[42] E.E. Petersen, G. Dudek-Wojciechowska, L. Sottrup-Jensen, S. Magnusson, The primary structure of antithrombin III (heparin cofactor): Partial homology between alpha1-antitrypsin and antithrombin III. In: The physiological inhibitors of coagulation and fibrinolysis,, D. Collen, B. Wiman, M. Verstraete (eds.), p.43, Elsevier Biomedical Press, Amsterdam, (1979).

[43] Damus, P.S.; Hicks, M.S.; Rosenberg, R.D., Anticoagulant action of heparin., Nature, 246 (1973), p.355

[44] Rosenberg, J.S.; McKenna, P.W.; Rosenberg, R.D., Inhibition of human factor IXa by human antithrombin-heparin cofactor., J. Biol. Chem., 250 (1975), p.8883

[45] Stead, N.; Kaplan, A.P.; Rosenberg, R.D., Inhibition of activated factor XII by antithrombin-heparin cofactor., J. Biol. Chem., 251 (1976), p.6481

[46] F. Kurachi, K. Fujikawa, G. Schmier, E.W. Davie, Inhibition of bovine factor IXa and factor Xa by antithrombin III, Biochemistry, 15 (1976), p.373

[47] J. Chan, C. Burrowes, F. Habal, H. Movat, Inhibition of activated factor XII (Hageman factor) by antithrombin III: the effect of other plasma proteinase inhibitors, Biochem. Biophys. Res. Commun., 74 (1977), p.150

[48] L. Summaria, I.G. Boreisha, L. Arzadon, K. Robbins, Activation of human glu-plasminogen to glum-plasmin by urokinase in presence of plasmin inhibitors: streptomyces leuteptin and human plasma alpha-1-antitrypsin and antithrombin III, Journal of Biological Chemistry, 252 (1977), p.3945

[49] R.D. Rosenberg, The heparin-antithrombin system: a natural anticoagulant mechanism, In: Haemostasis and Thrombosis, Basic Principles and clinical practice, R.W. Colman, J. Hirsch, V.J. Marder and E.W. Salzman (eds.), J.B. Lippincott Company, Philadelphia, (1982).

[50] Ofosu, F.A.; Buchanan, M.R.; Anvari, N,; Smith, L.M.; Blajchman, M.A., Plasma anticoagulant mechanisms of heparin, heparan sulfate, and dermatan sulfate, Ann. N. Y. Acad. Sci., 556 (1989), p.123

[51] I. Björk, S.T. Olson, J.D. Shore, Molecular mechanisms of the accelerating effect of heparin on the reactions between antithrombin and clotting proteinases, in: Heparin, chemical and biological properties, clinical applications, D.A. Lane and U. Lindahl (eds.), Edward Arnold, London, UK, (1989)

[52] J. Jesty, Dissociation of complexes and their derivatives formed during inhibition of bovine thrombin and activated factor X by antithrombin III, Journal of Biological Chemistry, 254 (1979), p.1044

[53] M.W. Pomerantz, W.G. Owen, A catalytic role for heparin. Evidence for a ternary complex of heparin cofactor thrombin and heparin, Biochimica et Biophysica Acta, 535 (1978), p.66

[54] Jordan, R.E.; Oosta, G.M.; Gardner, W.T.; Rosenberg, R.D., The kinetics of hemostatic enzyme-antithrombin interactions in the presence of low-molecular-weight heparin., J. Biol. Chem., 255 (1980), p.10081

[55] Jordan, R.E.; Oosta, G.M.; Gardner, W.T.; Rosenberg, R.D., The binding of low-molecular-weight heparin to hemostatic enzymes., J. Biol. Chem., 255 (1980), p.10073

[56] Oosta, G.M.; Gardner, W.T.; Beeler, D.L.; Rosenberg, R.D., Multiple functional domains of the heparin molecule., Proc. Natl. Acad. Sci. USA, 78 (1981), p.829

[57] Hoylaerts, M.; Owen, W.G.; Collen D., Involvement of heparin chain length in the heparin-catalyzed inhibition of thrombin by antithrombin III., J. Biol. Chem., 259 (1984), p.5670

[58] Laurent, T.C.; Tengblad, A.; Thunberg, L.; Höök, M.; Lindahl, U. The molecular weight dependence of the anticoagulant activity of heparin. Biochem. J., 175 (1978) p.691

[59] Andersson, L.O.; Barrowcliffe, T.W.; Holmer, E.; Johnson, E.A.; Sims, G.E., Anticoagulant properties of heparin fractionated by affinity chromatography on matrix-bound antithrombin III and by gel titration., Thromb. Res., 9 (1976), p.575

[60] Höök, M.; Björk, I.; Hopwood, J.J.; Lindahl, U., Anticoagulant activity of heparin: separation of high-activity and low-activity heparin species by affinity chromatography on immobilized antithrombin., Fed. Eur. Biochem. Soc. Lett., 66 (1976), p.90

[61] Lam, L.H.; Silbert, J.E.; Rosenberg, R.D., The separation of active and inactive forms of heparin., Biochem. Biophys. Res. Comm., 69 (1976), p.570

[62] Casu, B., Structure of heparin and heparin fragments., Ann. N. Y. Acad. Sci., 556 (1989), p.1

[63] J. Choay, M. Petitou, J.-C. Lormeau, P. Sinay, B. Casu and G. Gatti, Structure-activity relationship in heparin: A synthetic pentasaccharide with high affinity for antithrombin III and eliciting high anti-factor Xa activity, Biochemical and Biophysical Research Communications, 116 (1983), p.492

[64] Choay, J., Chemically synthesized heparin-derived oligosaccharides., Ann. N. Y. Acad. Sci., 556 (1989), p.61

[65] E. Holmer, K. Kurachi and G. Soderstrom, The molecular-weight dependence of the rate-enhancing effect of heparin on the inhibition of thrombin, factor Xa, factor IXa, factor XIa, factor XIIa and kallikrein by antithrombin, Biochemical Journal, 193 (1981), p.395

[66] A. Danielsson, E. Raub, U. Lindahl and I. Bjork, Role of ternary complexes, in which heparin binds both antithrombin and proteinase, in the acceleration of the reactions between antithrombin and thrombin or factor Xa, Journal of Biological Chemistry, 261 (1986), p.-467

[67] V. Ellis, M.F. Scully and V.V. Kakkar, The relative molecular mass dependence of the anti-factor Xa properties of heparin, Biochemical Journal, 238 (1986), p.329

[68] E. Holmer, U. Lindahl, G. Backstrom, L. Thunberg, H. Sanberg, G. Soderstrom and L.-O. Andersson, Anticoagulant activities and effects on platelets of a heparin fragment with high affinity for antithrombin, Thrombosis Research, 18 (1980), p.861

[69] D.L. Lane, J. Denton, A.M. Flynn, L. Thunberg and U. Lindahl, Anticoagulant activities of heparin oligosaccharides and their neutralization by platelet factor 4, Biochemical Journal, 218 (1984), p.725

[70] L. Thunberg, U. Lindahl, A. Tengblad, T.C. Laurent and C.M. Jackson, On the molecular-weight dependence of the anticoagulant activity of heparin, Biochemical Journal, 181 (1979), p.214

[71] J. Fareed, J.M. Walenga, D. Hoppenstedat, X. Huan, A Racanelli, Comparative study on the in vitro and in vivo activities of seven low-molecular weight heparins, Haemostasis, 18 (1988), p.3

[72] E. Holmer, Low-molecular weight heparin, in: Heparin, chemical and biological properties, clinical applications, D.A. Lane and U. Lindahl (eds.), Edward Arnold, London, UK, (1989).

[73] T.W. Barrowcliffe, E.A. Johnson, D.P. Thomas, Low molecular weight heparin, John Wiley & Sons, Chichester, UK, (1992).

[74] J. Hirsh, M.N. Levine, Low molecular weight heparin, Blood, 79 (1992), p.1

[75] F.A. Ofosu, P. Sie, G.J. Modi et al., The inhibition of thrombin-dependent positive-feedback reactions is critical to the expression of the anticoagulant effect of heparin, Biochem. J., 243 (1987), p.579

[76] F.A. Ofosu, C.T. Esmon, M.A. Blajchman, G.J. Modi, L.A. Smith, N. Anvari, M.R. Buchanan, J.W. Fenton II, J. Hirsh, Unfractionated heparin inhibits thrombin-catalyzed amplification reactions of coagulation more efficiently than those catalyzed by factor Xa, Biochem. J., 257 (1989), p.143

[77] S. Beguin, T. Lindhout, H.C. Hemker, The mode of action of heparin in plasma, Thrombosis and Haemostasis, 60 (1988), p.457

[78] F.A. Ofosu, Antithrombotic mechanisms of heparin and related compounds, in: Heparin, chemical and biological properties, clinical applications, D.A. Lane and U. Lindahl (eds.), Edward Arnold, London, UK, (1989)

[79] H.C. Hemker, The mode of action of heparin in plasma. In: Thrombosis and Haemostasis, M. Verstraete, J. Vermylen, R. Lijnen, J. Arnout (eds.), Leuven University Press, Leuven, (1987), p.17

[80] S. Béguin, J. Mardiguian, T. Lindhout, H.C. Hemker, The mode of action of low molecular weight heparin preparation (PK 10169) and two of its major components on thrombin generation in plasma, Thromb. Haemostas., 61 (1989) p.30

[81] W.H. Howell, Heparin: an anticoagulant, American Journal of Physiology, 63 (1923), p.434

[82] T.W. Barrowcliffe, Heparin assays and standardization, in: Heparin, chemical and biological properties, clinical applications, D.A. Lane and U. Lindahl (eds.), Edward Arnold, London, UK, (1989).

[83] T.W. Barrowcliffe, A.D. Curtis, T.P. Tomlinson, A.R. Hubbard, E.A. Johnson, D.P. Thomas, Standardization of low molecular weight heparins: a collaborative study, Thromb. Haemostas., 54 (1985), p.675

[84] T.W. Barrowcliffe, A.D. Curtis, E.A. Johnson, D.P. Thomas, An international standard for low molecular weight heparin, Thromb. Haemostas., 60 (1988) p.1

[85] T.D. Björnsson, K.M. Wolfram, Intersubject variability in the anticoagulant response to heparin in vitro, European Journal of Clinical Pharmacology, 21 (1982), p.491

[86] N.A. Teien, U. Abildgaard, On the value of the activated partial thrombo-plastin time (APTT) in monitoring heparin therapy, Thrombosis and Haemostasis, 35 (1976), p.592

[87] J.J. van Putten, M. van de Ruit, M. Beunis and H.C. Hemker, Interindividual variation in relationships between plasma heparin concentration and the results of five heparin assays, Clinica Chimica Acta, 122 (1982), p.261

[88] J. Hirsh, Mechanism of action and monitoring of anticoagulants, Seminars in Thrombosis and Haemostasis, 12 (1986), p.1

[89] M.J. O'Shea, P.T. Flute and G.M. Pannell, Laboratory control of heparin therapy, Journal of Clinical Pathology, 24 (1971), p.542

[90] K.W.E. Denson, The sensitivity of human and bovine thrombin to heparin in plasma, Thrombosis Research, 23 (1981), p.297

[91] C. Eika, H.C. Godal and P. Kierulf, Detection of small amount of heparin by the thrombin clotting time, Lancet, 2 (1972), p.276

[92] J.D. Philips, Plasma heparin estimation based upon a thrombin clotting time technique, Medical Laboratory Sciences, 36 (1979), p.141

[93] N.A. Teien, M. Lie, Heparin assay in plasma. A comparison of five clotting methods, Thrombosis research, 7 (1975), p.777

[94] H.C. Godal, The assay of heparin in thrombin systems, Scandinavian Journal of Clinical and Laboratory Investigation, 13 (1961), p.154

[95] J. Refn, L. Vesterggard, The titration of heparin with protamine, Scandinavian Journal of Clinical and Laboratory Investigation, 6 (1954), p.284

[96] E.T. Yin, S. Wessler and J.V. Butler, Plasma heparin: a unique, submicrogram-sensitive assay, Journal of Laboratory and Clinical Medicine, 81 (1973), p.298

[97] K.W.E. Denson, J. Bonnar, The measurement of heparin. A method based on the potentiation of anti-factor Xa, Thrombosis et Diathesis Haemorrhagica, 30 (1973), p.471

[98] E.T. Yin, Appraisal of clot-based and amidolytic anti-Xa methods for the monitoring of heparin and its derivatives, Seminars in Thrombosis and Haemostasis, 11 (1985), p.243

[99] T.W. Barrowcliffe, A.D. Curtis, Principles of bioassay of haemostatic components. In: Haemostasis and Thrombosis, pp. 996, A.L. Bloom and D.P. Thomas (eds.), Churchill Livingstone, Edinburgh, (1987).

[100] U. Abildgaard, Monitoring heparin treatment, in: Heparin, chemical and biological properties, clinical applications, D.A. Lane and U. Lindahl (eds.), Edward Arnold, London, UK, (1989)

[101] K. Bartl, E. Dorsch, H. Lill and J. Ziegenhorn, Determination of the biological activity of heparin by use of a chromogenic substrate, Thrombosis and Haemostasis, 42 (1980), p.1446

[102] N.A. Teien, M. Lie, Evaluation of an amidolytic heparin assay method: Increased sensitivity by adding purified antithrombin III, Thrombosis Research, 10 (1977), p.399

[103] H. Bounameaux, G.A. Marbet, B. Lammle, R. Eichlisberger and F. Duckert, Comparison of thrombin time, activated partial thromboplastin time and plasma heparin concentration, and analysis of the behaviour of antithrombin III, American Journal of Clinical Pathology, 74 (1980), p.68

[104] H. Vinazzer, Zur bestimmung von Heparin im Plasma. Qualitatsvergleich verschiedener Methoden, Anaesthesist, 28 (1979), p.299

[105] H.A. Holm, S. Kalvenes, U. Abildgaard, Changes in plasma antithrombin (heparin cofactor activity) during intravenous heparin therapy: observations in 198 patients with deep venous thrombosis, Scand. J. Haemost., 35 (1985), p.564

[106] H.A. Holm, U. Abildgaard, M.L. Larsen, S. Kalvenes, Monitoring of heparin therapy: should heparin assays also reflect the patient's antithrombin concentration?, Thromb. Res., 46 (1987), p.669

[107] S.W. Levy, L.B. Jaques, Appearance of heparin anti-thrombin-active chains in vivo after injection of commercial heparin and in anaphylaxis, Thromb. Res., 13 (1978), p.429

[108] T.D. Björnsson, K.M. Wolfram, B.B. Mitchell, Heparin kinetics determined by three assay methods, Clin. Pharmacol. Ther., 31 (1982), p.104

[109] M.D. Klein, R.A. Drongowski, R.J. Lindhardt, R.S. Langer, A colorimetric assay for chemical heparin in plasma, Anal. Biochem., 124 (1982), p.59

[110] L.B. Jaques, S.M. Wice, L.M. Hiebert, Determination of absolute amounts of heparin and of dextran sulfate in plasma in microgram quantities, J. Lab. Clin. Med., 115 (1990), p.422

[111] Gitel, S.N.; Medina, V.M.; Wessler, S., Antiheparin antibodies: their preparation and use in a heparin immunoassay., J. Lab. Clin. Med., 109 (1987), p.672

[112] J. Dawes, D.S. Pepper, A sensitive competitive binding assay for exogenous and endogenous heparins, Thromb. Res., 27 (1982), p.387

[113] R.J. Lindhardt, An important drug enters its seven decade, Chemistry & Industry, January 21 (1991), p.45

[114] S.-C. Ma, V.C. Yang, M.E. Meyerhoff, Heparin-responsive electrochemical sensor: a preliminary study, Anal. Chem., 64 (1992), p.694

[115] H.-S. Yim, C.E. Kibbey, S.-C. Ma, D.M. Kliza, D. Liu, S.-B. Park, C. Espadas Torre, M.E. Meyerhoff, Polymer membrane-based ion-, gas- and bio-selective potentiometric sensors, Biosensors & Bioelectronics, 8 (1993), p.1

[116] V.C. Yang, S.-C. Ma, D. Liu, R.B. Brown, M.E. Meyerhoff, A novel electrochemical heparin sensor, ASAIO J., 39 (1993), p.195

[117] S.-C. Ma, V.C. Yang, B. Fu, M.E. Meyerhoff, Electrochemical sensor for heparin: further characterization and bioanalytical applications, Anal. Chem., 65 (1993), p.2078

The ion-step measuring method

3

3.1 Introduction

The ion-step measuring method was introduced by Schasfoort as a method to determine changes in charge density in a porous membrane mounted on top of an ISFET [1]. The membranes which Schasfoort used were made of polystyrene beads (∅ 0.1 μm), which were immobilized in an agarose gel. The typical thickness of the membranes (in dry condition) was 10 μm. The measuring method is schematically shown in fig.3.1. A stepwise increase in the electrolyte concentration at a constant pH value (the ion-step), causes a transient response of the membrane-covered ISFET. This transient response is a function of the charge density in the membrane. By immobilizing an affinity ligand in the membrane, concentrations of a specific charged analyte can be determined. To achieve this, the ISFET with immobilized ligand is incubated for a certain time in a sample which contains the specific analyte. Then the ISFET is removed from the sample solution and the ion-step response is recorded in a specific measurement set-up and compared with the ion-step response before incubation.

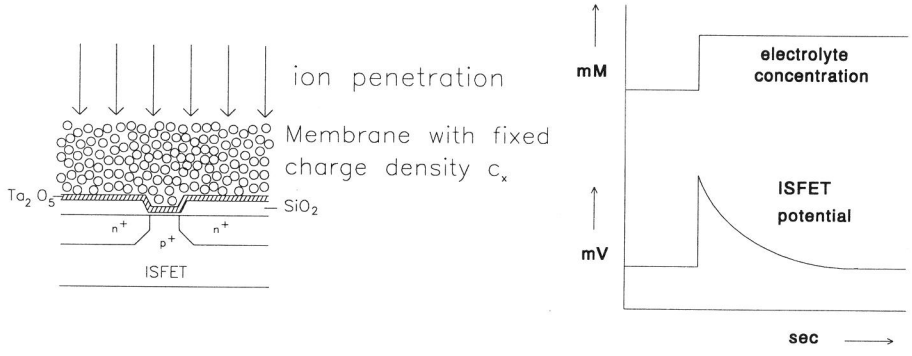

Fig.3.1 The ion-step measuring method

In this chapter, the ion-step measuring method is described in more detail. The chapter can be divided in two parts. In the first part, section 3.2, the ion-step

response of a membrane-covered ISFET is described. The different processes in the membrane, which take place after an ion-step, will be explained in more detail and some typical experimental results will be presented. From these experimental results it is concluded that the ISFET cannot simply be considered as an ideal transducer for these dynamic measurements, but also shows a response to an ion-step.

This dynamic behaviour of the ISFET itself is further explained in section 3.3 which forms the second part of this chapter. It will be shown that the mechanism which describes the ion-step response of the ISFET gate oxide is in fact similar to the mechanism describing the ion-step response of a charged membrane. The understanding of this dynamic behaviour of the ISFET leads to new possibilities for the ion-step measuring method. The role of the charged membrane might be fulfilled by the surface charge of the oxide itself.

PART A

3.2 The origin of the ion-step response of a membrane covered ISFET

3.2.1 Introduction

In this part, the transient ion-step response of a membrane-covered ISFET will be described. The porous membrane contains a fixed, homogeneously distributed negative charge. The ISFET is considered as an ideal transducer, measuring an oxide-surface potential which is at any time only dependent on the pH at the membrane-ISFET interface. Because the surface potential of the ISFET is measured with respect to a reference electrode in the bulk solution, possible potentials at the membrane-solution interface are also detected by the ISFET.

To interpret the ion-step responses of an ISFET with a membrane, Schasfoort used the Teorell-Meyer-Sievers (TMS) theory [2]. This theory describes the steady state conditions of a charged membrane between two solutions with different ion-concentrations. The total TMS membrane potential consists therefore of two Donnan potentials (see chapter 1) at the membrane solution interfaces, and a diffusion potential inside the membrane as a result of the unequal mobility of cations and anions. Schasfoort interpreted the measured transient ion-step responses as diffusion potentials, whereas the contribution of the Donnan potentials were believed to be negligible. However, a more detailed study of the ion-step responses by J. Eijkel showed that Schasfoort misinterpreted the measured results. It appeared that

diffusion potentials do not play a significant role and that the origin of the transient ion-step response is a changing Donnan potential followed by a release or uptake of protons as will be described in the following [3].

To elucidate the exact mechanism of the ion-step responses, Eijkel did not use the static TMS-theory but developed a dynamic simulation model for the transient responses [3]. The model consists of the Nernst-Planck flux equations and the Poisson-Boltzmann equations for several variables in the solution phase as well as in the membrane phase. Since a pH-sensitive ISFET is used as transducer, also the pH in the membrane, together with all factors influencing it, is incorporated in the model. The variables which are considered in the solution phase and in the membrane phase, are the concentrations of the water ions OH^- and H_3O^+, the concentration of the ion-step ions, usually K^+ and Cl^- or NO_3^-, and the electrical field and the electrical potential. In the membrane phase also the concentration of the fixed charge groups are considered which might be protonated or deprotonated. All variables are considered as functions of both time and place.

With this model Eijkel has been able to interpret the measured ion-step responses and to describe the essential mechanisms. The different mechanisms will be briefly described in the next two subsections. First a situation is considered where the fixed charge in the membrane does not interact with the mobile protons in the membrane. Subsequently, the situation is described where the fixed charge consists of mildly acidic groups which do interact with the mobile protons via the proton association equilibrium constant.

3.2.2 Contribution of the changing Donnan potential at the membrane-solution interface

Assume an ISFET with a membrane with a negative fixed charge density c_x of -40 mM, which is in equilibrium in a solution of 10 mM KCl at pH 7. The charged groups do not interact with the mobile protons in the membrane. In chapter 1 it has been explained that in this case a Donnan potential ϕ_D exists at the membrane-solution interface which is given by:

$$\phi_D = \phi_m - \phi_e = \frac{RT}{F} \ln r_D = \frac{RT}{F} \ln \frac{a_{K^+,e}}{a_{K^+,m}} = \frac{RT}{F} \ln \frac{a_{Cl^-,m}}{a_{Cl^-,e}} \qquad (3.1)$$

where the subscripts m and e refer to respectively the membrane and the solution (electrolyte) phase.

By considering the electroneutrality condition in the bulk solution as well as in the membrane with fixed charge density c_x (including its sign) and assuming that activities equal concentrations:

$$c_{K^+,e} - c_{Cl^-,e} = 0 \qquad \text{and} \qquad c_{K^+,m} - c_{Cl^-,m} + c_x = 0 \tag{3.2}$$

and defining $c_{K^+,e} = c_{Cl^-,e} = c_e$, the Donnan potential ϕ_D can also be written as (assuming concentrations equal to activities):

$$\phi_D = \frac{RT}{F} \ln r_D = \frac{RT}{F} \ln \frac{\sqrt{4c_e^2 + c_x^2} + c_x}{2c_e} \tag{3.3}$$

Equation 3.3 shows that the Donnan potential is thus a function of the fixed charge density in the membrane and the electrolyte concentration. For the assumed values of c_x and c_e (resp. -40 and 10 mM) the Donnan ratio r_D is 0.236 and the corresponding potential ϕ_D is -37.1 mV (at 298 K).

The protons (and OH^--ions) are however also distributed according to the Donnan ratio (eq.3.1), resulting in a pH difference between the membrane and the solution. In chapter 1 it has already been shown that this pH difference is equal to log r_D (eq.1.6). When using an ISFET with a (Nernstian) sensitivity of -59.2 mV/pH, the ISFET response to this pH difference is 37.1 mV. The Donnan potential at the membrane solution interface is therefore exactly compensated by the ISFET response to the pH difference between solution and membrane.

Now assume a stepwise increase in the electrolyte concentration c_e from 10 to 50 mM KCl (ion-step). The Donnan ratio for an electrolyte concentration c_e of 50 mM and a fixed charge density c_x of -40 mM is 0.677 which corresponds with a potential ϕ_D of -10.0 mV (eq.3.3). This means that as a response to an ion-step from 10 to 50 mM KCl, the ions in the membrane will redistribute according to the new Donnan ratio. This redistribution will start in the double layer at the membrane solution interface, which follows almost instantly on the concentration step. As a result, the potential across this interface changes from -37.1 to -10.0 which means that also the potential which is measured by the ISFET (with respect to the bulk solution) increases with 27.1 mV. However, simultaneously to this process, protons will diffuse out of the membrane because the new Donnan ratio r_D is higher than the old ratio, and the proton concentration at the surface of the ISFET will decrease, which causes the surface potential to decrease until equilibrium is reached again.

In the new equilibrium situation, the Donnan potential at the membrane-solution interface is -10.0 mV and the difference in pH between the membrane and the solution results in an ISFET response of +10.0 mV. The measured surface potential of the ISFET with respect to the reference electrode in the bulk is therefore the same as before the ion-step. The time constant of the decaying part of the ion-step response is determined by the diffusion of the protons away from the ISFET (or the diffusion of OH^- ions towards the ISFET surface). By simulating a proton

mobility in the membrane which has a value of about 0.4 times the mobility in an aqueous solution, the best fit with the experimental results was obtained [3].

The amount of protons (per unit of volume) that is transported as a response to an ion-step from 10 to 50 mM (the so-called Donnan amount, ΔH^+_{Don}) is simply given by:

$$\Delta H^+_{Don} = \left(c_{H^+,50} - c_{H^+,10}\right)_m = c_{H^+,e}\left(\frac{1}{r_{D,50}} - \frac{1}{r_{D,10}}\right) \tag{3.4}$$

where $c_{H^+,50}$ and $c_{H^+,10}$ are the proton concentrations in the membrane for c_e=50 and 10 mM respectively, $c_{H^+,e}$ the proton concentration in the solution and $r_{D,50}$ and $r_{D,10}$ the Donnan ratios in 50 and 10 mM electrolyte concentration respectively.

As a response to a stepwise change in the ion-concentration from 10 to 50 mM, the amplitude of the transient response will equal the theoretical maximum, ΔV_{max}, which is equal to the difference in the Donnan potentials at the membrane-solution interface before and after the ion-step. This theoretical maximum is given by:

$$\Delta V_{max} = \phi_{Don,50} - \phi_{Don,10} = \frac{RT}{F}\ln\left(\frac{r_{D,50}}{r_{D,10}}\right) \tag{3.5}$$

However, in practice the change in the ion-concentration will not be an ideal step but more likely an exponential increase with a certain rise time. This means that the diffusion of protons away from the ISFET surface might already take place while the increase in ion-concentration (the ion-step) is not completed yet. In other words, there is insufficient separation between the two processes. The result will be a transient response with an amplitude which is lower than the theoretical maximum.

3.2.3 Contribution of a proton release from acidic groups in the membrane

In the example as described above, a fixed charge density in the membrane is assumed without taking into account possible interactions of these charged groups with the protons in the membrane phase. However, in practical applications, the fixed charge in the membrane will consist of acidic or basic groups capable of exchanging protons. Therefore the possible proton-association reactions in the membrane must be taken into account.

If a membrane is considered with a fixed concentration of acidic HA-groups with a proton dissociation constant K_a, the dissociation equation is given by:

$$K_a = \frac{c_{A^-} \cdot c_{H^+,m}}{c_{AH}} \qquad \text{or after rearranging:}$$

$$c_{A^-} = \frac{c_{tot} K_a}{K_a + c_{H^+,m}} = \frac{c_{tot} K_a}{K_a + \frac{1}{r_D} c_{H^+,e}} \tag{3.6}$$

where c_{A^-} is the concentration of dissociated AH groups, c_{tot} the sum of dissociated and undissociated AH groups ($c_{tot}=c_{A^-}+c_{AH}$) and $c_{H^+,m}$ and $c_{H^+,e}$ the proton concentration in the membrane and in the solution respectively. It is obvious from eq.3.6 that the degree of dissociation, corresponding with c_{A^-}, depends on the Donnan ratio r_D and on the proton concentration in the solution. The Donnan ratio r_D is given by eq.3.3 where the fixed charge density is now the concentration of dissociated groups c_{A^-}, and c_e the ion-concentration in the solution.

$$r_D = \frac{\sqrt{4c_e^2 + c_{A^-}^2} - c_{A^-}}{2c_e} \tag{3.7}$$

For a negative fixed charge, the value of the Donnan ratio r_D can vary between 0 and 1. This means that the existence of a Donnan potential results in less dissociated AH groups in comparison with the situation where no Donnan potential is present (according to eq.3.6). In other words, the dissociation of AH groups, corresponding with c_{A^-}, is suppressed by a Donnan potential. The suppression is stronger in a low electrolyte concentration, due to a high Donnan potential, than in a high electrolyte concentration.

Eijkel has calculated proton titration curves by using eqs.3.6 and 3.7 of three membranes each with c_{tot}=40 mM but with different values of pK_a (pK_a =-2, 0.7 and 4). The pK_a values are chosen because strongly acidic groups have a pK_a of -2, while sulphate groups, which are responsible for the surface charge of polystyrene beads, have a pK_a of about 0.7 and carboxyl groups, which are very common amino-acid side- and end-chain groups, have a pK_a of about 4. The proton titration curves are calculated for two different values of the electrolyte concentration c_e (10 and 50 mM, 1:1 salt) and are plotted in fig.3.2.

Fig.3.2 shows that the difference between the titration curves for c_e=10 mM and c_e=50 mM, is the largest for the acid with pK_a=4. In this case, the suppression of the dissociation by the Donnan potential for c_e=10 mM is the strongest. The difference between the two curves for pK_a=4, Δc_{A^-}, is also plotted in fig.3.2. For the acid groups with pK_a=-2, the curves for both salt concentrations coincide. No

Donnan potential is developed in the titration region, because of the high proton concentration in the electrolyte. For the acid groups with pK_a=0.7, the titration curves only differ for pH values higher than 0.5.

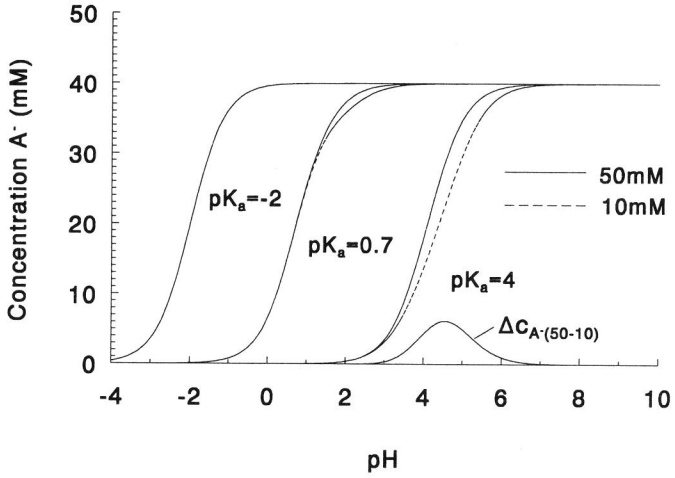

Fig.3.2 Calculated titration curves of three different membranes containing acidic groups with a pK_a of -2, 0.7 and 4 respectively, *for two different electrolyte concentrations [3].*

In the previous subsection it has been shown that as a response to an ion-step (for a negatively charged membrane), protons diffuse out of the membrane, because of a redistribution of protons according to a changed Donnan ratio. However, if the membrane contains proton associating AH groups, the mobile protons in the membrane are in equilibrium with these groups according to eq.3.6. If mobile protons diffuse out of the membrane, a certain amount of bound protons will be released by the AH groups (depending on the pK_a). This means that the total amount of protons that has to be transported, as a result of an ion-step, can be much larger than the Donnan amount (eq.3.4).

The amount of released protons ΔH^+_{rel} as a response to an ion-step of 10 to 50 mM in a membrane with a volume of V_m, can be calculated by using eq.3.6 and calculating the difference in c_{A^-} before and after the ion-step.

$$\Delta H^+_{rel} = V_m \Delta c_{A^-} = V_m \left(\frac{c_{tot} K_a}{K_a + \frac{1}{r_{D,50}} c_{H^+,e}} - \frac{c_{tot} K_a}{K_a + \frac{1}{r_{D,10}} c_{H^+,e}} \right) \tag{3.8}$$

where V_m is the membrane volume and $r_{D,50}$ and $r_{D,10}$ refer to the Donnan ratios for c_e=50 and c_e=10 mM respectively. For the case of an ion-step from 10 to 50 mM at pH 7 and a membrane of 1 dm^3 containing 40 mM AH groups with a pK_a of 4 (c_{tot}=40 mM), this amount is given in fig.3.2 as function of the pH (curve Δc_{A^-}). For this membrane, it can be calculated that the amount of released protons ΔH^+_{rel} is 400 times larger than the Donnan amount ΔH^+_{Don} [3]. However, if the acidic groups have a pK_a of 0.7 or -2, the amount of released protons is negligible in comparison with the Donnan amount (at pH 7).

Fig.3.3 shows the simulated ion-step responses (10 to 50 mM, pH 7) of three ISFETs with membranes containing 40 mM acidic groups with a pK_a of -2, 0.7 and 4 [3]. The ion-step was simulated by a description of the electrolyte concentration at the membrane-solution interface as function of the time, which followed from a model of a specific flow-through system. This function approaches an exponential increase with a rise time of about 1 sec. As can be seen in fig.3.3, the initial potential rise is identical for all three devices. This is caused by an increase of the Donnan potential at the membrane-solution interface. The theoretical extreme of this potential increase is equal to the difference in the Donnan potentials at the membrane-solution interface before and directly after the ion-step (eq.3.5), assuming that the concentration of dissociated groups (c_{A^-}) is not changed yet and equal to the value at c_e=10 mM.

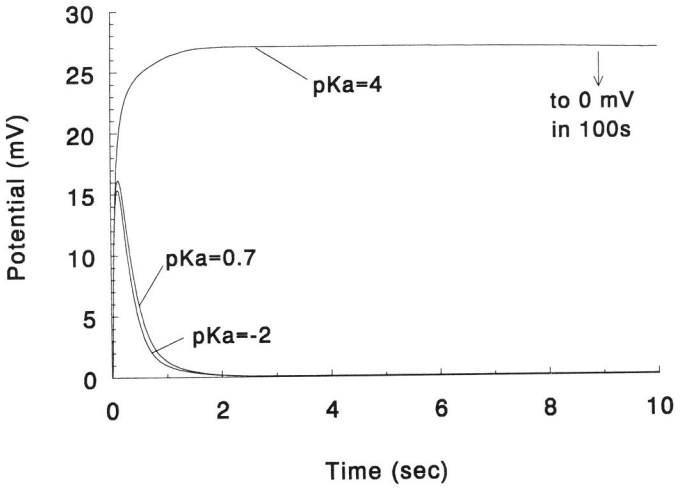

Fig.3.3. Simulated responses of an ion-step from 10 to 50 mM at pH 7, of three different ISFETs with membranes (8 μm) containing 40 mM acidic groups with a pK_a of -2, 0.7 and 4 respectively [3].

The return to zero of the measured potential, occurs with a different slope for the different membranes. As mentioned before, this process is determined by the diffusion of protons out of the membrane, and the diffusion of OH^- ions into the membrane. Fig.3.3 shows that the return to equilibrium is about the same for the membranes with the groups having a pK_a of -2 or 0.7 but is much slower in the case of the membrane with the groups having a pK_a of 4. This can fully be explained by the amount of protons that has to be transported. In the case of the membranes with pK_a of -2 or 0.7, only the Donnan amount of protons has to be transported because the released amount of protons is negligible. The return to equilibrium is relatively fast and the theoretical maximum amplitude is not reached because the change of the Donnan potential at the membrane-solution interface and the diffusion of protons from the ISFET surface partly coincide. In the case of the membrane with pK_a=4, the released amount is 400 times the Donnan amount and therefore it takes much longer to return to the equilibrium situation. The potential reaches the theoretical maximum and within the 10 seconds which are shown in the figure, the proton concentration at the membrane-ISFET interface hardly changes. It will take about 100 seconds before the potential is returned to zero.

The pH of the solution will influence the transport of protons and OH^- ions by determining both the Donnan and the released amounts. Eijkel has shown that the amount of mobile H^+ and OH^- ions in the negatively charged membrane which was used as example, is minimal at pH 7.4 [3]. Below pH 6.9, protons are the main transporting ions, and above pH 7.9 OH^- ions. Consequently, the flux of H^+ and OH^- ions will be minimal around pH 7.4. The exact minimum flux will however occur at a pH higher than 7.4 because protons are more mobile than OH^- ions. This means that the chance that the proton concentration at the ISFET surface already changes before the ion-step is completed, is minimal around pH 7.4. In other words, the chance of reaching the theoretical maximum amplitude for these membranes is maximal around pH 7.4.

In a practical application (e.g. proteins), the fixed charge in the membrane will consist of several types of acidic or basic groups, all with different pK_a values. In this case the intrinsic buffer capacity of the membrane can be used to describe the total contribution of all different groups to the charge density. The intrinsic buffer capacity of the membrane is defined as the change of the total negative fixed charge per change of the pH in the membrane.

To calculate the amount of released protons in a membrane with intrinsic buffer capacity β, Eijkel derived an equation which describes the change in the equilibrium total fixed charge concentration, $c_{x,tot}$, as a result of a change in the ion-concentration in the solution [3].

$$\frac{\delta \Delta H_{rel}^{+}}{\delta c_e} = \frac{-\delta c_{x,tot}}{\delta c_e} = \frac{-c_{x,tot}}{c_e} \frac{1}{\frac{2.3\sqrt{(4c_e)^2 + (c_{x,tot})^2}}{\beta} + 1} \qquad (3.9)$$

The change in the total fixed charge concentration, which results from an ion-step is equal to minus the amount of released protons. This amount is calculated by integration of eq.3.9, and therefore depends on the buffer capacity β and the square root term. In most cases β will be much smaller than the square root term, which means that the fixed charge concentration will change with an amount proportional to β. If the buffer capacity is zero, the fixed charge will not change at all and there will be no proton release. In this case only the Donnan amount of protons is transported. If β is much larger than the square root term, the fixed charge will change with the same factor as the change in c_e. In that case there will be no change in r_D and the Donnan potential at the membrane-solution interface will remain constant, as follows from eq.3.3. No change in the Donnan potential means that there is no Donnan amount of protons that has to be transported and the ion-step response will only be determined by the released amount of protons.

3.2.4 A double-layer model of the charged membrane

In the description of the charged membrane in subsections 3.2.2 and 3.2.3, the charged groups were considered to be homogeneously distributed in the membrane. The Donnan theory was used to describe the membranes and in this Donnan model, an electrical double layer only exists at the membrane-solution interface. However, the membranes which are actually used with the ion-step measuring method, consist of polystyrene beads in an agarose gel. The charged groups are not homogeneously distributed but are concentrated on the surface of the beads. Charged surfaces are usually described by a double-layer theory, and Eijkel has described the implication of using a double-layer model for the ion-step responses of a charged membrane [3].

The double-layer model of the membrane consists of many particles (assume a diameter of 0.1 μm), which are impenetrable for solution and carry a surface charge. Electrical double layers exist around each particle and because the dimensions of the membrane pores are of the same order as the double layers around the particles, double layers exist throughout the membrane pores. The potential which is measured by the underlying ISFET, with respect to the bulk potential, is on one hand determined by the mean pore potential, which is the net result of the contribution of all surface potentials of the charged particles, and on the other hand by the pH at the membrane-ISFET interface. The measured ISFET

response in equilibrium is therefore the same as of an ISFET without a membrane, because the distribution of the protons between the membrane and solution results in a pH difference, which compensates the mean membrane potential (this is the same mechanism as in the Donnan model). The relation between the surface charge on the particles σ (C/cm^2) and the surface potential ψ of each particle is given by:

$$\sigma = C_{dl}\psi \tag{3.10}$$

where C_{dl} is the double-layer capacitance (F/cm^2).

First, assume that the surface charge on the membrane particles does not interact with the mobile protons (no proton release or uptake). An ion-step will result in an increase in the double-layer capacitances of the particles and consequently in a decrease of the surface potentials ψ, because the charge densities remain constant. The ISFET will measure a transient change in the mean pore potential. As a result of the potential changes, an ion redistribution will take place and the equilibrium situation is re-established. The theoretical maximum ion-step response is the change in the mean pore potential. This is comparable with the Donnan model where the theoretical maximum is determined by the change in the Donnan potential at the membrane solution interface.

If the surface groups at the particles are mildly acidic or basic, the change in surface potential after an ion-step additionally results in a release or uptake of protons, depending on the pK_a of the groups. In this case the theoretical maximum of an ion-step response will not be determined by the change in the mean pore potential but by the change in the surface potentials at the particles, which will change more then the mean pore potential [3]. The buffer capacity of the surfaces is much higher than the mean buffer capacity of the pores, and therefore the release or uptake of protons resulting from the change in surface potential, will now fully determine the pH in the membrane pores, which is measured by the underlying ISFET.

Eijkel found that using the double-layer model, measured amplitudes of ion-step responses better matched calculated values than using a Donnan model. Especially when larger beads are used (up to 1 μm), which actually have been used in the research project described in this thesis, the double-layer model seems to be more realistic.

3.2.5 Experimental

Materials

Agarose (low IEE, zero M_r) was purchased from Biorad and the different suspensions of polystyrene beads (2.5% solids-Latex) from Polysciences Inc. Protamine sulphate (grade X, from salmon) and glutaraldehyde (grade 1), were products of Sigma. PBS solutions were made by dissolving PBS tablets (product of Sigma) in water.

Measurement set-up

The measurement set-up for the ion-step measurements with membrane-covered ISFETs consists of a computer-controlled flow through system in which a peristaltic pump ensures a flow of 2.7 ml/min. The ISFET is mounted in a wall-jet cell in which the liquid flow is perpendicular to the ISFET surface. A cross-section of the wall-jet cell is shown in fig.3.4. A saturated calomel electrode, placed downstream, is used to define the potential of the solution. Two bottles containing the two ion-step solutions are connected via valves to the measurement cell in such a way that the electrolyte concentration at the ISFET surface can be increased with a rise time (to 90% of the final value) of about 200 ms.

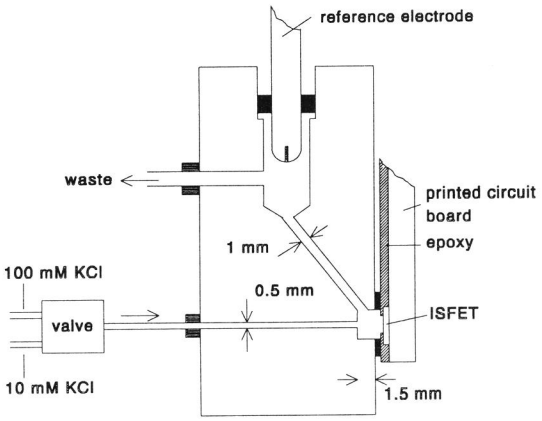

Fig.3.4 Cross-section of the wall-jet cell.

The ISFETs are connected to a source-drain follower and the output of this amplifier is connected to a Nicolet 310 digital oscilloscope, which has the ability to store recorded curves on a floppy disk. The data can then be modified on a PC using the software package Vu-Point. For presentation purposes, the curves can be

filtered with a software low-pass filter using a cut-off frequency of 40 Hz for elimination of the 50 Hz main supply interference which has a top-top amplitude of typically 0.2 mV.

Measurement devices

ISFETs with a Ta_2O_5 gate insulator were fabricated in the MESA cleanroom laboratory following the usual ISFET processing steps [4]. The ISFETs showed a response of about -58 mV/pH. The ISFET chips were mounted on a piece of printed circuit board and encapsulated with Hysol epoxy. Around the gate a circular area with a diameter of 2.5 mm and a depth of about 150 μm was left uncovered. The membranes were made by 1:1 mixing and ultrasonication of a 0.25% agarose solution with a suspension of polystyrene beads at 40-50°C and subsequently casting portions of 3 μl on top of the gate area of the ISFETs. After overnight drying at 4°C and a temperature step of 55°C, during one hour, membranes with a thickness of about 10-15 μm (in dry condition) resulted.

Protamine was immobilized in the membrane by physical adsorption or by covalent binding. In the case of immobilization by physical adsorption, ISFETs with membranes were exposed to a solution of 0.1 mg/ml protamine sulphate in phosphate buffered saline (PBS) at pH 7.4 for about 16 hours. In the case of immobilization by covalent binding, polystyrene beads with functional amino groups were washed in a buffer solution and subsequently the amino groups were activated by 8% glutaraldehyde in PBS at pH 7.4. Next, the beads were washed again and exposed to a solution of 0.25 mg/ml protamine sulphate in PBS for 4-5 hours. After washing, the beads were used to make membranes.

3.2.6 Results and discussion

Fig.3.5 shows a typical response of an ISFET with a membrane of 0.12 μm polystyrene beads with immobilized protamine (by physical adsorption) to an ion-step of 10 to 50 mM KCl at pH 7.3. The solutions were buffered with 0.2 mM HEPES. The ion-step response is a negative transient signal, corresponding with a changing Donnan potential (or surface potential of the beads) followed by a proton uptake by the protamine molecules in the membrane causing a temporary pH increase in the membrane. However, in the first decreasing part of the response, the potential shows a small temporary increase, indicated in the figure by an arrow, which is characteristic for these types of membranes. This small increase is the result of the response of the underlying ISFET gate oxide to an ion-step, as will be discussed later.

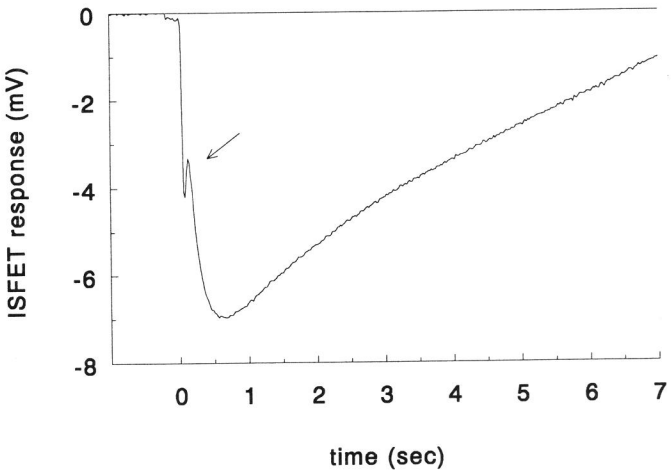

Fig.3.5 Typical ion-step response (10 to 50 mM KCl, pH 7.3) of an ISFET with a membrane of 0.12 μm beads with immobilized protamine

Fig.3.6 shows a typical response of an ISFET with a membrane of 1.0 μm polystyrene beads with immobilized protamine (covalently coupled via glutaraldehyde) on an ion-step of 10 to 50 mM KCl at pH 7.3. Both solutions were again buffered with 0.2 mM HEPES. The response is again a negative transient caused by a proton uptake of the protamine. However, the small increase in the potential in the beginning of the response, as in the case of the membrane with the 0.1 μm beads, is now a significant positive peak. This peak is the result of the ion-step response of the underlying ISFET, which apparently can not be considered as an ideal transducer for these dynamic measurements.

The interfering response of the ISFET itself seemingly is a positive transient signal. In the second part of this chapter it will be explained that this positive response can be described in the same way as the change in surface potential of the charged particles in the double-layer model of the membrane [5].

In case of the membrane with the 0.1 μm beads, the membrane itself has a potential with respect to the bulk solution. This can be described as a Donnan potential in the Donnan model of the membrane, or as a mean pore potential in the double-layer model. After an ion-step, first the potential at the membrane-solution interface will decrease which is detected by the ISFET. However, when the KCl ions reach the ISFET surface, the ISFET reacts with a positive transient. Apparently this transient is heavily suppressed by the membrane because only a small effect is visible. In case of the membrane with the 1.0 μm beads, there probably exists no potential at the membrane-solution interface, because as a result to an ion-step, the

first effect is the positive ISFET response and not a decreasing membrane potential. The electrical fields of the charged beads do not extend to the pore centres anymore and the mean pore potential is (almost) zero. After the ISFET itself is in equilibrium again, the ISFET measures the temporary increase in the pH caused by a proton uptake by the protamine molecules at the surface of the beads.

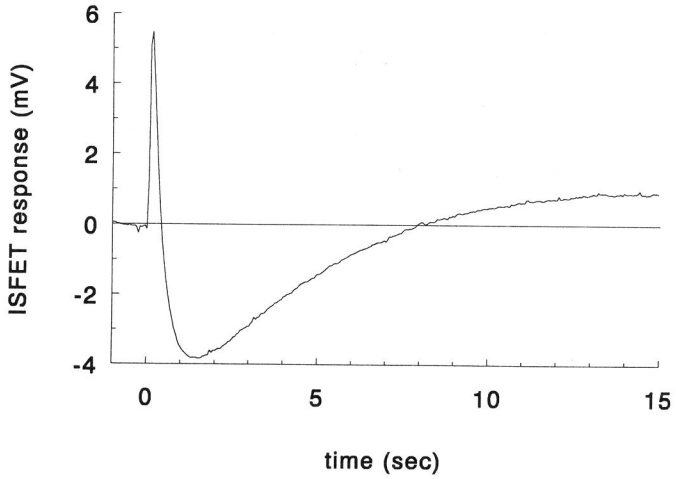

Fig.3.6 Typical ion-step response (10 to 50 mM KCl, pH 7.3) of an ISFET with a membrane of 1.0 μm beads with immobilized protamine

3.2.7 Conclusions

In the previous subsections, the origin of an ion-step response of a charged membrane is described. In a practical application, the charge in the membrane will consist of mildly acidic or basic groups (e.g. proteins). In this case the release or uptake of protons by the membrane groups is the dominating mechanism determining the ion-step responses. The experimental results show that the ISFET cannot simply be considered as an ideal transducer for these dynamic measurements, because the ISFET gate oxide also responds to an ion-step. This interfering ISFET response is more significant in case of a membrane consisting of 1.0 μm beads then in the case of a membrane consisting of 0.1 μm beads. However, for both membrane types the ion-step response of a charged membrane and the response of the underlying ISFET gate oxide are clearly distinguishable in time.

PART B

3.3 The ion-step response of a bare ISFET

3.3.1 Introduction

In the previous section, the ion-step response of a charged membrane deposited on top of a pH-sensitive ISFET is described. From the experimental results it was concluded that also the ISFET gate oxide responds to an ion-step with a transient potential change. It has been mentioned that the mechanism behind this response is the same as the mechanism of the change in surface potential of a charged membrane particle, which has very briefly been described in subsection 3.2.4. In this part of this chapter, the ion-step response of a bare ISFET is described in more detail.

First the operational mechanism of the static pH sensitivity of an ISFET is described in more detail, because this theory is needed to be able to explain the dynamic behaviour of the ISFET. After the subsequent description of the dynamic behaviour, an electrical equivalence model of the ISFET oxide-solution interface is presented, which can be used to explain both the static and dynamic behaviour of the ISFET.

3.3.2 The static pH sensitivity of an ISFET

The model which is nowadays commonly used to describe the oxide-solution interface, and thereby the pH sensitivity of an ISFET, was presented by Bousse in 1982 [6]. This model is based on the site-binding model which is used in colloid chemistry to describe an oxide-solution interface and which was introduced in 1974 by Yates et al. [7]. Very recently, Van Hal and Eijkel have presented a more simple theory to describe the pH sensitivity of ISFETs [8]. This theory is initially based on the site-binding model but is also valid for other models which describe the charging mechanism of an oxide-solution interface. In this subsection, this theory will be used to explain the operational mechanism of an ISFET.

As indicated in chapter 1, the threshold voltage of an ISFET is dependent on the surface potential ψ_0 at the oxide-solution interface which is the result of a charged oxide surface. The mechanism responsible for the oxide surface charge can be described by the site-binding model which describes the equilibrium between amphoteric AOH surface sites and H^+ ions in the solution. The reactions are [7]:

$$AOH \rightleftarrows AO^- + H_s^+ \quad \text{and} \quad AOH_2^+ \rightleftarrows AOH + H_s^+ \tag{3.11}$$

where H_s^+ refers to the protons in the vicinity of the surface. The equilibrium constants of these equations are:

$$K_a = \frac{n_{AO^-} a_{H_s^+}}{n_{AOH}} \quad \text{and} \quad K_b = \frac{n_{AOH} a_{H_s^+}}{n_{AOH_2^+}} \tag{3.12}$$

where n_i is the number of surface i-sites per cm^2 and $a_{H_s^+}$ the dimensionless activity of the protons in the vicinity of the surface.

The total number of surface groups per cm^2 is referred to as N_s:

$$N_s = n_{AOH_2^+} + n_{AO^-} + n_{AOH} \tag{3.13}$$

and the resulting surface charge density σ_o (C/cm^2) can now be calculated by:

$$\sigma_o = q\left(n_{AOH_2^+} - n_{AO^-}\right) \qquad \text{with } q=1.6*10^{-19}C \tag{3.14}$$

Combining eqs. 3.12, 3.13 and 3.14 gives:

$$\sigma_o = qN_s\left(\frac{a_{H_s^+}^2 - K_a K_b}{K_a K_b + K_b a_{H_s^+} + a_{H_s^+}^2}\right) \tag{3.15}$$

The pH at which the surface charge $\sigma_o=0$, is called the point of zero charge, pH_{pzc}.

The relation between the surface charge σ_o and the surface potential ψ_0 is given by:

$$\sigma_o = \psi_0 C_{dl,i} \tag{3.16}$$

where $C_{dl,i}$ is the integral double-layer capacitance (in F/cm^2) which is defined as the ratio of the charge density σ_0 to the potential difference ψ_0.

The integral double-layer capacitance $C_{dl,i}$ can be calculated by using the Gouy-Chapman-Stern model [9]. In this model the double-layer capacitance consists of a series network of a Helmholtz layer capacitance (the Stern capacitance) and a diffuse-layer capacitance. The Helmholtz layer models the effect that the ions in the solution have a finite size and the centres of the ions cannot approach the surface any closer than the ionic radius including a possible water layer which means that there exists a plane of closest approach for the centres of the ions at some distance x_H. The diffuse layer, starting from x_H, is containing the same amount of charge (but with opposite sign) as the oxide surface charge, because the Helmholtz layer is by definition not containing any charge. The charge in the diffuse layer σ_{dl} is given by [9]:

$$\sigma_{dl} = -\left(8kT\epsilon_r\epsilon_0 n^0\right)^{1/2} \sinh\left(\frac{zq\psi_1}{2kT}\right) = -\sigma_o = -C_{dl,i}\psi_0 \tag{3.17}$$

where ψ_1 is the potential at x_H, n^0 the concentration of each ion in the bulk solution in number/litre, and z the valence of the ions. The parameters ε_r, ε_0, k, q and T have their usual meaning.

The difference between the potential ψ_1 at x_H and the surface potential ψ_0, is the potential difference across the Stern capacitance. The Stern capacitance has a value of $\varepsilon_r\varepsilon_0/x_H$ (F/m^2) and is usually assumed to be constant with a value of 20 μF/cm^2 (with $\varepsilon_r \approx 11$ in the Helmholtz layer, and $x_H \approx 5$ Å). The potential ψ_1 can therefore be described by:

$$\psi_1 = \psi_0 - \frac{\sigma_0}{C_{Stern}} = \psi_0 - \frac{\sigma_0 x_H}{\epsilon_r \epsilon_0} \qquad \text{with } C_{Stern} = 20\mu F/cm^2 \qquad (3.18)$$

With eqs. 3.17 and 3.18 it is now possible to calculate the integral double-layer capacitance as a function of ψ_0 and the electrolyte concentration.

Van Hal and Eijkel derived a general expression for the pH sensitivity of an ISFET, defined as the change in the surface potential ψ_0 as a response to a change in the pH of the bulk solution, which is referred to as pH_e ($\delta\psi_0/\delta pH_e$) [8]. This sensitivity is expressed in terms of the chemical intrinsic buffer capacity of the oxide surface and the electrical capacitance of the double layer. The intrinsic buffer capacity β_i of the oxide surface is defined as the change in the net number B of basic groups, as a result of an infinitesimal change in pH_s, which is the pH in the vicinity of the surface. The number B is equal to $B=n_{AO^-} - n_{AOH_2^+}$ and using eqs. 3.14 and 3.15, β_i is given by:

$$\beta_i = \frac{\delta B}{\delta pH_s} = -\frac{1}{q}\frac{\delta \sigma_0}{\delta pH_s} = N_s \frac{K_b a_{H_s^+}^2 + 4K_a K_b a_{H_s^+} + K_a K_b^2}{\left(K_a K_b + K_b a_{H_s^+} + a_{H_s^+}^2\right)^2} 2.3 a_{H_s^+} \qquad (3.19)$$

The ability of the double layer to store charge in response to a small change in the potential $\delta\sigma_0/\delta\psi_0$ is defined as the differential double-layer capacitance, C_{dif}, and can be calculated using eqs. 3.17 and 3.18 [9]:

$$\frac{\delta\sigma_o}{\delta\psi_o} = -\frac{\delta\sigma_{dl}}{\delta\psi_o} = \frac{\left(\frac{2\epsilon_r\epsilon_0 z^2 q^2 n^0}{kT}\right)^{1/2} \cosh\left(\frac{zq\psi_1}{2kT}\right)}{1 + \left(\frac{1}{C_{stern}}\right)\left(\frac{2\epsilon_r\epsilon_0 z^2 q^2 n^0}{kT}\right)^{1/2} \cosh\left(\frac{zq\psi_1}{2kT}\right)} = C_{dif} \qquad (3.20)$$

If the differential capacitance is written as the inverse, it can be clearly seen that the capacitance is made up of two components in series.

$$\frac{1}{C_{dif}} = \frac{1}{C_{Stern}} + \frac{1}{\left(\frac{2\epsilon_r\epsilon_0 z^2 q^2 n^0}{kT}\right)^{\frac{1}{2}} \cosh\left(\frac{zq\psi_1}{2kT}\right)} \qquad (3.21)$$

The change in the surface potential ψ_0 as a response to a change in pH_s, can now simply be derived by combining eqs.3.19 and 3.20 which result in:

$$\frac{\delta\psi_0}{\delta pH_s} = \frac{\delta\psi_0}{\delta\sigma_0}\frac{\delta\sigma_0}{\delta pH_s} = \frac{-q\beta_i}{C_{dif}} \qquad (3.22)$$

The relation between the pH in the bulk solution pH_e and the pH in the vicinity of the surface pH_s is given by the Boltzmann equation which describes the relation between the potential ψ_0 and the difference in the H^+ concentration in the bulk solution $c_{H_e^+}$ and in the vicinity of the surface $c_{H_s^+}$.

$$c_{H_s^+} = c_{H_e^+}\exp\left(\frac{-q\psi_0}{kT}\right) \quad \text{or} \quad (pH_s - pH_e) = \frac{q\psi_0}{2.3kT} \qquad (3.23)$$

The general expression for the pH sensitivity of an ISFET can now be derived by combining eq.3.22 and 3.23:

$$\frac{\delta\psi_0}{\delta pH_e} = -2.3\frac{kT}{q}\alpha \quad \text{with} \quad \alpha = \frac{1}{\frac{2.3kTC_{dif}}{q^2\beta_i} + 1} \qquad (3.24)$$

The parameter α is a dimensionless sensitivity parameter which varies between 0 and 1, depending on the intrinsic buffer capacity β_i of the oxide surface and the differential double-layer capacitance C_{dif}. If α=1, the ISFET has a so-called Nernstian sensitivity of -59.2 mV/pH (at 298K).

Van Hal and Eijkel calculated the sensitivities for ISFETs with an SiO_2, Al_2O_3 or Ta_2O_5 gate oxide [8]. The values for K_a, K_b and N_s were obtained from the literature. It appeared that the intrinsic buffer capacity β_i of the oxide surface is the key parameter which is determining the pH sensitivity. The value of the differential double-layer capacitance is limited to a maximum of 20 $\mu F/cm^2$ by the Stern capacitance. Fig.3.7 shows the calculated intrinsic buffer capacities using eq.3.19 and the values for K_a, K_b and N_s as given in table 3.1. The calculated pH-sensitivities for an electrolyte concentration of 100 mM are shown in fig.3.8 using eqs.3.18, 3.19, 3.20 and 3.24. It is obvious that the Ta_2O_5 ISFET has the largest intrinsic buffer capacity resulting in a calculated sensitivity of -58 mV/pH over the entire pH range.

Table 3.1 Some oxide parameters as found in literature

	pK_a	pK_b	pH_{pzc}	N_s (groups/cm^2)	reference
SiO_2	6	-2	2	$5*10^{14}$	[6]
Al_2O_3	10	6	8	$8*10^{14}$	[6]
Ta_2O_5	4	2	3	$1*10^{15}$	[10]

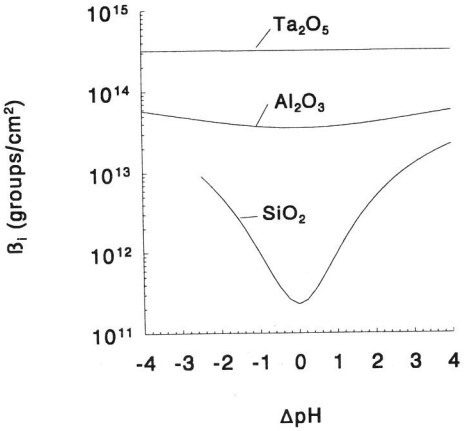

Fig.3.7 Calculated intrinsic buffer capacities β_i for SiO_2, Al_2O_3 and Ta_2O_5 surfaces as function of ΔpH, which is the difference between the pH of the electrolyte and the pH at the point of zero charge of the oxide [8].

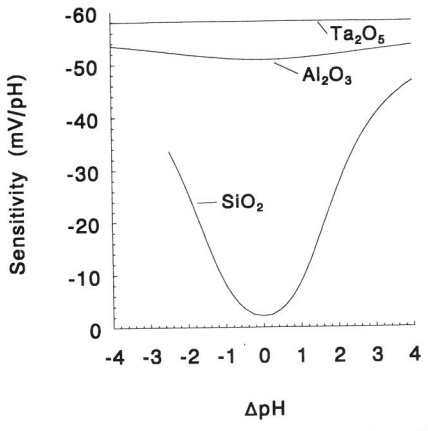

Fig.3.8 Calculated pH sensitivities for SiO_2, Al_2O_3 and Ta_2O_5 ISFETs for an electrolyte concentration of 100 mM as function of ΔpH, which is the difference between the pH of the electrolyte and the pH at point of zero charge of the oxide [8].

3.3.3 The dynamic behaviour of an ISFET after an ion-step

Now the static pH sensitivity of the ISFET has been described, the dynamic behaviour after an ion-step can also be described. To elucidate the mechanism [11] the simulation model, which was developed to simulate ion-step responses of a charged membrane as described in section 3.2, was slightly adapted [3]. The chemical equilibria at the ISFET surface, as described in the previous subsection, were incorporated in the model to describe a Ta_2O_5 ISFET surface (pH_{pzc}=3) together with a stagnant layer of 8 μm in which ion-transport is caused by diffusion only. The ion-step is simulated by a stepwise increase in the electrolyte concentration at the outside of the stagnant layer. Fig.3.9 shows simulations of a Ta_2O_5-ISFET response to an ion-step from 10 to 100 mM KCl at t=0 sec, and

subsequently from 100 to 1000 mM KCl at t=3 sec. The electrolytes all have a pH of 7 and do not contain a buffer. The electrolyte concentration c_e, the (integral) double-layer capacitance C_{dl}, the surface potential ψ_0 and the surface charge density σ_0 are plotted as function of the time. The relation between the last three parameters is given by eq.3.16: $\sigma_0=\psi_0 C_{dl}$.

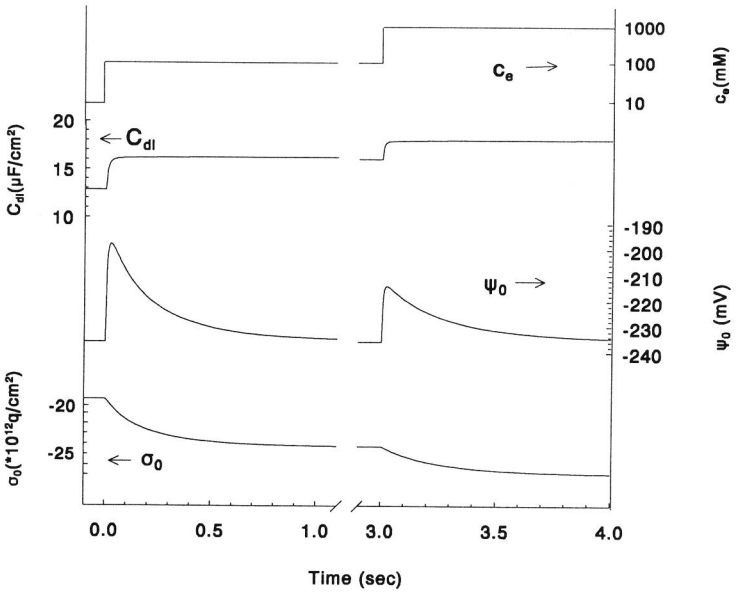

Fig.3.9. Simulated ion-step responses from 10 to 100 mM KCl at t=0 and from 100 to 1000 mM KCl at t=3 sec, of a Ta_2O_5 ISFET at pH 7

In the equilibrium situations of the simulations shown in fig.3.9, t<0, 1<t<3 and t>4 sec., ψ_0 (and thus σ_0/C_{dl}) has the same value. Because a Ta_2O_5 ISFET shows a constant pH sensitivity over the entire pH range, the value of ψ_0 is equal to (pH_e-pH_{pzc}) times the sensitivity, which gives (7-3)*-59=-236 mV. The difference between the simulated values of ψ_0 at 10 mM and 1 M KCl is only 1.5 mV, which indicates that the pH sensitivity should hardly be influenced by the electrolyte concentration. This is in agreement with the theory as described in the previous subsection. The parameter α in eq.3.24 is mainly determined by the buffer capacity β_i of the Ta_2O_5 surface whereas the double-layer capacitance C_{dif}, which changes with the electrolyte concentration together with the integral double-layer capacitance, plays a minor role. The independence of the static pH sensitivity on the electrolyte concentration has also been verified by experimental results [5].

For the non-equilibrium situations directly after an ion-step the mechanism is as follows. After an ion-step, C_{dl} increases very fast due to a sudden increase of the diffuse capacitance. As a result, the surface potential ψ_0 will decrease (become less negative) according to eq.3.16. According to the Boltzmann equation (eq.3.23), the proton concentration in the vicinity of the oxide surface, will tend to decrease because of the decreased ψ_0. However, due to the very large intrinsic buffer capacity of the Ta_2O_5 surface, the surface will dissociate AOH groups to keep the H_s^+ concentration constant. As a result of the dissociation, σ_0 will become more negative and consequently, ψ_0 will increase again (become more negative). When a new equilibrium is reached, σ_0/C_{dl} ($=\psi_0$) has the same value as before the ion-step. The time constant of adapting σ_0 by dissociating AOH groups is determined by the flux of the H^+ ions away from the surface. A larger flux will result in faster responses and a smaller flux in slower responses. Since the proton flux in an aqueous solution (without additional buffer) is minimal at pH 7.12, the ion-step response will have a maximum time constant at this pH. Above pH 7.12, OH^- ions will be the main transporting ions, and below pH 7.12, the protons will be the main transporting ions. If the solution contains an additional amount of buffer (with a relevant pK_a), the buffer molecules and ions will in most cases determine the proton flux. For example, in a solution of 0.1 mM buffer at pH 7, the total concentration of buffer molecules is 1000 times higher than the proton concentration.

The amplitude of the simulated response to the ion-step from 100 to 1000 mM at t=3 sec. is smaller than the amplitude of the response to the ion-step from 10 to 100 mM (at t=0 sec). This is because the change in C_{dl} is smaller at higher ion concentrations, which is caused by the constant Stern capacitance.

If the double-layer capacitance changes from C_{dl1} to C_{dl2}, the theoretical maximum change in ψ_0 ($\Delta\psi_{max}$) directly after the ion-step (assuming σ_0 is not changing yet from $\sigma_{0,1}$ to $\sigma_{0,2}$) is:

$$\Delta\psi_{max} = \frac{\sigma_{0,1}}{C_{dl2}} - \frac{\sigma_{0,1}}{C_{dl1}} = \psi_{0,1}\left(\frac{C_{dl1}}{C_{dl2}} - 1\right) \qquad (3.25)$$

For the example given in fig.3.9, this gives a $\Delta\psi_{max}$ of 49 mV at t=0 and 26 mV at t=3 sec. The simulated values in fig.3.9 are 38 and 22 mV respectively. The reason for this discrepancy is an insufficient time separation of the changes in C_{dl} and σ_0 which is caused by the thickness of the stagnant layer. The oxide surface is already dissociating protons, thereby changing σ_0, before the ion-step is completed. Sufficient separation can only be realized if a smaller stagnant layer is assumed, which is not realistic. Therefore, submaximal responses are to be expected in experiments. The chance of reaching the theoretical maximum is maximal if the flux of protons is minimal.

3.3.4 An electrical model of the oxide-solution interface

In this subsection an electrical model of the oxide-solution interface will be presented, which can be used to explain the static pH sensitivity as well as the dynamic behaviour of the ISFET after an ion-step [3]. Fig.3.10 shows in a schematic way the ISFET gate oxide-solution interface together with equivalent electrical components. In front of the oxide surface and the electrical double layer, a stagnant layer is defined in which ion-transport is caused by diffusion only. The stagnant layer is connected to the bulk solution in which the concentrations are assumed to be constant and change instantaneously at an ion-step.

In fig.3.11 an electrical equivalence model of fig.3.10 is shown. The voltage source u, corresponding with the pH difference between the bulk solution and the pH at the point of zero charge of the oxide surface, is converted by the network $C_1/C_2/R_p$ to the surface potential ψ_0. Capacitor C_1 corresponds with the intrinsic buffer capacity of the oxide surface, capacitor C_2 with the electrical double-layer capacitance and resistor R_p is the reciprocal of the proton and OH^- conductivity of the stagnant layer. Note that in this model only protons and OH^- ions are considered because these are the potential-determining ions. The proton currents flowing through the stagnant layer will not create a significant diffusion potential across the stagnant layer due to the background electrolyte concentration of at least 10 mM KCl.

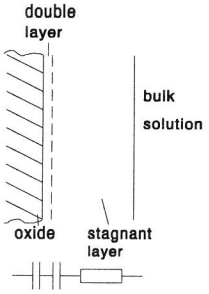

Fig.3.10 Schematic presentation of the ISFET oxide-solution interface.

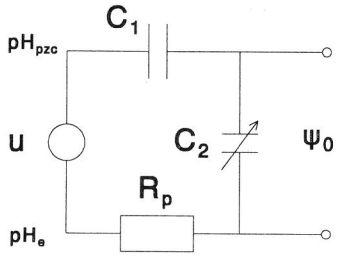

Fig.3.11 Electrical model of the ISFET oxide-solution interface

The voltage source u of the network is the electrical potential difference corresponding with a difference between the bulk pH and the pH at the point of zero charge of the ISFET given by the Boltzmann equation:

$$u = (pH_{pzc} - pH_e)2.3\frac{RT}{F} \qquad [V] \qquad (3.26)$$

Capacitor C_1 is the electrical equivalence of the intrinsic buffer capacity β_i, and is equal to (using eq.3.19 and the Boltzmann equation):

$$C_1 = \beta_i \frac{F^2}{2.3RT} \qquad [F/m^2] \tag{3.27}$$

The value of capacitor C_2 equals the integral electrical double-layer capacitance:

$$C_2 = C_{dl,i} \qquad [F/m^2] \tag{3.28}$$

The value of the resistor R_p is the reciprocal of the proton and OH^- conductivities in the stagnant layer. Assuming a potential difference $\delta\psi/\delta x$ over the stagnant layer, and thus over R_p, the corresponding current density j_p of H^+ and OH^- ions is:

$$j_p = F\left(c_{H^+} U_{H^+} + c_{OH^-} U_{OH^-}\right) \frac{\delta\psi}{\delta x} \qquad [A/m^2] \tag{3.29}$$

where c_i the concentration of ion i and U_i the mobility of ion i. The specific proton conductance χ follows from Ohms law:

$$\chi = F\left(c_{H^+} U_{H^+} + c_{OH^-} U_{OH^-}\right) \qquad [\Omega^{-1}m^{-1}] \tag{3.30}$$

The relation between the mobility and the diffusion coefficient of ion i is given by the Nernst-Einstein èquation:

$$U_i = \frac{F}{RT} D_i \qquad [m^2 s^{-1} V^{-1}] \tag{3.31}$$

Combination of eqs. 3.30 and 3.31 gives the following expression for the specific proton resistance ρ_p:

$$\rho_p = \frac{RT}{F^2} \frac{1}{\left(c_{H^+} D_{H^+} + c_{OH^-} D_{OH^-}\right)} \qquad [\Omega m] \tag{3.32}$$

The proton resistance R_p of a stagnant layer with a thickness Δx and an area of one square meter is now given by:

$$R_p = \frac{RT}{F^2} \frac{\Delta x}{\left(c_{H^+} D_{H^+} + c_{OH^-} D_{OH^-}\right)} \qquad [\Omega m^2] \tag{3.33}$$

If the solution contains a certain amount of buffer BH with a certain pK_B, the proton resistance decreases and is given by:

$$R_p = \frac{RT}{F^2} \frac{\Delta x}{\left(c_{H^+} D_{H^+} + c_{OH^-} D_{OH^-} + \text{buf. term}\right)} \qquad [\Omega m^2] \tag{3.34}$$

The buffer term is a function of the concentration and diffusion coefficients of the

dissociated and undissociated buffer molecules and the pK_B of the buffer.

Now assume a Ta_2O_5-ISFET (pH_{pzc}=3) in thermodynamical equilibrium at pH 7. The potential source u is now equal to -236 mV. The value of C_1 can be calculated by taking the value for β_i from fig.3.7 ($3.25*10^{19}$ groups/m^2) which results in a value of 202 F/m^2. The value of C_2 (the double-layer capacitance) is constant and determined by the electrolyte concentration but will always be smaller than 0.2 F/m^2 due to the constant Stern capacitance. In an equilibrium situation, no proton current will flow and the potential ψ_0 is given by:

$$\psi_0 = u\frac{C_1}{(C_1 + C_2)} \tag{3.35}$$

Due to the very large value of C_1, in comparison with the value of C_2 (C_1/C_2>1000), the potential ψ_0 of a Ta_2O_5-ISFET will always equal the source u, resulting in a Nernstian sensitivity over the entire pH-range, which is not influenced by the electrolyte concentration. This is in agreement with the theory and experimental results. In the case of Al_2O_3 and SiO_2-ISFETs, the value of C_1 is lower and varies with the pH. The potential ψ_0 is now also influenced by the value of C_2 which explains the non-Nernstian behaviour of the Al_2O_3 and SiO_2-ISFETs.

The dynamic behaviour of the ISFET after an ion-step can be simulated in the electrical model by a sudden increase of the value of capacitor C_2. Assume a Ta_2O_5 ISFET to which an ion-step is applied at constant pH 7 (no additional buffer). Due to the increase in C_2, the potential ψ_0 will first decrease (become less negative) followed by a redistribution of charge which causes a temporary proton current through resistor R_p. Assuming a stagnant layer of 8 μm, R_p has a value of $1.5*10^3$ Ωm^2 in equilibrium at pH 7, according to eq.3.33. However, if the oxide is releasing protons, the value of the proton resistance decreases due to the increasing term ($c_{H^+}D_{H^+} + c_{OH^-}D_{OH^-}$). The proton resistance R_p is therefore a potential dependent resistance with a maximum of 1.5 kΩm^2 at pH 7. If an ion-step from 10 to 100 mM is considered at pH 7, the double-layer capacitance changes from 0.128 to 0.161 F/m^2 as is shown in the previous subsections. The transient change of the potential ψ_0 is now determined by the RC time consisting of the proton resistance R_p and the change in double-layer capacitance which is 0.033 F/m^2. This yields a maximum RC time of 49 sec. which will decrease very rapidly because of the decreasing value of R_p.

3.3.5 Experimental

The measurement set-up which was used for the measurement of ion-step responses of bare ISFETs, slightly differed from the set-up described in subsection

3.2.5. The measurement set-up consists of two vessels containing the two ion-step solutions, which are connected to a flow-through system in such a way that the electrolyte in front of the ISFET can be changed with a rise time (to 90% of final value) of about 1 second by switching a valve. Note that the ion-step is applied slower than in the set-up described in section 3.2.5. The two vessels contain solutions of equal pH and different KCl concentration c_{e1} and c_{e2} (without additional buffer) and are continuously purged with nitrogen to prevent CO_2 to dissolve. The pH in each vessel is monitored by a battery-supplied Radiometer pH meter. Two Metrohm burettes are connected to the vessels to adjust the pH with KOH. The ISFET is mounted in a wall-jet cell where the liquid flow is perpendicular to the ISFET surface. The cell is almost identical with the cell which is shown in fig.3.4, but some of the dimensions are slightly different which result in the slower rise time. A peristaltic pump ensures a flow of 2.7 ml/min and a calomel reference electrode, which is placed downstream, defines the potential of the bulk solution. All solutions used were of analytical grade.

Ta_2O_5, SiO_2 and Al_2O_3 ISFETs were made according to the usual ISFET processing steps, and were encapsulated in the same way as described in subsection 3.2.5. The data-acquisition procedure was also the same as described in subsection 3.2.5.

3.3.6 Results and discussion

A typical response of a Ta_2O_5-ISFET to an ion-step from 10 to 50 mM KCl, is shown in fig.3.12, curve 1. In this case the pH was 8.3 (adjusted with KOH), and no buffer was added. The three other curves in fig.3.12 show ion-step responses after addition of respectively 0.1, 0.5 and 1 mM of TRIS buffer to both solutions, while keeping the pH at 8.3. As can be seen, the amplitude as well as the duration of the response become smaller with increasing buffer capacity, which is caused by the decreasing proton resistance R_p. The buffer molecules and ions are fully determining the proton flux at this value of the pH.

In fig.3.13 the amplitudes of ion-step responses from 10 to 100 mM KCl are shown as function of the pH for three different ISFETs with different types of gate oxide. The pH was adjusted with HCl and KOH and no buffer was added. The curves of the Ta_2O_5 and Si_3N_4 ISFETs reach a maximum around pH 8 and only the curve of the Al_2O_3 ISFET intersects the zero axis (around pH 4.2). The Al_2O_3 ISFET which was used for the experiment apparently has a point of zero charge at pH 4.2. In literature, values of 4.8 to 9 have been reported [12]. Although the ion-step measuring method seems to be a very direct method to determine the point of zero charge of a gate oxide of an ISFET, more results of specific experiments are

needed to make a realistic comparison between this measured value of the pH_{pzc} of Al_2O_3 and the values reported in literature. The other ISFETs do not intersect the x-axis and therefore the points of zero charge must be found at lower values of the pH. However, it must be noted that at pH values lower than 3 (and higher than 11), the ion-step response will always be very small because of the high proton flux in the stagnant layer (corresponding with a very low proton resistance R_p in the electrical model).

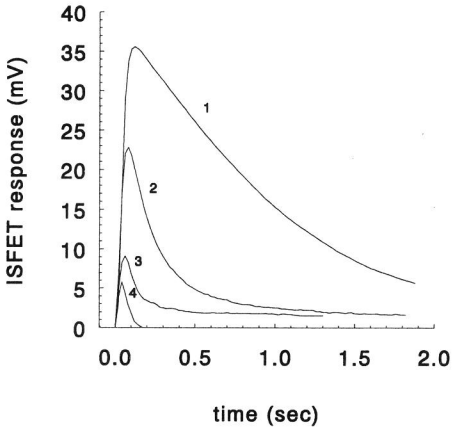

Fig.3.12 Ta_2O_5-ISFET response to an ion-step (10 to 50 mM KCl) at pH 8.3. Curve 1, no buffer added; curve 2, 0.1 mM TRIS; curve 3, 0.5 mM TRIS and curve 4, 1 mM TRIS.

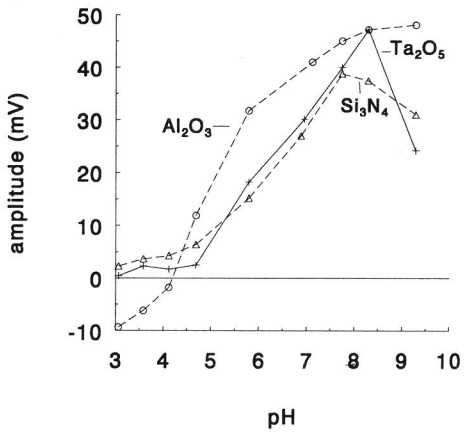

Fig.3.13 Amplitude of ISFET-responses to an ion-step of 10 to 100 mM KCl (no buffer added) as a function of the pH.

If the difference between the pH and the pH_{pzc} increases, the surface potential ψ_0 increases and consequently the amplitude of the ion-step response increases. The amplitude of the ISFET response to an ion-step from 10 to 100 mM KCl has a theoretical limited value of 59 mV (Nernst). The measured amplitude reaches a maximum around pH 7.5 to pH 8 for the Ta_2O_5 and Si_3N_4 ISFETs. Around pH 7 the proton flux is minimal which means that the ratio of the measured amplitude and the theoretical maximum will be maximal. With increasing values of the pH, the surface potential ψ_0 will increases and therefore the theoretical maximum will increase (limited to 59 mV). However, the ratio of the measured amplitude and the theoretical maximum will decrease for pH>8 due to an increasing proton flux, which apparently is a stronger effect because the amplitudes decrease. For the Al_2O_3 ISFET the relative increase in ψ_0 is higher with increasing pH (due to a lower absolute value) which apparently is a stronger effect then the decreasing ratio of the

measured amplitude and the theoretical maximum for pH>8.

To determine the dependence on the absolute electrolyte concentration, ion-step responses of a Ta_2O_5-ISFET were recorded using different electrolyte concentrations c_{e1} and c_{e2} while keeping the step ratio constant at 5 ($c_{e2} = 5*c_{e1}$). In fig.3.14 the amplitude of the ion-step response is plotted as function of the initial concentration c_{e1}. The amplitude of the ISFET responses decreases with increasing concentration, which was also observed in the simulations and expected from the theory because the change in the double-layer capacitance decreases with increasing electrolyte concentration due to the constant Stern capacitance.

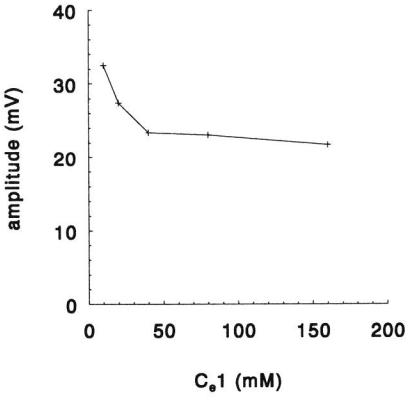

Fig.3.14 Amplitude of a Ta_2O_5-ISFET response to an ion-step from c_{e1} to $5*c_{e1}$ as function of c_{e1}.

3.3.7 Conclusions

In part B of this chapter, the dynamic behaviour of a bare ISFET (ISFET without a membrane) after a step-wise increase in the electrolyte concentration (the ion-step) has been explained. The theoretical maximum amplitude of the response is dependent on the surface charge density of the ISFET gate oxide and the change in the double-layer capacitance. Because in the practical measurement set-up the ion concentration at the ISFET surface does not change in an ideal step-wise way, the change in concentration and the resulting adaptation of the surface charge might partly coincide, which results in an amplitude that does not reach the theoretical maximum. The time constant of the re-establishment of equilibrium, is determined by the proton flux in the stagnant layer in front of the ISFET. At pH 7 (no buffer), the amount of transporting ions reaches a minimum and therefore, the time constant reaches a maximum. This means that the chance of reaching the theoretical

maximum amplitude is maximal at pH 7. If the solutions contain a certain amount of buffer, the buffer molecules and ions will in most cases determine the proton flux in the stagnant layer (eq.3.34) and lower the time constant.

Since the ion-step response of a bare ISFET is determined by the surface charge density of the gate oxide, it is interesting to investigate the possibility of modifying the ISFET surface in such a way that it becomes specific for a certain charged analyte. If the analyte binds to the surface, the ion-step response would change. In chapters 5 and 6, results are presented of different procedures to modify Ta_2O_5 ISFETs in such a way that heparin directly binds to the modified surfaces.

If ISFETs are used in combination with a porous membrane of polystyrene beads, as described in section 3.2, it is inevitable that the ISFET gate oxide also responds to the ion-step which introduces an artefact for the membrane characterization. Only at the point of zero charge, the ISFET response is nihil. The already mentioned possible surface modification might be used to 'tune' the pH_{pzc} of an ISFET to eliminate the interfering ion-step response of the ISFET. Some results of 'tuned' ISFETs with a membrane of polystyrene beads are presented in chapter 5.

The ion-step response of the ISFET gate oxide can also be reduced by ensuring a large proton flux from the ISFET surface as is described in the previous subsections. In a practical application a membrane will have a certain buffer capacity which in most cases is higher than the buffer capacity of the solution. If a dense membrane is used, the buffer capacity directly at the surface of the ISFET will reduce the ion-step response of the gate oxide by ensuring a relatively large proton release or uptake. However, in case of a more porous membrane, the buffer capacity directly at the surface of the ISFET will be smaller, which will give a relatively smaller proton release or uptake. This results in a more significant ISFET response which has also been observed in the experiments presented in section 3.2.5. In general, when using an ISFET under a membrane and when the interfering response of the ISFET gate oxide must be limited, the buffer capacity directly at the oxide surface-membrane interface must be as high as possible. In practice, this means using a dense membrane which is in close contact with the oxide surface.

References

[1] R.B.M. Schasfoort, R.P.H. Kooyman, P. Bergveld, J. Greve, A new approach to ImmunoFET operation, Bios. Bioelectron., 5 (1990), p.103

[2] R.B.M. Schasfoort, P. Bergveld, R.P.H. Kooyman, J. Greve, The ion-step-induced response of membrane-coated ISFETs: theoretical description and experimental verification, Bios. Bioelectron., 6 (1991), p.477

[3] J.C.T. Eijkel, Thesis University of Twente, the Netherlands, in preparation.

[4] P. Bergveld, A. Sibbald, in G. Svehla (ed.), Comprehensive Analytical Chemistry, Vol XXIII, Elsevier, Amsterdam (1988)

[5] P. Bergveld, R.E.G. van Hal, J.C.T. Eijkel, The remarkable similarity between the acid base properties of ISFETs and proteins and the consequences for the design of ISFET biosensors, Submitted to Biosensors and Bioelectronics

[6] L.J. Bousse, The chemical sensitivity of electrolyte/insulator/silicon structures. Thesis University of Twente (1982)

[7] D.E. Yates, S. Levine, T.W. Healy, Site-binding model of the electrical double layer at the oxide/water interface, J. Chem. Soc. Faraday Trans., 70 (1974), 1807-1818

[8] R.E.G. van Hal, J.C.T. Eijkel, P. Bergveld, The pH sensitivity of ISFETs described in terms of buffer capacity and double layer capacitance. Technical digest of the fifth international meeting on Chemical Sensors, Rome, 11-14 July (1994)

[9] A.J. Bard, L.R. Faulkner, Electrochemical methods, fundamentals and applications, John Wiley & Sons, New York (1980), Chapter 12.3.

[10] L.J. Bousse, S. Mostarshed, B.H. van der Schoot, N.F. de Rooij, P. Gimmel, W. Göpel, Zeta potential measurements of Ta_2O_5 and SiO_2 thin films, J. Colloid Interface Sci., 147 (1991) 22-32.

[11] J.C. van Kerkhof, J.C.T. Eijkel, P. Bergveld, ISFET responses on a stepwise change in electrolyte concentration at constant pH, Sensors and Actuators B, 18 (1994) 56-59.

[12] A.S. Wong, Theoretical and experimental studies of cvd aluminium oxide as a pH sensitive dielectric for the back contacts ISFET sensor, PhD Thesis, Case Western Reserve University (1985)

The ISFET-based heparin sensor with a membrane of polystyrene beads

4

4.1 Introduction

In this chapter a heparin sensor is described based on the ion-step measuring method and a membrane of polystyrene beads with immobilized protamine acting as affinity ligand. Binding heparin in the membrane will change the charge density in the membrane, which can be detected by the ion-step response.

Protamine sulphate is clinically used to neutralize heparin and to counteract its anticoagulant effects. The protamines are a family of basic proteins which typically contain 22 arginines out of 32 amino acids (MW ±4000). Because arginine contains a basic functional group with a pK of 12.5, the protamine molecules are highly positively charged at physiological pH values. The three acid functional groups in heparin are fully dissociated at physiological pH values, to yield $-OSO_3^-$, $-NHSO_3^-$ and $-COO^-$ groups, thus resulting in a highly negatively charged heparin molecule. It is found that the interaction of protamine with heparin consists of 1:1 pairing of anionic heparin sites with cationic protamine sites, which provides enough binding energy for a firm and stable complex formation [1]. The use of the positively charged protamine as affinity ligand for the negatively charged heparin will result in a substantial change in charge density in the membrane which is very beneficial when using the ion-step measuring method.

Because of the purely electrostatic nature of the interaction of heparin with protamine, the interaction does not distinguish heparin molecules with high affinity for antithrombin III (AtIII) or factor Xa (fXa) from heparin molecules with low affinity to AtIII or fXa. This means that using protamine as affinity ligand, absolute concentrations of heparin are determined. Since heparin is very heterogeneous (see chapter 2), the best way to express absolute concentrations would be in milligrams per millilitre. However, the heparin which was used in the experiments was a commercial heparin solution for clinical application, and the concentration was defined in anticoagulant activity units per millilitre (U/ml). Consequently, the results of our experiments are also given as function of this concentration. The range which

is of physiological importance for monitoring, and therefore chosen as specification for the heparin sensor, is 0.1-1.0 U/ml.

The protocol which will be used to determine the calibration curve of the sensor response as function of the heparin concentration is as follows:

- Immobilization of the affinity ligand protamine in the membrane.
- Calibration of the device by measuring the response to an ion-step.
- Incubation of the device in a solution with a known heparin concentration for a certain incubation time.
- Determination of the ion-step response.
- Determination of the shift in response with respect to the calibration.
- Repetition of the previous steps for different heparin concentrations using a new device for each heparin concentration.
- Plotting the shift in response as a function of the heparin concentration.

4.2 Materials and methods

The measurement set-up consists of a computer controlled flow-through system in which the pH can be varied by mixing two buffers with variable ratio. The electrolyte concentration at the surface of the membrane-covered ISFET can be changed within 200 msec from a 10 mM KCl to a 50 mM KCl solution by switching a valve. A cross-section of the wall-jet cell which was used, has been shown in fig.3.4. For some of the experiments the 10 mM KCl solution was buffered with a mixture of 0.2 mM citric acid and 0.5 mM TRIS to vary the pH between 4 and 9 while the 50 mM KCl solution was not buffered. Other experiments were performed with 10 and 50 mM KCl solutions which were both buffered with respectively 0.5 and 0.2 mM HEPES (pH 7.55).

The responses of the Ta_2O_5 ISFETs were measured with a source and drain follower [2] and recorded with a Nicolet 310 digital storage oscilloscope.

The membranes were made according to the process described by Schasfoort et al. [3]. A 0.25% agarose solution (low IEE, zero M_r, Biorad) was mixed 1:1 with a suspension of polystyrene beads (2.5% solids-Latex, Polysciences inc.) at 40-50°C and portions of 3 µl were cast on the ISFETs. After overnight drying at 4°C and a temperature step of 55°C (for one hour), membranes with a thickness of about 10-15 µm (in dry condition) resulted. An additional step with respect to the original process, was ultrasonication of the mixture for 1-2 minutes before casting it on the ISFETs. This resulted in more homogeneous membranes as is shown on the SEM photographs in fig.4.1.

Protamine sulphate (grade X, from salmon) was purchased from Sigma and

heparin from Organon Teknika (Thromboliquine®, 5 ml ampoules containing 25000 Units). Protamine was immobilized in the membrane by physical adsorption or by covalent binding. In the case of immobilization by physical adsorption, ISFETs with membranes were exposed to a solution of 0.1 mg/ml protamine sulphate in phosphate buffered saline (PBS) for 1-17 hours. In the case of immobilization by covalent binding, polystyrene beads with functional amino groups were washed in a buffer solution, and subsequently the amino groups were activated by glutaraldehyde. Next, the beads were washed again and exposed to a solution of 0.25 mg/ml protamine sulphate for about 4-5 hours. After washing, the beads were used to make membranes.

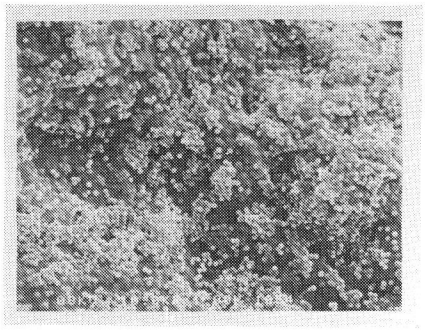

Fig.4.1a SEM photograph of a membrane of 0.12 μm beads without ultrasonication of the membrane mixture.

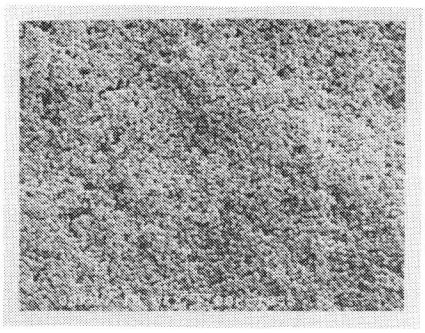

Fig.4.1b SEM photograph of a membrane of 0.12 μm beads after ultrasonication of the membrane mixture.

For the experiments in blood plasma, citrated normal plasma was used which was a gratefully accepted gift from the laboratory of the 'Medisch Spectrum Twente' hospital. Small amounts of the concentrated heparin solution were added to the citrated normal plasma to obtain plasma samples with different heparin concentrations.

4.3 Results

A typical ion-step response of an ISFET provided with a membrane of 0.12 μm polystyrene beads is given in fig.4.2. In this case the 10 mM KCl and the 50 mM KCl solutions were both buffered at pH 7.3. The top curve represents a typical ion-step response of an ISFET with a bare membrane without immobilized proteins. The negative surface charge on the beads (and possibly the agarose) result in a

positive response.

The bottom curve in fig.4.2 represents a typical ion-step response of an ISFET with a membrane (0.12 μm beads) with immobilized protamine. To immobilize the protamine, the device was incubated for 15 hours in 0.1 mg/ml protamine sulphate. The positively charged groups of the protamine result in a net positive charge in the membrane and thus in a negative ion-step response. The small negative peak that precedes the larger response is caused by the interfering ISFET response, as described in chapter 3, section 3.2.6. Experiments showed that already after two hours of incubation in 0.1 mg/ml protamine sulphate, the ion-step response reaches a maximum value indicating that the membrane is saturated with protamine. Yet the reason for incubating the membranes for 15 hours is the experience that protamine which was immobilized by long incubation times did not desorb at all during at least 48 hours, while short incubation times did result in some desorption of the protamine from the polystyrene beads.

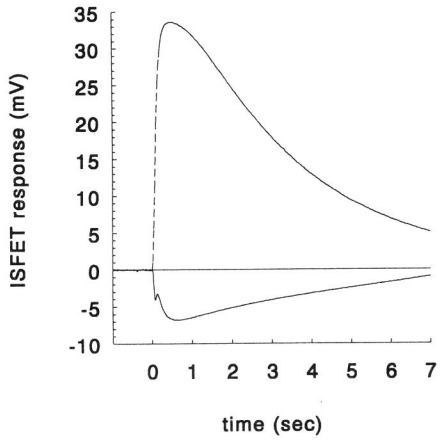

Fig.4.2 Top curve: typical ion-step response of an ISFET with a membrane of 0.12 μm beads without coupled proteins. Bottom curve: typical ion-step response of an ISFET with a membrane of 0.12 μm beads with adsorbed protamine.

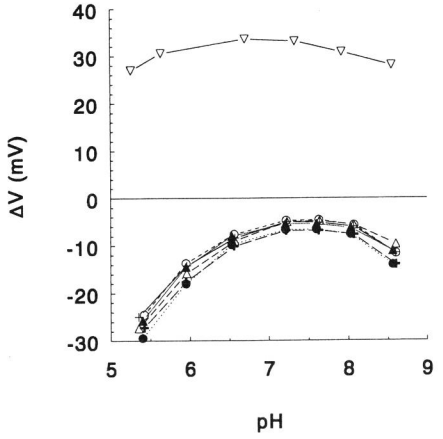

Fig.4.3 Top curve: amplitude ΔV of an ion-step response of an ISFET with a bare membrane as function of the pH. Bottom curves: amplitude ΔV of ion-step responses of six ISFETs with a protamine loaded membrane as function of the pH.

Ion-step responses were also recorded as function of the pH. Fig.4.3 shows the amplitude ΔV of the ion-step response as function of the pH for an ISFET with a bare membrane (upper curve, typical result) and of a series of six ISFETs provided with a protamine loaded membrane (lower curves). The pH of the 10 mM KCl

solution was varied by mixing a citric acid and a TRIS buffer solution. The 50 mM KCl step solution was not buffered (pH ± 5.5) because the transient response of the membrane to an ion-step is much faster then the establishment of the new pH equilibrium in the membrane.

As a result of the dissociation of titratable groups, the charge density in a positively charged membrane should decrease with increasing pH, until the charge density becomes zero at the iso-electric point of the charged membrane and then changes sign. If the ion-step response should only be a function of the charge density, the bottom curves in fig.4.3 should continuously rise with increasing pH and eventually cross the X-axis at the iso-electric point of the membrane. This effect is however not seen. The reason of this deviation might be that because the ion-step response is mainly caused by a release or uptake of protons, which result in a temporary pH change in the membrane, the buffer capacity of the solutions and the membrane also play a very important role. Further experiments did indeed show a different response when using different buffer capacities. More experiments need to be done to determine the exact influence of the buffer capacity and to interpret the shape of the ΔV-pH curves[1]. Up to now we decided that, in order to compare ion-step responses before and after modulation of the charge density in the membrane, the buffer capacity must be kept constant. In a practical application of the sensor, the buffer capacity as well as the pH will be kept constant before and after modulation of the charge in the membrane and only one ion-step response is needed (after calibration) to determine the concentration. The exact shape and nature of the ΔV-pH curve is then of minor importance.

Each of the six ISFETs with protamine-loaded membranes was subsequently immersed in a PBS solution with a different heparin concentration. After 18 and 40 hours of incubation, the ion-step responses were again recorded as a function of the pH. In fig.4.4 the amplitudes of the transient ion-step responses after 40 hours of incubation are shown as a function of the pH. The shape of the ΔV-pH curves doesn't significantly change after incubation in different heparin solutions. It is therefore concluded that the change in the ion-step response as function of the heparin concentration does practically not depend on the pH. In fig.4.5 we have shown the change in the amplitude of the ion-step response at pH 7.4 for the six different ISFETs with respect to the response before incubation in the heparin solutions. The change in the amplitude of the ion-step response is plotted as a

[1] This chapter was published before the ion-step response of bare ISFETs was examined as described in chapter 3. From this investigation it is now known that the ISFET itself also shows a response to an ion-step and that this response can interfere with the membrane response. It was also shown that this response is maximal around pH 7 (in unbuffered solutions) which effect might contribute to the maximum in the curves shown in fig.4.3.

function of the heparin concentration. The curves which are fitted through the points, show a linear relation between the change in response and the heparin concentration in the range 0.1-1.0 U/ml.

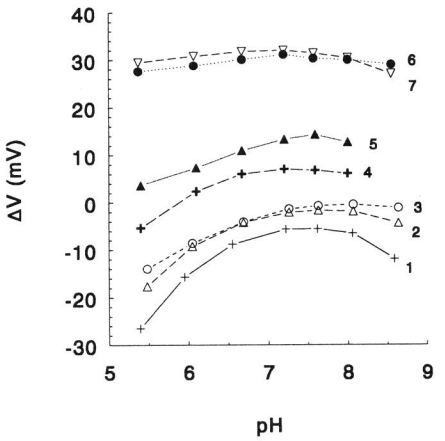

Fig.4.4 Amplitude ΔV of ion-step responses after incubation for 40 hours in heparin as function of the pH. Curve 1 is the average of the six bottom curves of fig.5. Curves 2-7 are recorded after incubation in respectively 0.1, 0.2, 0.4, 0.8, 1.6 and 3.2 U/ml heparin in PBS.

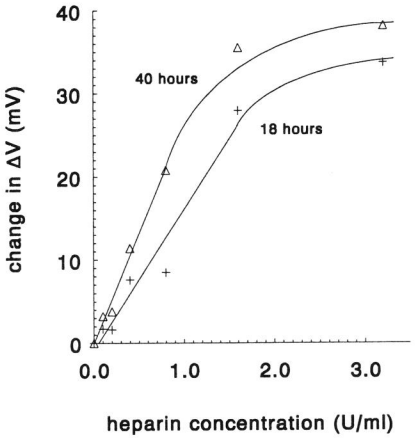

Fig.4.5 Change in amplitude ΔV of the ion-step responses at pH 7.4 as function of the heparin concentration after 18 hours and 40 hours of incubation.

Aiming at a practical application of the sensor, incubation times of 18 or 40 hours are not very auspicious. To determine whether more porous membranes result in shorter incubation times, ISFETs were provided with membranes of three different sizes of polystyrene beads (0.12, 0.43 and 1.14 μm diameter). Protamine was immobilized by physical adsorption after which the response to an ion-step was recorded. Subsequently the devices were immersed in a PBS solution containing 0.5 U/ml heparin and the ion-step response was recorded as a function of the incubation time. Fig.4.6 shows the change in the amplitude of the ion-step response (with respect to the response before incubation in the heparin solution) for the different ISFETs as function of the incubation time (typical result). From this figure it is obvious that larger beads lead to more porous membranes and facilitate the diffusion of heparin into the membrane.

Based on these results we decided to use 1.14 μm beads for a new series of devices and determine the change in the ion-step response as function of the heparin concentration. Protamine was again immobilized by physical adsorption and before

exposing the device to a heparin solution, a calibration ion-step response was recorded. Fig.4.7 shows the change in the amplitude of the ion-step response after 30, 60 and 170 minutes of incubation in the heparin solutions.

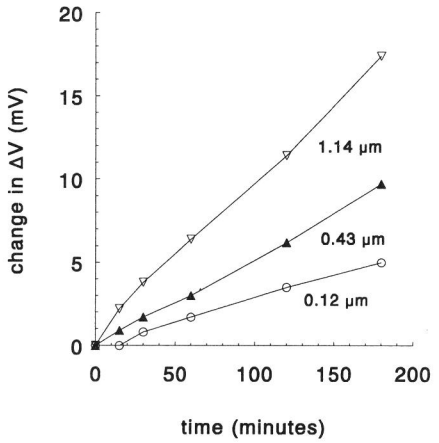

Fig.4.6 Change in amplitude ΔV of ion-step responses of ISFETs with protamine-loaded membranes of different beads as function of the incubation time in 0.5 U/ml heparin.

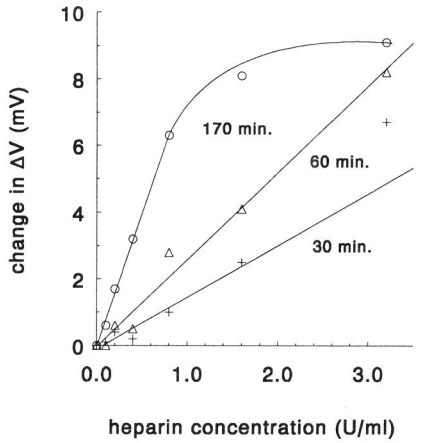

Fig.4.7 Change in amplitude ΔV of ion-step responses of ISFETs with membranes of 1.14 μm polystyrene beads with adsorbed protamine as function of the heparin concentration in PBS after three incubation times.

Another series of six ISFETs was provided with a membrane of 1.0 μm polystyrene beads containing functional amino groups. Protamine was immobilized by covalent binding via glutaraldehyde after which the devices were immersed in different heparin solutions. Fig.4.8 shows the results of this experiment. The same type of devices were used to determine the ion-step response, in blood plasma with different heparin concentrations. In fig.4.9 the change in the amplitude of the ion-step response with respect to the response before incubation, is shown as function of the heparin concentration in blood plasma.

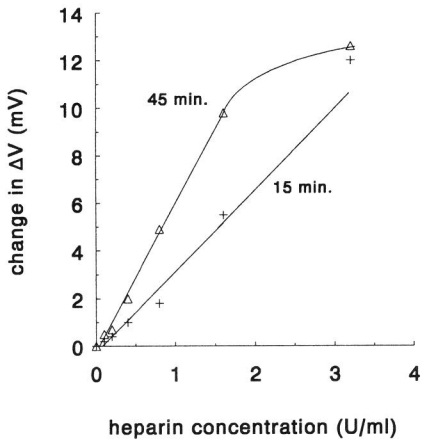

Fig.4.8 Change in amplitude ΔV of ion-step responses of ISFETs with membranes of 1.0 μm polystyrene beads with covalently bound protamine as function of the heparin concentration in PBS after two incubation times.

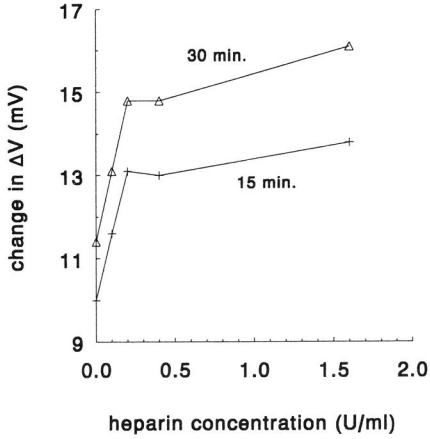

Fig.4.9 Change in amplitude ΔV of ion-step responses of ISFETs with membranes of 1.0 μm polystyrene beads with covalently bound protamine as function of the heparin concentration in blood plasma after two incubation times.

4.4 Discussion and conclusions

The results of the experiments as described in the previous section show that it is possible to determine heparin concentrations with the ion-step measuring method by using protamine as affinity ligand. The relation between the change in the amplitude of the ion-step response and the heparin concentration in PBS can be described as linear in the range 0.1-1.0 U/ml. As described in the previous section, the measurements of the different heparin concentrations were performed with different devices because the ion-step measuring method is a 'single use' method. Due to the fabrication process, the membrane thickness of the different devices varies about 20%. This is the main reason for the individual deviations of the measured heparin concentrations from the fitted curve. Another fabrication process which controls the membrane thickness, for instance spinning the membrane mixture on a wafer of ISFETs, will reduce these deviations. For higher concentrations and longer incubation times, the curves deviate from the linear relation as a result of saturation of the membrane with heparin.

The slope of the response-concentration curve is a function of the incubation time, the bead diameter and the way of immobilization of the protamine. The slope varies from 26 mV/U.ml^{-1} for 0.12 μm beads after 40 hours of incubation to about

3 mV/U.ml^{-1} for 1.0 μm beads after 15 minutes of incubation. The minimum acceptable slope of the response-concentration curve is determined by the specifications for a practical application together with the technical specifications of the measurement system. If we assume that the required accuracy for determining heparin concentrations is 0.05 U/ml and that the ion-step response is reproducible within 0.1 mV, the minimum acceptable slope is 2 mV/U.ml^{-1}.

Immobilization of protamine by covalent binding results (after a certain incubation time) in a larger slope of the response-concentration curve than physical adsorption (see figs. 4.7 and 4.8). Covalent coupling by glutaraldehyde results in protein binding 6-10 atoms from the surface, while coupling by adsorption results in protein binding on the surface. The covalently coupled protamine is therefore better attainable for heparin than the adsorbed protamine.

To increase the response after only 15 minutes of incubation, there are a few parameters that still can be optimized. The use of larger beads will result in more porous membranes which facilitates diffusion of heparin in the membranes. However, larger beads will also give a smaller charge density in the membrane which results in a smaller temporary pH change in the membrane in response to an ion-step. The thickness of the membranes can also be reduced to facilitate diffusion of heparin in the membrane, but this will also result in a smaller ion-step response. More experiments have to be carried out to optimize these two parameters.

The curves in fig.4.9 which represent the results of the measurement in blood plasma show a significant offset caused by nonspecific adsorption of plasma components in the membrane. To reduce nonspecific adsorption it is common practice to block all redundant adsorption sites after coupling the affinity ligand. This is usually done with albumin or small polypeptides. We expect that also in our application, blocking of the adsorption sites will reduce the nonspecific adsorption of plasma components.

The measured relation between the shift in the ion-step response and the heparin concentration in blood plasma is not linear. It is unclear whether this is caused by the nonspecific binding of other plasma components or that it is caused by the binding of plasma proteins to the heparin. More experiments will be necessary to determine the relation between the ion-step response and the heparin concentration in blood plasma.

The results presented in this chapter show the possibility of detecting heparin concentrations of 0.1 U/ml using the ion-step measuring method. It has been reported that 1 Unit of heparin corresponds with about 8 microgram for many commercial preparations [4]. The average molecular weight of the used heparin preparation is about 15000; thus 0.1 U/ml corresponds with $5.3*10^{-8}$ mol/l. This makes the ion-step measuring method a very interesting method for a broad scale

of applications.

References

[1] R.B. Cundall, G.R. Jones, D. Murray, Polyelectrolyte complexes, 3 The interaction between heparin and protamine. Makromol. Chem., 183 (1989) p.849-61.

[2] P. Bergveld, The operation of an ISFET as an electronic device. Sensors and Actuators, 1 (1981), p.17-29.

[3] R.B.M.. Schasfoort, P. Bergveld, R.P.H. Kooyman, J. Greve, A new approach to ImmunoFET operation. Bios. Bioelectron. 5 (1990), p.103-24.

[4] L.B. Jaques, S.W. Wice, L.M. Hierbert, Determination of absolute amounts of heparin and of dextran sulfate in plasma in microgram quantities. J. Lab. Clin. Med., 115 (1990), p.422-32.

Ion-step responses of surface-modified ISFETs

5

5.1 Introduction

In chapter 3 it has been suggested that surface modification of the ISFET gate oxide might be interesting, because the ion-step response of a bare ISFET (which can interfere with the ion-step response of a membrane) is directly related to the oxide surface charge density. Modifying the surface charge density will thus also modify the ion-step response and in this chapter results are presented of experiments with ISFETs with a modified gate oxide surface. The modification which has been investigated is treatment of the Ta_2O_5 gate oxide with an amino-functionalized silane, which results in the introduction of NH_2 groups at the surface. Functional NH_2-groups at the surface might be favourable for several reasons:

- Amino groups are frequently used functional groups for covalent coupling of proteins to the surface. They can be used for covalent coupling of, for instance, protamine as an affinity ligand to bind heparin.
- The point of zero charge, pH_{pzc}, of a Ta_2O_5 ISFET (pH_{pzc}=3) might be 'tuned' to higher values by introducing positively charged amino groups. This option can be useful because at pH_{pzc} the ISFET itself does not respond to an ion-step and the response of an additional layer of proteins or a membrane can then be measured without an interfering ISFET response.
- If the density of the positively charged amino groups is sufficiently high, then the modified surface might directly be used to bind heparin, without using an additional affinity ligand.

In this chapter results are presented of different types of ion-step experiments with different objectives. First, ion-step responses are used to characterize the silylated Ta_2O_5 ISFETs. Then, the sensitivity of the silylated ISFETs to heparin is determined by means of ion-step responses. The amino-functionalized silane is now used as an affinity ligand for binding heparin molecules from a buffer solution as well as from blood plasma. Next, the silylation procedure is used to change the point of zero charge of the Ta_2O_5 ISFET to pH 7, as determined by the ion-step response. On top of these silylated ISFETs, different membranes of polystyrene beads are mounted, as described in chapters 3 and 4. It will be shown that the

measured ion-step response is now fully determined by the membrane because the ISFET itself does not show an ion-step response in this case,.

Before the results are presented, a brief introduction is given on silane coupling agents in general but focused on the used amino-functionalized silane.

5.2 Silane coupling agents

Organofunctional silanes are hybrid organic-inorganic compounds that are used as coupling agent across organic-inorganic interfaces such as organic polymers and mineral substrates [1,2]. The reactions between the inorganic part of a silane coupling agent and the hydrophilic mineral substrate (e.g. a metal oxide) are equilibrium reactions. Bonds are formed and broken in reversible reactions determined by concentrations and equilibrium constants. The organic reactions between the organofunctional group and other organic molecules (e.g. proteins) are determined by thermodynamics and kinetics of different competing reactions. Formation and breaking of these bonds are generally irreversible.

A silane coupling agent may function as a surface modifier or as a primer. When it is used as a surface modifier, the material is used only to chemically modify a surface without forming a layer with any mechanical properties. A primer, however, must have good mechanical film properties to carry the mechanical load, formed by the layer to be attached to the primer. A silane layer used for surface modification usually has a thickness of one or several monolayers, whereas a primer layer can have a thickness up to several micrometers.

A specific class of silane coupling agents is the class of organofunctional alkoxysilanes with the general formula $(OCH_3)_3Si\text{-}RY$. These silanes contain three hydrolysable ethoxy groups and one organofunctional group RY. The three hydrolysable groups are intermediates in the formation of silanol (Si-OH) groups for bonding to mineral surfaces. The RY group is chosen for reactivity or compatibility with the specific organic molecules which are to be coupled. Several of these silanes with different organofunctional groups are commercially available. Some examples of the functional group RY are vinyl, chloropropyl, methacrylate, mercapto and primary amine.

In the following, one specific silane and one specific mineral substrate is considered. The silane is γ-aminopropyltriethoxysilane (APS) and the substrate is Ta_2O_5 which is applied as gate-oxide for the ISFETs, used for the ion-step experiments.

APS in aqueous solutions

APS can be applied to a Ta_2O_5 surface from aqueous solutions, organic solvents or a mixture of an organic solvent and water. First, the reactions of APS with water will be considered. The reaction with the Ta_2O_5 surface and the subsequent formation of an APS layer is considered later.

When in contact with water, APS hydrolyses irreversibly in a two-step reaction. The three ethoxy groups will hydrolyse very fast which results in the formation of silane triols (reaction 5.1). These silane triols have good stability in water at pH 3 to 5, but condense rapidly to siloxanes at a pH of 7 to 9 according to reaction 5.2 [1].

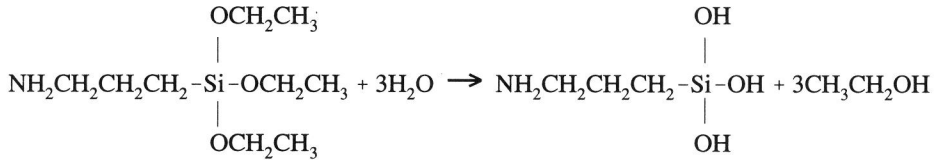

(5.1)

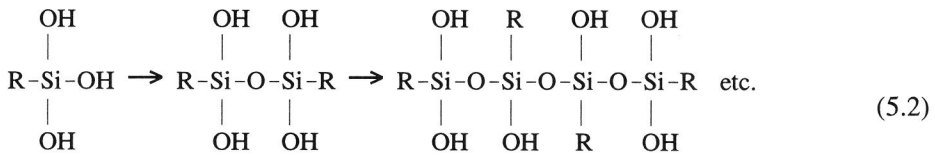

(5.2)

$R = -CH_2CH_2CH_2NH_2$

If APS is hydrolysed in excess acetic acid at pH 4, silane triols are immediately formed and solutions up to concentrations of 50% (by weight) are stable, due to the strong hydrophilic nature of the aminopropyl group. When an aqueous solution of APS is prepared at its natural pH (which is very high, due to the aminogroup), siloxane oligomers will be formed immediately, which retain solubility in water to moderate concentrations. It is assumed that the solutions are an equilibrium mixture of low-molecular-weight siloxanes (oligomers) with silanols, stabilized by hydrogen bonds to aminegroups, forming cyclic cage structures. However, in very diluted aqueous solutions of APS (<1% by weight), a significant amount of monomeric silanetriol will be present. This proportion of monomeric silanetriol increases rapidly with decreasing concentration of APS for concentrations <1% [3]. Other silanes from the class of APS, with other organic functional groups, are not very stable in aqueous solutions because the formation of siloxanes results

within a few hours in a insoluble gel.

Formation of APS layers on Ta_2O_5 surfaces from an aqueous solution

To bind to a Ta_2O_5 surface, silanol groups of a silane triol or a siloxane oligomer, must condense with hydroxyl groups at the oxide surface as is shown in reaction 5.3. It is known that neutral silanes (with a neutral functional organic group), condense very slowly on an oxide surface and may require a catalyst for optimum condensation. Amine functional silanes, like APS, seem to be self-catalytic for surface condensation.

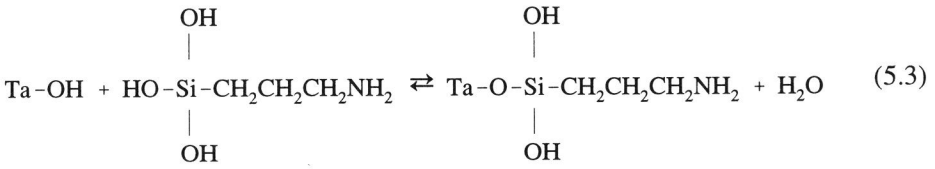

$$Ta\text{-}OH + HO\text{-}Si(OH)\text{-}CH_2CH_2CH_2NH_2 \rightleftarrows Ta\text{-}O\text{-}Si(OH)\text{-}CH_2CH_2CH_2NH_2 + H_2O \qquad (5.3)$$

As mentioned before, the inorganic reaction between APS and a Ta_2O_5 surface (reaction 5.3) is an equilibrium reaction and the oxane bonds between APS and Ta_2O_5 can hydrolyse again depending on the availability of water and the equilibrium constant.

Plueddemann has estimated equilibrium constants for hydrolysis of different coupling agents on silica, schematically presented by reaction 5.4 [4].

$$Si\text{-}O\text{-}Si\text{-}(\text{coupling agent}) + H_2O \rightleftarrows Si\text{-}OH + HO\text{-}Si\text{-}(\text{coupling agent}) \qquad (5.4)$$

For an organofunctional trialkoxysilane (e.g. APS), the estimated value of the equilibrium constant of reaction 5.4 is 10^{-4}. Although there is no firm evidence that silane coupling agents have a similar interaction with metal hydroxide surfaces (such as Ta_2O_5) as with silica, it seems most probable, because almost all metals are found in nature as silicate minerals. Nevertheless, it can be expected that equilibrium constants for hydrolysis of various metal-oxane bonds differ from those of silica-oxane bonds, but the factors that determine such constants are unknown.

The stability with respect to hydrolysis of APS-treated glass was studied by Royer and Liberatore under continuous flow conditions over a pH range of 4 to 9 [5]. They determined the amine concentration, remaining on the surface of commercially available porous glass (550 Å pores and a particle size of 125-177 microns), after pumping 1 liter of aqueous solution through a packed bed at a flow rate of 1 ml/min. At pH 4 about 5% of the amine was lost, at pH 6 about 25% and at pH 8 about 65%. It was concluded that retention of amine function on glass is

poor at any pH above 6. It is known that both acids and bases are powerful catalysts for hydrolysis. However, since the hydrolysis reaction is an equilibrium reaction, only the rate of hydrolysis is affected by the pH but not the point of equilibrium.

A good bond between APS and Ta_2O_5 requires that the equilibrium of reaction 5.3 does not move too far to the left. Conditions favourable for bonding are therefore a maximum initial formation of Ta-oxane bonds and a minimum equilibrium concentration of water at the interface.

Since each silane triol has three silanol groups, they are able to condense with the Ta_2O_5 surface as well as with adjacent molecules. Moreover, aqueous APS solutions already contain low-molecular-weight siloxanes which create a multilayer structure after condensation at the oxide surface. Additional crosslinking in this layer can improve the resistance to water which is favourable for a good bonding according to reaction 5.3. Further crosslinking can be achieved by drying the layer at elevated temperatures to ensure complete condensation in the multilayer itself as well as at the Ta_2O_5 surface. The polysiloxane layer now forms a protection against water which prevents hydrolysis at the Ta_2O_5 surface. Therefore, a multilayer APS coverage is more stable than a monolayer APS coverage.

To accomplish a stable multilayer coverage, aqueous silane baths and silane baths containing a mixture of organic solvent and water, are generally stored for at least a few hours after preparation to ensure the formation of oligomers. After contact with Ta_2O_5, these oligomers will form a polysiloxane layer which can be stabilized by baking the layer. A drawback of baking APS layers at elevated temperatures, is the possible damage to the aminopropyl group. To avoid damaging by peroxide formation, the treated surface could be heated in an inert atmosphere, but this has not yet been demonstrated.

The resulting thickness of an APS film on a Ta_2O_5 surface depends on the availability of water and on the pH (catalyst) and age of the silane solution. Tutas et al. observed that the thickness of an APS film deposited on glass was the same after a minute of contact as after an hour of contact with the aqueous silane bath [6]. However, it is not clear whether the degree of crosslinking, and therefore the mechanical stability of the layer, changes during contact with the silane bath. Normally, surfaces are allowed to contact the silane bath for a few hours.

Formation of APS layers on oxide surfaces from an organic solution

When APS is applied to an oxide surface from water free organic solvents, it is necessary for the APS to migrate to the oxide surface, react with the surface moisture (physically and chemically adsorbed water) and condense on the surface. Because no siloxane oligomers are formed, silylation from a dilute solution of APS in an anhydrous organic solvent will probably lead to thinner layers (a few

monolayers) than silylation from an aqueous solution.

5.3 Materials and methods

Materials

APS (γ-aminopropyltriethoxysilane) was purchased from Sigma, heparin from Organon Teknika (Thromboliquine®, 5 ml ampoules containing 25000 Units) and agarose (low IEE, zero M_r) was a product of Biorad. A 2.5% suspension of 0.12 μm negatively charged polystyrene beads (sulphate groups) in water was purchased from Polysciences, and a 4% suspension of 1.03 μm positively charged polystyrene beads (amidine groups) was purchased from Interfacial Dynamics Corp. (Portland, Oregon). All salt and buffer solutions were of analytical grade. Normal blood plasma was a gratefully accepted gift from the laboratory of the 'Medisch Spectrum Twente' hospital.

Measurement set-up

The measurement set-up used for the experiments described in this chapter, is the same flow-through system as used for the experiments with the membrane covered ISFETs as described in section 3.2.5. However, the flow is now controlled by an effective pressure (0.1 bar) of nitrogen in the two bottles containing the solutions, resulting in a constant flow-rate of 1.3 ml/min. Using an effective pressure instead of a peristaltic pump, reduces the occurrence of small air bubbles in the flow system. The ISFET is mounted in a wall-jet cell in which the liquid flow is perpendicular to the ISFET surface (see fig.3.4). A saturated calomel electrode, placed downstream, is used to define the potential of the solution. Two bottles containing the two ion-step solutions (10 and 100 mM KCl) are via valves connected to the wall-jet cell in such a way that the electrolyte concentration at the ISFET surface can be increased with a rise time (to 90% of the final value) of 200 ms. The 10 mM KCl solution is buffered with 0.5 mM HEPES and the 100 mM KCl solution with 0.2 mM HEPES. In some cases the solutions were both buffered with 0.1 mM phosphate buffer.

The ISFETs are connected to a source-drain follower and the output of this amplifier is connected to a Nicolet 310 digital oscilloscope which has the ability to store recorded curves on a floppy disk. The data can then be modified on a PC with the software package VuPoint. For presentation purposes, the curves can be filtered with a software low-pass filter using a cut-off frequency of 40 Hz for elimination of the 50 Hz main supply interference which has a top-top amplitude of typically 0.2 mV.

Measurement devices

ISFETs with a Ta_2O_5 gate insulator were fabricated in the MESA cleanroom laboratory following the usual ISFET processing steps. The ISFETs showed a response of about -58 mV/pH. The ISFET chips were mounted on a piece of printed circuit board and encapsulated with Hysol epoxy. Around the gate a circular area with a diameter of 2.5 mm and a depth of about 150 μm was left uncovered.

Several methods were used to silylate Ta_2O_5 ISFETs with APS [1,7]. The methods are referred to as method 1 to 8 and are listed below.

Method 1: The ISFETs are immersed in a solution of 2% (v/v) APS in acetone for 3 hours. Subsequently, the ISFETs are rinsed in acetone and dried for 2 hours at 115°C.

Method 2: A 10% (v/v) APS solution in water is adjusted to pH 3-4 with 6 M HCl directly after preparing. The ISFETs are immersed for 2 hours in this solution which is placed in a water bath at 75°C. After this, the ISFETs are rinsed in water and dried for 2 hours at 115°C.

Method 3: The ISFETs are immersed for 3-6 hours in a 10% (v/v) APS solution in toluene. Subsequently, the ISFETs are rinsed in acetone and dried for 2 hours at 115°C.

Method 4: The ISFETs are immersed for 3 hours in a mixture of 19ml methanol, 1 ml water and 100 μl APS which was stored for some time (at least one day) to ensure the formation of oligomers. After rinsing in ethanol, the ISFETs are dried at 115°C for 2 hours or more.

Method 5: The ISFETs are immersed for one hour in a 0.25% (v/v) solution of APS in 50 mM HAc, pH 4. Subsequently the ISFETs are rinsed in water and dried at 115°C for one hour.

Method 6: The ISFETs are immersed for one hour in a 0.25% (v/v) solution of APS in acetone. After rinsing in acetone the ISFETs are dried at 115°C for one hour.

Method 7: The ISFETs are immersed for one hour in a 0.25% (v/v) solution of APS in toluene which is placed in a water bath at 75°C. Afterwards, the ISFETs are rinsed in toluene.

Method 8: The ISFETs are placed in a vessel which is surrounded by an oil bath at 115°C. A nitrogen flow is led through a bottle containing water or through a bottle containing pure APS, and subsequently through the heated vessel which contains the ISFETs. The nitrogen flow enters the vessel through the bottom which consists of sintered glass, and leaves the vessel through the cover. First the nitrogen flow is directed through the bottle containing demi water (for one hour) to ensure a certain degree

of surface moisture at the ISFET surfaces. Then the nitrogen is led through the bottle containing pure APS (at room temperature) for one hour. The nitrogen is transporting APS vapour which can react with the Ta_2O_5 surface of the ISFETs in the heated vessel.

The membranes of polystyrene beads were made by 1:1 mixing and ultrasonication of a 0.25% agarose solution with a 2.5% suspension of polystyrene beads in water at 40-50°C and subsequently casting portions of 3 µl on top of the gate area of the ISFETs. After overnight drying at 4°C and a temperature step of 55°C, during one hour, membranes with a thickness of about 10-15 µm (in dry condition) resulted.

Measurement protocol

Each time the ion-step response had to be determined, 3-5 responses were successively recorded, and the amplitude of the ion-step response was defined as the mean value of these responses. For the determination of heparin concentrations in PBS solutions, small 15 ml vessels were used in which the ISFET was placed for 10 minutes while the solution was not stirred. After incubation the ISFET was rinsed with PBS and mounted in the wall-jet cell of the measurement set-up. The ion-step response was recorded and the change in the amplitude, with respect to the response before incubation, was taken as parameter.

For the measurements in normal plasma, a test-tube containing 2 ml of normal plasma was used to which small amounts of a 100 U/ml heparin solution (in 0.9% NaCl) were added to obtain the different concentrations. The ISFET was incubated in the plasma for 10 minutes (without stirring), rinsed in PBS and subsequently the ion-step response was determined.

5.4 Results and discussion

Characterization of silylated ISFETs by the ion-step response

Fig.5.1 shows a typical ion-step response (10 to 100 mM KCl, pH 7) of an unmodified Ta_2O_5 ISFET (curve 1) and of some different silylated ISFETs (curves 2-4). It is obvious from the figure that the effect of silylation on the ion-step response can be quite different. The ISFETs showing the ion-step responses 2-4, were silylated by method 4 using solutions of different age and after storage of the silylated ISFETs for different times in PBS. Later in this section it will become clear which effects cause the differences between the ion-step responses. The fact that the responses can become negative, indicates that the negative charge of the Ta_2O_5 can

fully be compensated by the positive charge of the APS.

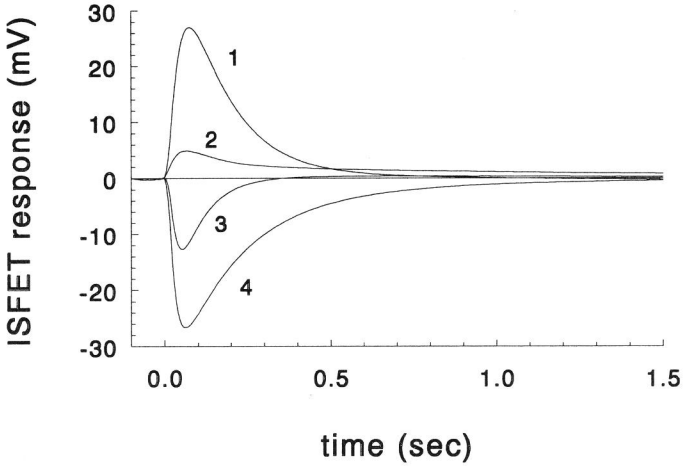

Fig.5.1 Ion-step responses (10 to 100 mM KCl, pH 7) of a bare ISFET (curve 1), and different silylated ISFETs (curves 2-4).

The time constants of the ion-step responses of the different silylated ISFETs are the same as the time constant of the untreated ISFET response. This indicates that the ion-step response of a silylated Ta_2O_5 ISFET can be described in the same way as the ion-step response of a bare ISFET, as described in chapter 3, assuming a different surface charge density σ_0. In other words, the silylation procedure can be seen as a surface modification. Most methods used for silylating Ta_2O_5 ISFETs will result in a multilayer coverage of the oxide as explained in section 5.2. However, if it is assumed that these layers remain relatively thin (<100 nm), the time to reach thermodynamical equilibrium in these layers (e.g. after an ion-step), is very short in comparison with the other time constants of the measuring method. In case of much thicker layers, membrane effects, as described in chapter 3, would become important which certainly would have influence on the time constant of the transient ion-step responses.

To evaluate the different silylation methods, several series of ISFETs (all the same type of Ta_2O_5 ISFETs) were silylated according to the different methods mentioned in the experimental section. After silylation, the response to an ion-step of 10 to 100 mM KCl at pH 7 was recorded. Table 5.1 shows the method of silylation, the number of ISFETs in each series, the moment of measurement and the amplitude range of the ion-step responses of the different ISFETs in each series. The measured amplitudes of the ISFET responses in each series were in most cases

randomly divided in the range determined by the limits given in table 5.1. The differences between the amplitudes of the ion-step responses within one series are very large in some cases and it seems that silylation from an aqueous solution (method 2 and to some extend method 4), results in more variance in the amplitudes than the non-aqueous methods. In an aqueous solution, siloxane oligomers are formed which have several hydroxyl groups by which they can bind to the oxide surface. It may be expected that these oligomers form a layer which shows more variance in the structure and thickness than a layer which is built from much smaller APS-molecules, as is the case in the non-aqueous methods.

Stability of the APS layer with respect to hydrolysis

During the experiments, it was noticed that the ion-step responses changed after the ISFETs were stored in aqueous solutions. This was not unexpected and most likely the result of hydrolysis of the Tantalum-oxane bonds as described in section 5.2. To characterize this hydrolysis, the amplitude of the ion-step response (10 to 100 mM KCl, pH 7) was recorded as a function of storage time in PBS, for different types of silylated ISFETs. Some typical results are shown in fig.5.2. The slowest change in amplitude (curve 3) is observed with APS layers obtained by silylation according to method 4 using a 13 days old silane bath and a drying time of 16 hours at 115°C. A 13 days old silane bath, will have a high concentration of siloxane oligomers which will result in a relative thick layer. The long drying time which was used in this case (16 hours) result in a high degree of condensation and thus cross-linking in the polysiloxane layer. In this way, the layer forms a protection against water which prevents hydrolysis at the Ta_2O_5 surface.

Silylation method 3 also resulted in very stable layers (with respect to hydrolysis in time), comparable with curve 3. In this case APS layers are formed from a 10% APS solution in toluene and dense layers of APS are formed, resulting in large ion-step responses as shown in table 5.1. Since no siloxanes are formed in the water-free toluene, most APS molecules will form oxane bonds with the Ta_2O_5 and a high degree of condensation will be reached. It might be expected that using this method, a relatively thick layer is formed because of the high APS concentration. This highly condensed layer will also protect the interface with the Ta_2O_5 surface against water. A less concentrated solution of APS in toluene, as used in method 7, initially also resulted in very large ion-step responses with comparable amplitudes (see table 5.1), but the ISFETs showed a faster hydrolysis in time (comparable with curve 2 in fig.5.2) in comparison with the ISFETs silylated by method 3. This might be explained by the fact that these layers were not dried at 115°C and that the layers will be thinner, due to the low APS concentration. The layers which were made according to method 1 (2% APS in acetone), also showed

a faster hydrolysis than the layers deposited from APS in toluene by method 3. It is known that acetone contains more water than toluene which can explain the poorer stability of APS layers deposited from acetone, together with the lower concentration of APS which was used in method 1 in comparison with method 3.

Table 5.1 Range of amplitudes of ion-step responses (10 to 100 mM KCl, pH 7) within one series, for different methods of silylation.

method of silylation	number of devices	moment of measurement	amplitudes of ion-step responses (mV)
1	8	direct	-25 to -16
1	11	overnight in pH 7	-20 to -12
1 (dried for 16 hours at 115°C)	8	direct	-45 to -23
2	8	direct	-29 to -3
3	4	direct	-51 to -48
3	5	overnight in pH 7	-48 to -38
4 (1 day)*	10	direct	-20 to -5
4 (1 day)*	15	overnight in pH 7	-5 to +4
4 (3 days)*	19	overnight in pH 5	-32 to -6
4 (3 days)*	20	overnight in pH 7	-20 to +2
4 (4 days)*	14	direct	-30 to -5
4 (4 days)*	14	overnight in pH 7	-23 to -3
4 (5 days)*	8	direct	-30 to -15
4 (5 days)*	10	overnight in pH 5	-27 to -11
4 (10 days)*	7	overnight in pH 7	-39 to +3
4 (13 days, 16 hours at 115°C)*	20	direct	-41 to -22
5	5	direct	-10 to -6
6	5	direct	-25 to -15
7	10	direct	-48 to -38
8	5	direct	-23 to -16

* number of days that the APS/methanol/water mixture was stored before use.

Method 2 resulted in layers which showed a relatively fast hydrolysis as given by curve 1. The other methods yielded layers of which the hydrolysis as function of time, was roughly comparable with curve 2.

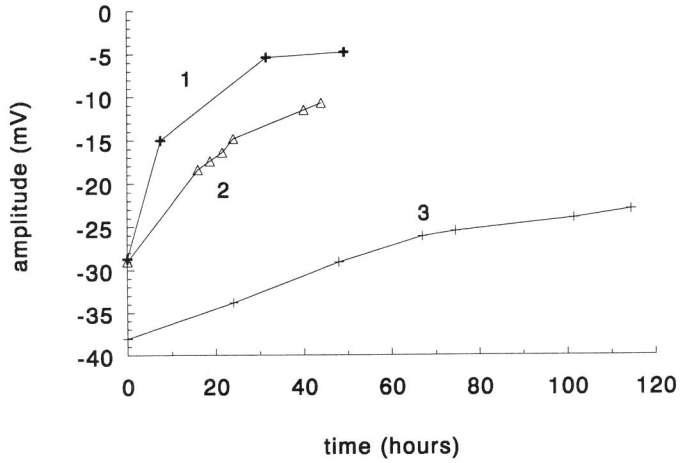

Fig.5.2 Amplitude of ISFET response to ion-step from 10 to 100 mM KCl at pH 7, as function of storage time in a PBS solution. Curve 1: ISFET silylated according to method 2. Curve 2: ISFET silylated according to method 1, also typical result for silylation methods 4 (until 5 days storage of APS solution) to 8. Curve 3: ISFET silylated according to method 4 using a silane bath of 13 days old and a drying time of 16 hours at 115°C, also typical result for silylation method 3.

The hydrolysis of APS layers which were made according to method 4, was found to be dependent on the age of the silane bath. Table 5.2 gives the range of the change in amplitude within each series after one night (about 16 hours) in buffer at pH 7, for ISFETs silylated by method 4 using silane baths of different age. It can be seen that the layers deposited from an older silane bath show a smaller change after one night than layers deposited from a more fresh silane bath. An older silane bath will probably contain more siloxane oligomers resulting in a thicker layer which forms a better protection against water after crosslinking during the baking time.

Table 5.2 Range of the change in ion-step response (10 to 100 mM KCl, pH 7) of ISFETs which are silylated according to method 4, for different ages of the APS/methanol/water mixture.

age of solution	number of devices	range of change in amplitude after overnight storage in buffer at pH 7
1 day	10	min 9, max 15 mV
4 or 5 days	22	min 1.5, max 9 mV

Heparin sensitivity of silylated ISFETs

Since an APS treatment introduces functional amino groups at the surface, it was examined whether or not the APS layers could directly be used as an affinity ligand for binding heparin to the surface. For a stable binding of heparin to the surface, the density of amino groups attainable for heparin must be as high as possible. When heparin is bound to the surface, the charge of the heparin molecules must at least compensate a substantial part of the APS charge, before it can be detected by a change in the ion-step response.

ISFETs which were silylated according to method 3, did not show a different ion-step response after incubation in a heparin solution. Increasing the heparin concentration up to 5000 U/ml did not change the ion-step response. Also silylation method 4, using a silane bath of 13 days old and a drying time of 16 hours at 115°C, was not successful in this regard. A possible explanation might be that the structure of these layers result in a density of surface NH_2-groups, attainable for heparin, which is not sufficient to firmly bind heparin molecules. The ion-step responses of these ISFETs do indicate highly positively charged surfaces (see table 5.1), but a significant number of these amino groups might not be accessible for heparin molecules because they are enclosed in the polysiloxane layer. Another possibility is that the amount of bound heparin does not significantly change the total charge density which is determined by the ion-step response.

Using the other silylation methods, including method 4 using shorter drying times and more fresh baths, did result in some kind of sensitivity towards heparin. After incubation in a heparin solution, ion-step responses with smaller (negative) amplitudes were obtained, indicating a decrease in positive charge density at the surface, caused by the binding of negatively charged heparin molecules. In some cases, the ion-step responses even changed from a negative transient into a positive transient.

To test whether different silylated ISFETs of one series showed a comparable sensitivity to heparin, several ISFETs of one series, silylated by method 4, were

incubated in the same buffer solution containing a specific heparin concentration. Before incubation, the ISFETs all showed very different initial responses after silylation and additional storage in a buffer solution. Table 5.3 shows the amplitudes of the ion-step responses (10 to 100 mM KCl, pH 7) of two series of silylated ISFETs (all Ta_2O_5 ISFETs silylated by method 4, in a 5 days-old bath) before and after incubation in a heparin solution. The only difference between the two series is that the ISFETs are incubated in different heparin concentrations. The error which is given for each value of the amplitude indicates the range of the amplitude of the 3-5 responses which are successively recorded each time the ion-step response has been determined, as described in the measurement protocol. Although the initial responses of the ISFETs are very different, the changes in the responses after incubation in a heparin solution are almost the same, taking into account the error. The last ISFET of the second series mentioned in table 5.3 is an exception, because the change in the amplitude of the ion-step response is much larger than for the other ISFETs within that series.

Table 5.3 Change in amplitude of ion-step responses of two series of silylated ISFETs (method 4, 5 days) after incubation for 10 min. in 0.4 or 0.5 U/ml heparin in PBS.

initial response of silylated ISFET (mV)	response after 10 min. in 0.4 U/ml heparin (mV)	change in response (mV)
-5.3 ± 0.2	-2.1 ± 0.2	3.2 ± 0.4
+12.4 ± 0.1	+16.0 ± 0.7	3.6 ± 0.8
-12.1 ± 0.2	-7.6 ± 0.2	4.5 ± 0.4
+2.1 ± 0.2	+7.1 ± 0.2	5.0 ± 0.4
+12.6 ± 0.1	+17.9 ± 0.2	5.3 ±0.3
initial response of silylated ISFET (mV)	response after 10 min. in 0.5 U/ml heparin (mV)	change in response (mV)
-17.2 ± 0.4	-12.1 ± 0.3	5.1 ± 0.7
-23.4 ± 0.3	-19.5 ± 0.2	3.9 ± 0.5
+1.0 ± 0.1	+5.8 ± 0.4	4.8 ± 0.5
-6.8 ± 0.3	-2.3 ± 0.2	4.5 ± 0.5
-2.0 ± 0.2	+7.1 ± 0.2	9.1 ± 0.4

The results of table 5.3 show that the change in the ion-step response after incubation in a heparin solution is comparable for most devices, although the

silylated ISFETs seem to have very different net surface charge densities. Because of the relatively short incubation time, no equilibrium will be reached and the amount of heparin which binds to the surface will be determined by diffusion of the heparin towards the surface (solution is not stirred). This might explain why the bound amount of heparin is about the same for the different surfaces, even if the surfaces have different initial charge densities. Another plausible explanation is that the density of NH_2 groups attainable for heparin is about the same for the different silylated ISFETs of table 5.3. The significant differences in the initial responses might be explained by a different thickness of the APS layers resulting in a different amount of NH_2 groups in the polysiloxane layer which are not attainable for heparin.

The next step was to examine whether the ISFETs showed different changes in ion-step response after incubation in different heparin concentrations. Fig.5.3a shows the change in the amplitude of the ion-step response (10 to 100 mM KCl, pH 7) as a result of incubation of silylated ISFETs (according to method 1) as a function of the heparin concentration in PBS. The incubation time during which the ISFETs were exposed to the heparin solutions was 10 minutes. The error bars indicate the variance in the values of the amplitude of the 3-5 responses which were recorded each time. Each measurement shown in the figure was carried out with a different silylated ISFET; the ISFETs were only used once.

Fig.5.3b shows the change in amplitude of ion-step responses of ISFETs which were silylated according to method 2, as a function of the heparin concentration in PBS. The two curves correspond with the change in ion-step response after 10 and 30 minutes of incubation. Again, for each different concentration, a different ISFET was used. Note that the slope of the fitted curve recorded after 10 minutes of incubation, is much lower than in fig.5.3a. Apparently, these ISFETs show a smaller sensitivity to heparin, resulting in a smaller slope, than the silylated ISFETS used for fig.5.3a. The structure of the layer seemingly has a strong influence on the heparin sensitivity.

In fig.5.3c the results are presented of ISFETs silylated according to method 4, using a silane bath of 5 days old and a drying time of 2 hours at 115°C. Each measurement was again carried out with a different ISFET from the same series.

It is obvious from figs.5.3a and 5.3b that not all measurements match the fitted curve within the error of the measurements. This can be explained by the fact that the individual silylated ISFETs, which were used to determine the different heparin concentrations, will have slightly different heparin sensitivities as also follows from the results of table 5.3. In fig.5.3c, the match with the fitted curve is better, which might mean that the difference in heparin sensitivity between individual ISFETs is larger in case of silylation methods 1 and 2 than in case of

method 4. It must be mentioned however that also with silylated ISFETs according to method 4, other experiments were performed which resulted in less better fits than shown in fig.5.3c, which is not unexpected considering the results of table 5.3.

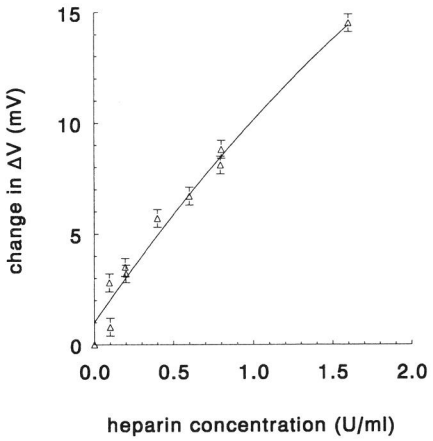

Fig.5.3a Change in amplitude ΔV, of ion-step response (10 to 100 mM KCl, pH 7) of silylated ISFETs (method 1) after 10 min. of incubation, as function of heparin concentration in PBS. Each measurement was carried out with another device.

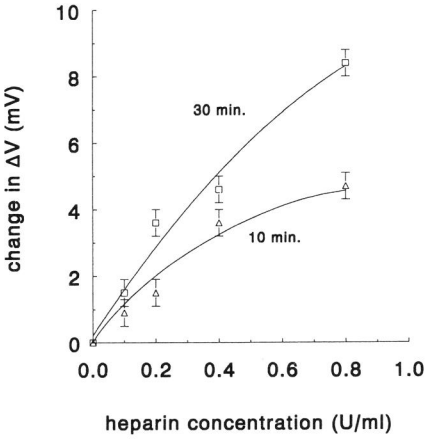

Fig.5.3b Change in amplitude ΔV, of ion-step response (10 to 100 mM KCl, pH 7) of silylated ISFETs (method 2) after 10 and 30 min. of incubation, as function of heparin concentration in PBS. Each measurement was carried out with another device.

All the curves representing the change in the amplitude of the ion-step response as function of the heparin concentration, show a linear relation for low concentrations and a deviation of the linear relation with a decreasing slope for higher concentrations. This behaviour indicates a saturation effect at higher concentrations.

ISFETs which were silylated according to methods 5-8 did show a change in ion-step response after incubation in a heparin solution, but the relation to the heparin concentration was not reproducible. It seemed that the binding of heparin to the APS layers was not very strong because bound heparin could partly be removed, simply by extensive stirring in a buffer solution. Especially when the ISFET was incubated in a relatively high heparin concentration (>0.7 U/ml), the results were not reproducible. Apparently, the density of surface NH_2 groups attainable for heparin, was not sufficient to firmly bind heparin molecules in these cases.

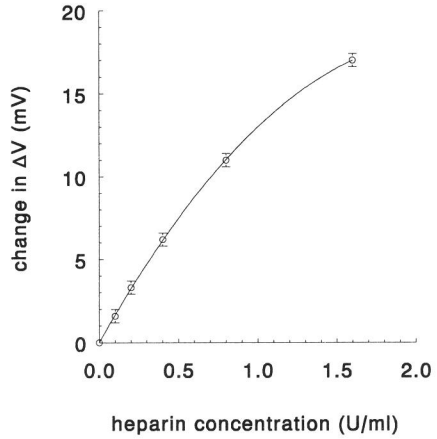

Fig.5.3c Change in amplitude ΔV, of ion-step response (10 to 100 mM KCl, pH 7) of silylated ISFETs (method 4, silane bath of 5 days, drying time 2 hours at 115°C) after 10 min. of incubation, as function of heparin concentration in PBS. Each measurement was carried out with another device.

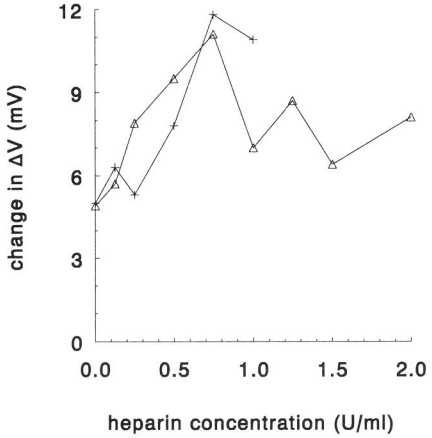

Fig.5.4 Change in amplitude ΔV, of ion-step response (10 to 100 mM KCl, pH 7) of silylated ISFETs (method 4, silane bath of 5 days, drying time 2 hours at 115°C) after 10 min. of incubation, as function of heparin concentration in blood plasma. Each measurement was carried out with another device.

The same type of silylated ISFETs as used in the experiments presented in fig.5.3c, were used to determine the change in ion-step response after incubation in blood plasma samples containing different concentrations of heparin. The results were, however, not very reproducible and no clear relation between the change in ion-step response and the heparin concentration could be determined. Some typical results of two series of ISFETs are shown in fig.5.4. Again, for each measurements another ISFET was used. The results suggest a non-specific binding (in case of a heparin concentration of 0 U/ml), which results in a change in amplitude of the ion-step response of 5 mV. Although the presence of heparin seems to result in an increase in the change in ion-step response, no clear relation between the change in ion-step response and the heparin concentration could be determined. This might be caused by the non-specific binding which results in a random number of bound molecules of different charge.

Silylation of Ta_2O_5 ISFETs to change the point of zero charge

Because it was found that a silylation procedure can result in negative ion-step responses (at pH 7), whereas untreated ISFETs show positive ion-step

responses, it was examined whether the initial negative surface charge density of a Ta_2O_5 ISFET (at pH 7) can be compensated by an APS layer to obtain a zero ion-step response at pH 7. In this way, these modified ISFETs can be used to determine the ion-step response of polystyrene bead membranes, because no interfering ISFET response will occur in this case.

Several Ta_2O_5 ISFETs were silylated according to method 4 and subsequently stored in PBS. Directly after the silylation procedure, the ISFETs showed responses of -20 to -25 mV on an ion-step from 10 to 100 mM KCl at pH 7. The ion-step responses were subsequently measured after several periods of storage in PBS, in which the APS layer slowly hydrated, resulting in decreasing amplitudes of the negative responses. When the responses were reduced to responses with an amplitude of <5 mV (but still negative), different membranes of polystyrene beads were deposited on the ISFETs as described in the experimental section. To determine the effect of the ISFET response on the total response, the same batches of the agarose/polystyrene mixtures were used to make membranes on top of untreated Ta_2O_5 ISFETs. Fig.5.5 shows an ion-step response (10 to 100 mM KCl, pH 7) of an untreated Ta_2O_5 ISFET with a membrane of positively charged 1.03 μm polystyrene beads with amidine surface groups. The positive ion-step response of the bare, untreated ISFET (before the membrane was mounted on top of it), is also shown in the figure. Although the membrane consists of positively charged beads, which will result in a proton uptake, the ion-step response is still positive due to the interfering ISFET response.

Fig.5.6 shows an ion-step response of a silylated Ta_2O_5 ISFET with the same type of membranes consisting of amidine polystyrene beads. The small, negative ion-step response of the silylated ISFET, before the membrane was deposited, is also shown in the figure. The interfering ISFET response is now limited and the total response is negative due to a proton uptake by the membrane groups.

Fig.5.7 shows two typical ion-step responses of Ta_2O_5 ISFETs with a membrane of 0.1 μm negatively charged (sulphate groups, pK_a ±0.8) polystyrene beads. Curve 1 is the response of an untreated Ta_2O_5 ISFET with a membrane and curve 2 is the response of a silylated Ta_2O_5 ISFET with a membrane. The silylated ISFET showed a small ion-step response <-5 mV before the membrane was mounted on top of it. Curve 2 can therefore be considered as the response of the membrane solely, whereas curve 1 is the combined response of the ISFET plus membrane. It is obvious, comparing the two curves, that the ISFET response has a significant influence on the total response. Even after the first few seconds, which is normally the maximum duration of the bare ISFET response, the total response is still influenced by the ISFET response. In this specific case, the buffer capacity of the membrane is very small because the sulphate groups at the beads have a pK_a of

about 0.7 and will all be protonated at pH 7. Therefore, the proton release of the membrane groups will be minimal and the membrane will hardly suppress the ISFET response. The protons which are released from the ISFET surface, have to diffuse from the surface which will be a slower process in the membrane phase than in the solution phase. This might explain why the ISFET response seem to last longer in the case of fig.5.7 than observed in the experiments with bare ISFETs described in chapter 3.

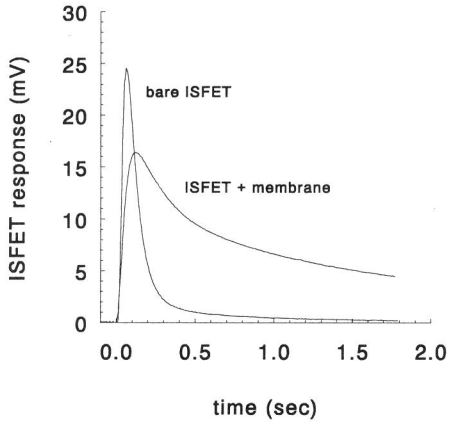

Fig.5.5 Response to an ion-step from 10 to 100 mM KCl at pH 7 of a bare, untreated ISFET and an untreated ISFET with a membrane of positively charged polystyrene beads of 1.03μm.

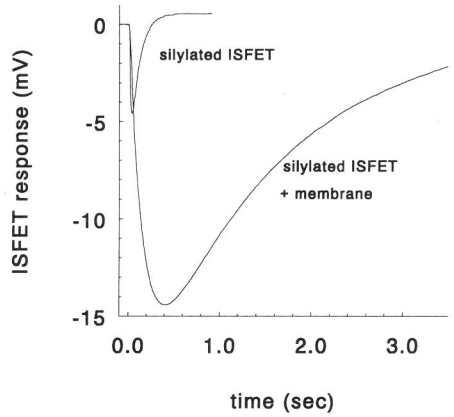

Fig.5.6 Response to an ion-step from 10 to 100 mM KCl at pH 7 of a 'tuned' silylated ISFET and the same silylated ISFET with a membrane of positively charged polystyrene beads of 1.03 μm.

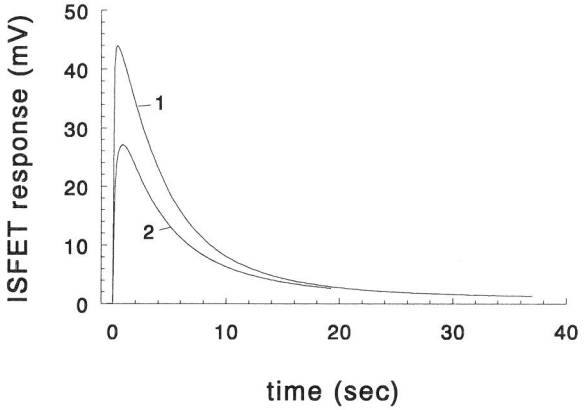

Fig.5.7 Response to an ion-step from 10 to 100 mM KCl at pH 7 of an untreated ISFET with a membrane of 0.1 μm negatively charged beads (curve 1) and of a silylated ISFET with the same membrane (curve 2).

5.5 Conclusions

In this chapter it has been shown that modification of the Ta_2O_5 surface of an ISFET results in a change in the ion-step response. The amino-functionalized silane γ-aminopropyl-triethoxysilane (APS) was used to introduce amino groups at the surface. Although several methods were used, it seemed very difficult to realize reproducible layers of APS, because the amplitude of the ion-step responses of the different ISFETs in the series showed a large variance. The condensation reaction of the silanol groups and the Ta_2O_5 (reaction 5.3) is an equilibrium reaction, which can only be forced to one side by avoiding contact with water. However, since APS is hydrophilic, this seems an impossible condition to realize. It was also noticed that the APS layers slowly hydrolysed as function of time, as determined by a slow change in the ion-step response after storage in aqueous solutions. The rate of hydrolysis did decrease as function of time but an equilibrium was not reached.

Because of this relative instability of the APS layers with respect to hydrolysis, it will be difficult to use the APS layer as a basis to covalently couple an affinity ligand. The coupling procedures often require long incubation times in aqueous solutions, during which APS might loosen from the surface. Therefore it will be impossible to make reproducible and stable layers of bound affinity ligand based on APS layers.

APS-silylated ISFETs can directly be used to determine heparin concentrations in PBS solutions, using the ion-step measuring method and an incubation time of 10 minutes. For each concentration a different ISFET was used. In this way, the contact of each ISFET with an aqueous solution is very limited which means that the slow loss of APS does not play a significant role. The sensitivity to heparin of the different ISFETs within one series, are comparable but do show a small variance which results in a variance in the measurements. Determining heparin concentrations in blood plasma appeared to be difficult due to non-specific binding of other plasma compounds.

Silylating ISFETs with APS can be used as an effective method to reduce the ISFET response to an ion-step at pH 7 by 'tuning' the point of zero charge (as determined by the ion-step response) to pH 7. This option makes it possible to determine the ion-step response of a charged membrane without an interfering ISFET effect. However, also in this case the APS layer will slowly hydrolyse which means that the point of zero charge, as determined by the ion-step response, also slowly changes.

References

[1] E.P. Plueddemann, Silane Coupling Agents, Plenum Press, New York, 2nd edition (1991)

[2] E.P. Plueddemann, Chemistry of silane coupling agents, in: Silylated Surfaces, D.E. Leyden and W.T. Collins (eds.), Gordon and Breach science publishers, New York, (1980)

[3] H. Ishida, S. Vaviroj, S.K. Tripathy, J.J. Fitzgerald, J.L. Koenig, SPI, 36th Ann. Tech. Conf. Reinf. Plast. 2-C (1981)

[4] E.P. Plueddemann, Silane Coupling Agents, Plenum Press, New York, 2nd edition (1991), p.125

[5] G.P. Royer, F.A. Liberatore, The use of silylated derivatives of porous glass as enzyme supports, in: Silylated Surfaces, D.E. Leyden and W.T. Collins (eds.), Gordon and Breach Science Publishers, New York, (1980), p.189

[6] D.J. Tutas, R. Stromberg, E. Passaglia, SPE Trans. 4 (1964), p.256

[7] H.H. Weetall, Covalent coupling methods for inorganic support materials. In: Methods of Enzymology, K. Mosbach (ed.), Academic Press, New York, Vol.44 (1976), ch.10

The ISFET-based heparin sensor with a monolayer of protamine as affinity ligand

6

6.1 Introduction

In chapter 4, the first results have been presented of a heparin sensor based on the ion-step measuring method. In this case a porous membrane of polystyrene beads in an agarose gel is mounted on top of a Ta_2O_5 ISFET. Protamine is serving as affinity ligand and is immobilized on the surface of the polystyrene beads. The measured ion-step responses are a combination of the ion-step response of the membrane and the ion-step response of the underlying ISFET. Although it has been shown that it is possible to determine heparin concentrations in buffer solutions with this sensor, the results in blood plasma were disappointing due to a large interfering effect of other plasma components. The incubation time for this sensor is 15 minutes, which might be long for a practical application.

In the previous chapter the possibility of direct modification of the ISFET surface has been investigated aiming at a surface with high affinity for heparin. In this case the ion-step response only consists of the response of the modified ISFET, and no membrane response is present. Ta_2O_5 ISFETs are treated with an amino-functionalized silane coupling agent which results in a coverage with a positively charged layer of polysiloxanes to which heparin binds by electrostatic interaction. Also with these devices it has been possible to determine heparin concentrations in buffer solutions. The incubation time was 10 minutes in this case. However, the stability of the layers, with respect to hydrolysis, appeared to be poor and the results in blood plasma were again disappointing. The poor stability makes it also very difficult to use the silane layer as a basis for the covalent coupling of another affinity ligand.

A better result is achieved by direct immobilization of protamine at the ISFET surface by physical adsorption. In this chapter it will be shown that with this sensor it is possible to determine heparin concentrations in buffer solutions as well as in blood plasma in the range of physiological importance. The interfering effect of other plasma components is limited and the incubation time is reduced to only 2 minutes.

6.2 Materials and Methods

Reagents

Protamine sulphate (grade X, from salmon) was purchased from Sigma Chemical Co. and heparin from Organon Teknika (Thromboliquine®, 5 ml ampoules containing 25,000 Units). For some of the experiments, heparin was used which was made in the pharmacy of the 'Medisch Spectrum Twente (MST)' hospital (sodium salt, 5 ml ampoules, 5000 U/ml) and which was a gratefully accepted gift. This heparin will be referred to as 'MST heparin'. Since the heparin concentration of both heparin preparations is defined in Units/ml, the heparin concentrations in this chapter are also given in Units/ml, although the response of the sensor is related to absolute concentrations. Phosphate buffer was a mixture of Na_2HPO_4 and NaH_2PO_4 (both products of Merck) in the appropriate ratio. HEPES was a product of Aldrich Chemical Co. and phosphate buffered saline (PBS) was purchased from Sigma Chemical Co. in tablet form. Normal plasma samples (platelet free, from a pool of a large group of healthy donors) were obtained from the laboratory of the MST hospital as well as the plasma samples of different heparinized patients of which the APTT was determined using a kaolin/cephalin APTT assay (Diagnostica Stago).

Measurement set-up

The measurement set-up consists of a flow system in which the flow is controlled by an effective pressure (0.1 bar) of nitrogen in the two vessels containing the solutions. The resulting flow rate is 1.3 ml/min. The ISFET is mounted in a wall-jet cell in which the liquid flow is perpendicular to the ISFET surface (see fig.3.4). The electrolyte at the surface of the ISFET can be replaced within about 0.2 s (ion-step). A saturated calomel electrode is used to define the potential of the solution. In all experiments described in this chapter, 10 mM and 100 mM KCl solutions were used as the 'ion-step' solutions. The solutions were buffered with 0.2 mM HEPES or 0.1 mM phosphate buffer. The responses of the ISFET, connected to a source-drain follower, were recorded with a Nicolet 310 digital oscilloscope which has the ability to store recorded curves on a floppy disk. The output potential of the source-drain follower in case of the equilibrium situation in 10 mM KCl was defined as 0 mV. For representation purposes, the curves were filtered with a software low-pass filter using a cut-off frequency of 40 Hz.

Measurement devices

ISFETs with a Ta_2O_5 gate insulator were fabricated in the MESA cleanroom laboratory following the usual ISFET processing steps. The ISFETs showed a pH response of -58 to -59 mV/pH. The protamine was immobilized by physical

adsorption. The ISFETs were immersed in a solution of 10 mg/ml protamine sulphate in PBS for at least 24 hours, rinsed in 4M NaCl and subsequently stored in a PBS solution.

Measurement protocol

Before each incubation period in a heparin containing sample, the ISFETs with the immobilized protamine were characterized by the response on an ion-step of 10 to 100 mM KCl. Each time the ion-step response had to be determined, 3-5 responses were successively recorded, and the amplitude of the ion-step response was defined as the mean value of the different responses.

For the determination of heparin concentrations in PBS solutions, small 15 ml vessels were used in which the ISFET was placed for two minutes while the solution was not stirred. After incubation the ISFET was rinsed with PBS and mounted in the wall-jet cell of the measurement set-up. The ion-step response was recorded and the change in the amplitude, with respect to the response before incubation, was taken as parameter. The ISFETs with protamine layer could be regenerated after each measurement in a heparin solution, by rinsing for about 1 minute in a 4M NaCl solution followed by an equilibration period in a PBS solution (varying from 5 minutes to 1 hour). When recording a calibration curve, which gives the change of the ion-step response as a function of the heparin concentration, only one ISFET was used, which was regenerated after each measurement.

For the determination of heparin concentrations in normal plasma, a test-tube containing 2 ml of normal plasma was used to which small amounts of a 100 U/ml heparin solution (in 0.9% NaCl) were added to obtain the different concentrations. The ISFET was incubated in the plasma for 2 minutes (without stirring), rinsed in PBS and subsequently the ion-step response was determined. The heparin concentration of the plasma samples of the different heparinized patients was also determined by placing the ISFET in a test-tube containing 0.5 or 1.0 ml of the plasma sample. After 2 minutes the ISFET was rinsed with PBS and the change in the amplitude of the ion-step response, with respect to the response before incubation, was determined. Then 5 µl of a 50 U/ml or 100 U/ml heparin solution was added to yield an increase in the heparin concentration of 0.5 U/ml. After regeneration in a 4M NaCl solution, the ISFET was used to measure this increased heparin concentration following the same procedure.

6.3 Results

Fig.6.1 shows some typical ion-step responses of 10 to 100 mM KCl at pH 7.0. Curve 1 represents a typical ion-step response of a 'bare' Ta_2O_5 ISFET without a protamine layer. Curve 2 represents a typical ion-step response of an ISFET with an adsorbed layer of protamine at the gate oxide surface and curve 3 is a typical ion-step response of an ISFET with a protamine layer after 2 minutes of incubation in a PBS solution containing 0.9 U/ml heparin. The change in the amplitude of the ion-step response after incubation (curve 3) with respect to the response before incubation (curve 2) is referred to as ΔA. The KCl solutions used for recording curve 1 were buffered with 0.2 mM HEPES whereas the solutions used for recording curve 2 and 3, were buffered with 0.1 mM phosphate buffer. It appeared however, that using 0.2 mM HEPES instead of 0.1 mM phosphate buffer (or vice versa) did not significantly change the responses. Because the pH of the 10 and 100 mM KCl solutions were not exactly the same, curve 2 and 3 do not return to 0 mV for $t \rightarrow \infty$. ISFETs with an adsorbed protamine layer could be stored in PBS for at least two weeks without any change in the ion-step response at pH 7.

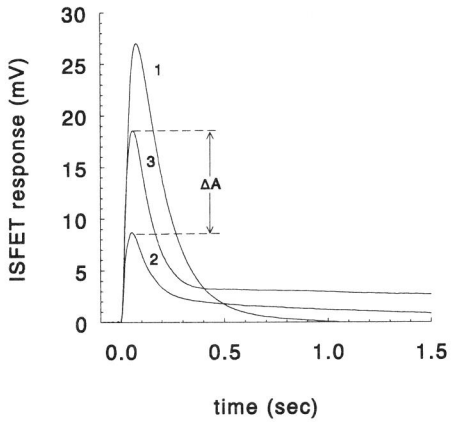

Fig.6.1 Typical responses to an ion-step of 10 to 100 mM KCl at pH 7.0. Curve 1 represents a bare ISFET, curve 2 an ISFET with a protamine layer and curve 3 an ISFET with protamine layer after incubation in PBS containing 0.9 U/ml heparin. ΔA is the change in amplitude after incubation in a heparin solution.

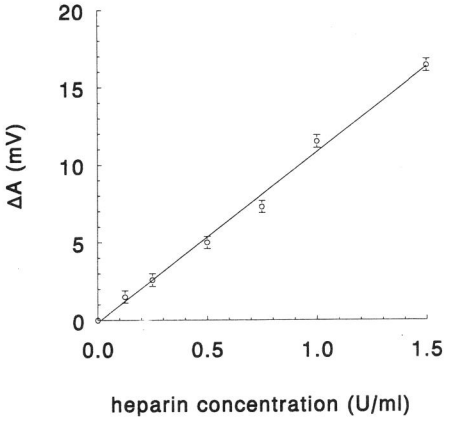

Fig.6.2 The change in amplitude of the ion-step response ΔA after 2 min. incubation in a PBS solution as a function of the heparin concentration (ISFET A).

In fig.6.2 ΔA is plotted as a function of the heparin concentration in a PBS solution. The KCl solutions were buffered with 0.1 mM phosphate buffer at pH 7.0 and the ISFET was incubated for 2 minutes in the heparin solution. In this case Thromboliquine® heparin was used. The difference between the amplitudes of the 3-5 different responses which were recorded for each measurement was about 0.4 mV (mean value ±0.2 mV). Since the parameter ΔA, which is shown in fig.6.2, is defined as the difference between the mean value (±0.2 mV) of the response before incubation and the mean value (±0.2 mV) of the response after incubation, the accuracy of this parameter is ±0.4 mV, as indicated by the error bars. The ISFET was regenerated after each measurement by rinsing with 4 M NaCl and used again for the following measurement.

The relation between the change in amplitude, ΔA (mV), of the ion-step response and the heparin concentration in PBS, c_b (U/ml), can be described by a linear curve fit of the data points as is shown in fig.6.2. The linear equation is given in table 6.1 (ISFET code A) together with the linear equations of the curve fit of three other ISFETs with a protamine layer which were used to determine ΔA as function of the heparin concentration in PBS.

Table 6.1. Linear curve fits of heparin concentration measurements of different ISFETs. The ion-step responses of ISFET D were recorded at pH 7.4 and MST heparin was used. The other ISFETs were measured at pH 7.0 and Thromboliquine was used as heparin. ΔA is the change in amplitude after incubation (mV), c_b is the heparin concentration in PBS and c_p the heparin concentration in normal plasma (both in U/ml).

ISFET code	linear curve fit of heparin concentration measurement in PBS	linear curve fit of heparin concentration measurement in normal plasma
A	$\Delta A=-0.15+11.0c_b$ (fig.6.2)	$\Delta A=2.53+6.10c_p$ (fig.6.3)
B	$\Delta A=-0.30+10.6c_b$	$\Delta A=2.38+4.51c_p$
C	$\Delta A=-0.25+11.6c_b$	------
D	$\Delta A=-0.01+11.3c_b$	$\Delta A=3.17+4.86c_p$ (fig.6.4)

Fig.6.3 shows ΔA (10 to 100 mM KCl, 0.1 mM phosphate buffer pH 7.0) as a function of the heparin (Thromboliquine®) concentration in normal plasma, in which the ISFET was incubated for 2 minutes. The same ISFET (code A) and the same solutions as for the measurement of the heparin concentration in PBS were used. The error bars indicate the accuracy of ΔA as explained in the description of fig.6.2. The relation between the change in amplitude ΔA (mV) and the heparin

concentration in plasma c_p (U/ml) can again be described by a linear curve fit of the data points, starting from 0.25 U/ml, and the linear equation is given in table 6.1 (code A). Note the difference in offset and slope in comparison with the curve fit of the measurements in PBS. The ISFET with code B was also used to determine heparin concentrations in normal plasma and the linear equation of the curve fit of the results is given in table 6.1. Also for this ISFET, note the difference in offset and slope in comparison with the curve fit of the measurements in PBS.

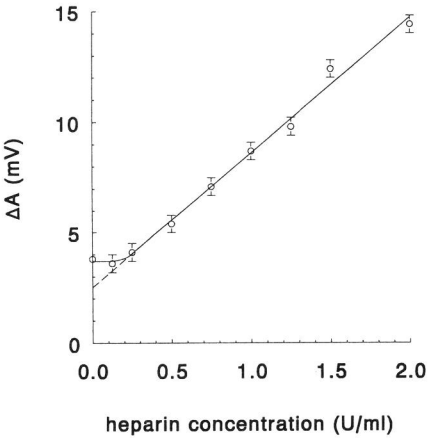

Fig.6.3 The change in amplitude of the ion-step response ΔA after 2 min. incubation in normal plasma as a function of the heparin concentration (ISFET A).

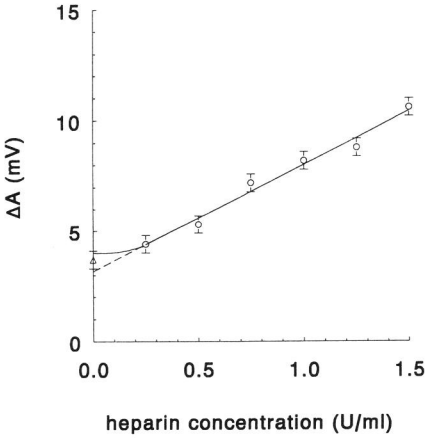

Fig.6.4 The change in amplitude of the ion-step response ΔA after 2 min. incubation in normal plasma as a function of the heparin concentration (ISFET D). Calibration curve for the experiments shown in table 6.2.

Fig.6.4 shows ΔA as a function of the heparin concentration in normal plasma, determined with another ISFET (code D). In this case the ion-step responses were recorded at pH 7.4 and the KCl solutions were buffered with 0.2 mM HEPES. The heparin that was used was MST heparin. The linear curve fit is again given in table 6.1. This curve was used as a calibration curve for the measurement of the heparin concentration in plasma samples of several patients who where heparinized with MST heparin. In table 6.2 the heparin concentrations of these samples are presented as determined with the ion-step measuring method, using fig.6.4 as a calibration curve. After each measurement of the heparin concentration of a specific sample, 0.5 U/ml heparin was added to the sample and the concentration was measured again. These values are also given in table 6.2. Thirteen different samples were tested, and in nine of the samples the increase in the heparin concentration of

0.5 U/ml was correctly measured within the range 0.5 ± 0.07 U/ml. In the other 4 samples the measured increase was less than the added 0.5 U/ml.

Table 6.2. Results of measurements in plasma samples of heparinized patients.

measured heparin concentration (U/ml)	measured change (in U/ml) after addition of 0.5 U/ml	APTT (sec)
1.18	0.47	141
1.22	0.51	86
1.00	0.45	144
0.85	0.49	156
1.30	0.47	73
1.00	0.47	92
1.02	0.43	55
0.79	0.54	93
0.97	0.43	87
1.06	0.35	134
1.06	0.37	67
0.75	0.23	72
0.95	0.27	119

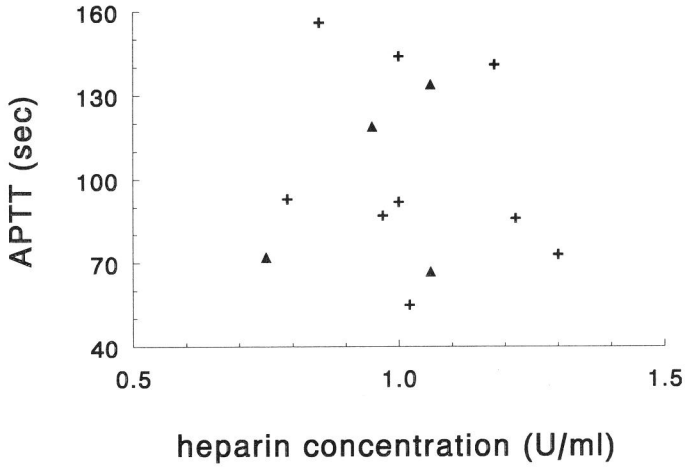

Fig.6.5 The APTT as function of the measured heparin concentration for the different plasma samples of heparinized patients. The plus signs represent the samples in which the addition of 0.5 U/ml was correctly measured, and the triangles represent the other samples.

The ISFET that was used for these experiments (code D), was regenerated more than fifty times. The amplitude of the calibration response, which was recorded after each regeneration procedure, only changed about 2 mV.

Table 6.2 also shows the values for the APTT of the different plasma samples. Fig.6.5 shows the relation between the APTT and the measured heparin concentrations for the nine samples in which the sensor correctly measured the increase of 0.5 U/ml as well as for the other 4 samples. It can be seen that no clear relation can be defined between the APTT value and the measured heparin concentration.

6.4 Discussion and conclusions

The mechanism behind the ion-step response of a 'bare' ISFET as shown in fig.6.1, curve 1, has already been described in chapter 3 but will be briefly reviewed.

The interface between the ISFET and the solution is described by the acid-base equilibria at the amphoteric surface of the Ta_2O_5-gate oxide. The surface OH groups can act as a proton donor as well as a proton acceptor yielding a charge density σ_0 (in C/cm^2) at the surface.

$$\sigma_0 = q\left([Ta\text{-}OH_2^+]-[Ta\text{-}O^-]\right) \tag{6.1}$$

The pH where σ_0=0 is called the point of zero charge pH_{pzc}, which lies around pH 3 for Ta_2O_5. This means that at pH 7 the Ta_2O_5 surface is negatively charged. The relation between the surface charge σ_0 and the surface potential ψ_0 is given by:

$$\sigma_0 = \psi_0 C_{dl} \tag{6.2}$$

with C_{dl} the integral double-layer capacitance (in F/cm^2).

The ISFET measures the surface potential ψ_0 with respect to the bulk potential which is defined by the reference electrode. This potential ψ_0 follows from the Boltzmann equation:

$$\left[H_s^+\right] = \left[H_b^+\right]\exp\left(\frac{-q\psi_0}{kT}\right) \tag{6.3}$$

where $[H_s^+]$ is the proton concentration directly at the ISFET surface and $[H_b^+]$ the proton concentration in the bulk solution. The combination of the large number of OH surface sites (about 10^{15}/cm^2), the chemical equilibria of the acid-base reactions and the relatively low value of the double-layer capacitance (maximum 20 μF/cm^2),

makes the Ta_2O_5 oxide surface act as a very good buffer for H_s^+, which results in a (almost) constant pH at the surface (pH_s). Consequently, the surface potential ψ_0 changes with -59 mV/pH_b [1] (see chapter 3).

Eqs.6.1-6.3 describe the statical behaviour of the ISFET in thermodynamical equilibrium. However, the transient response to an ion-step cannot directly be described by these equations. To elucidate the mechanism behind these responses, a dynamical simulation model was developed based on the Nernst-Planck and Poisson equations which are solved by a finit difference procedure. The chemical equilibria at the ISFET surface are incorporated in this model of the ISFET together with a stagnant layer in which ion transport is caused only by diffusion. With this model it has been possible to understand the dynamic mechanism and verify the experimental results [2].

After an ion-step, C_{dl} increases very fast due to a sudden increase in the diffuse capacitance, which results in a decrease in the absolute value of the surface potential ψ_0, according to eq.6.2. According to the Boltzmann eq.6.3, the H_s^+ concentration will tend to decrease because of the decreased ψ_0. However, the oxide surface act as a very good buffer for H_s^+ and will keep the H_s^+ concentration constant by dissociating Ta-OH groups. This will change σ_0 until a new equilibrium is reached when σ_0/C_{dl} ($=\psi_0$) has the same value as before the ion-step. The time constant of adapting σ_0 by dissociating Ta-OH groups is determined by the diffusion of the H^+ ions and the buffer capacity of the electrolyte. A thick stagnant layer and/or a low buffer capacity will delay the establishment of a new equilibrium. This was indeed observed in experiments which were in agreement with the simulation results.

If the double-layer capacitance changes, as a result of an ion-step of 10 to 100 mM KCl, from C_{dl1} to C_{dl2}, the theoretical maximum change in ψ_0 directly after the ion-step (assuming that σ_0 is not changing yet) is:

$$\Delta\psi_{max} = \psi_{0,2} - \psi_{0,1} = \frac{\sigma_0}{C_{dl2}} - \frac{\sigma_0}{C_{dl1}} = \psi_{0,1}\left(\frac{C_{dl1}}{C_{dl2}} - 1\right) \qquad (6.4)$$

The double-layer capacitance can be calculated using the Gouy-Chapman-Stern model and depends on the electrolyte concentration and on the potential ψ_0 across the double layer. Fig.6.6 show the values of C_{dl1} (in 10 mM) and C_{dl2} (in 100 mM), as well as the ratio C_{dl1}/C_{dl2}, as a function of the potential ψ_0, calculated according to the Gouy-Chapman-Stern model, assuming a constant Stern capacity of 20 $\mu F/cm^2$ [3].

At pH 7, the surface potential ψ_0 of a Ta_2O_5 ISFET (pH_{pzc}=3) is (7-3)*-59=-236 mV. The double-layer capacitance at 10 mM KCl is 12.7 $\mu F/cm^2$, which results according to eq.6.2 in a surface charge σ_0 of -3.00*10^{-6} C/cm^2,

corresponding with $1.87*10^{13}$ negatively charged groups per cm^2. The value of C_{dl} at 100 mM KCl is 16.1 $\mu F/cm^2$, which gives a value of 50 mV for $\Delta\psi_{max}$ as defined by eq.6.4.

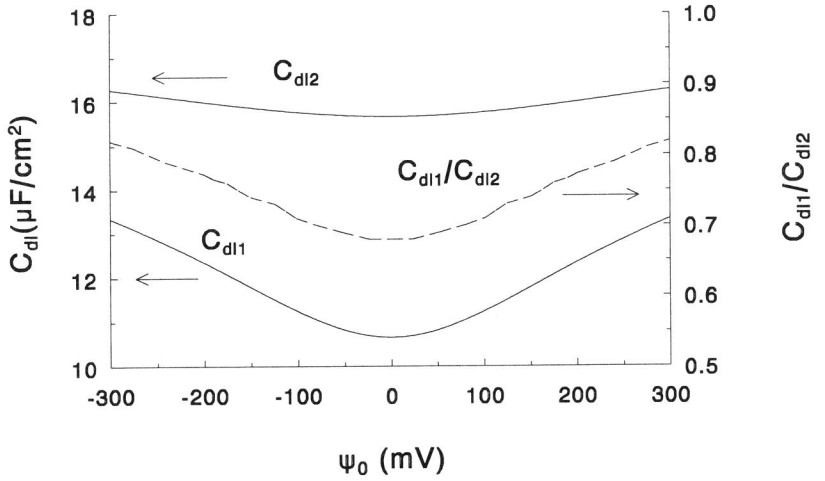

Fig.6.6 The double-layer capacitance C_{dl} as function of the potential ψ_0 across the double layer. C_{dl1} is the capacitance in 10 mM KCl, C_{dl2} the capacitance in 100 mM KCl (left Y-axis) and C_{dl1}/C_{dl2} represents the ratio of the two capacitances as used in eq.4 (right Y-axis).

Because of an insufficient time separation of the changes in C_{dl} and σ_0, which is caused by the stagnant layer and related to the buffer capacity of the solution, the real value of the amplitude of the ion-step response is smaller than the theoretical maximum. This effect was clearly observed in the simulation results [2]. The experimental result of 27 mV (fig.6.1) implies that the response reaches 54% of its maximum value due to the insufficient time separation between the changes in C_{dl} and σ_0.

Immobilization of protamine by physical adsorption will result in a coverage with a maximum thickness of a few monolayers, but since the ISFETs are rinsed in 4M NaCl, a monolayer coverage seems most plausible. Due to the small size of the protamine molecules (MW 4000), the protamine layer will be very thin, which makes it acceptable to assume that the immobilization of a protamine layer can be described as a modification of the surface charge of the ISFET. The ion-step response can therefore be described in the same way as the ion-step response of a bare ISFET, but with a different surface charge density σ_0 and point of zero charge pH_{pzc}. Therefore, the contribution of membrane responses, which were described in chapter 3 and 4, can be neglected. These responses include a changing Donnan

potential at the protamine-solution interface and a temporary increase in the pH inside the protamine layer as a result of an uptake of protons by the protamine molecules, induced by the stepwise increase in the electrolyte concentration.

The measured ion-step response of an ISFET with a protamine layer, as shown in fig.6.1 (curve 2), supports the assumption to describe the effect of a protamine layer coverage as a surface modification. The ion-step has a smaller amplitude due to the positive charge of the protamine, compensating a part of the negative charge of the Ta_2O_5, but the time constants of the ion-step responses shown in fig.6.1 are about the same. This is shown in fig.6.7 where the responses of fig.6.1 are shown again but in this case the responses are normalized to an amplitude of 1. It can be seen that the time constants are all comparable, including those of curve 3 which represents the response after incubation in heparin. Apparently, also the binding of heparin can still be described as modification of the surface charge. If the earlier mentioned membrane effects should contribute to the ion-step response, this would certainly influence the time constants of the ion-step response of the ISFET. It should be noted that curve 1 was recorded in solutions that were buffered with 0.2 mM HEPES of which the buffer capacity differs a little from the solutions buffered with 0.1 mM phosphate buffer, used for recording curve 2 and 3. Because the pH was not exactly the same in both ion-step solutions, curve 2 and 3 do not return to 0 mV for $t \rightarrow \infty$.

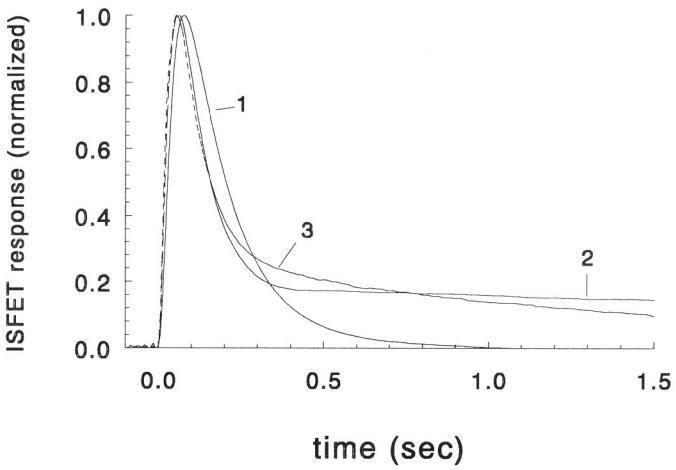

Fig.6.7 The same ion-step responses as in fig.6.1 but now normalized to the amplitude. Curve 1 is the response of a bare ISFET, curve 2 of an ISFET with a protamine layer and curve 3 the response after incubation in a heparin solution.

The amplitude of the ion-step response of an ISFET with a protamine layer is typically 9 mV (fig.6.1, curve 2). If it is assumed that also in this case the response reaches 54% of its maximum response as described by equation 4, a value of 17 mV is obtained for $\Delta\psi_{max}$. Since the binding of the protamine results in a decrease in the absolute value of the surface potential ψ_0, the value for the ratio C_{dl1}/C_{dl2} is also changed (see fig.6.6). From eq.6.4 and fig.6.6, it can be calculated that the new ratio C_{dl1}/C_{dl2} is 0.69 which corresponds with a potential $\psi_{0,1}$ of -55 mV (at 10 mM KCl). This potential results in a surface charge of $-0.70*10^{-6}$ C/cm^2, or $4.4*10^{12}$ negatively charged groups per cm^2. With respect to a bare ISFET, the net surface charge is therefore decreased from 18.7 to $4.4*10^{12}$ negatively charged groups per cm^2. This means that the adsorbed protamine contributes to a positive charge density of $14.5*10^{12}$ groups per cm^2. According to the amino acid content of protamine [4], a molecule charge of +20 can be assumed, which yield a coverage of $7*10^{-3}$ molecules per nm^2. This indicates that the protamine layer is not a dense layer, which means that the Ta_2O_5 surface is not completely covered with protamine.

The results of the measurements of heparin concentrations in PBS show, that four different ISFETs behave in virtually the same way with respect to the heparin concentration in PBS, as is shown in table 6.1 (ISFET D at another pH, using another heparin). The offsets fall within the accuracy of the measurement of ΔA (mean value ± 0.4 mV) and the slopes are almost equal. According to the accuracy of ΔA (± 0.4 mV), the accuracy in the measurement of the heparin concentration in PBS should be ± 0.04 U/ml (using a mean slope of 11.1 mV.Unit^{-1}.ml). However, the curve fit does not include all data points within the accuracy as given by the error bars. A possible cause for this extra inaccuracy might be found in the procedure. During the two minutes incubation time, the sample is not stirred which makes the affinity reaction at the surface very sensitive for convection in the solution to which no special attention was paid. Moreover, the incubation is manually timed, which introduces an estimated error of about 5 sec. (4%).

The interaction of heparin with a protamine-loaded surface has been described by a Langmuir adsorption model [5]. As a function of time, Kim and co-workers found a rapid increase in the heparin concentration at the surface during the first 10 minutes, followed by an asymptotic approach to a steady state value. It can therefore be concluded that during the 2 minutes of incubation time, which was used in our procedure, no equilibrium or steady state value could have been reached. Therefore, the binding to the ISFET cannot be described by a Langmuir adsorption model as is also obvious from the linear relation between the heparin concentration and ΔA. More experiments will be needed to study the binding of heparin to the protamine-treated ISFET as a function of time. The observation that the amount of bound heparin increases rapidly during the first minutes indicates, that it is important to

time the incubation period accurately.

The measurements in normal blood plasma show a significant offset which is probably caused by a non-specific interaction of plasma components with the ISFET surface. Since it has been reasoned that the coverage of protamine is not very dense, the non-specific interaction might include interaction with protamine molecules as well as adsorption on 'free' Ta_2O_5. This non-specific interaction reduces the detection limit of heparin in plasma to about 0.25 U/ml. A more dense coverage of the surface with protamine, for instance by covalently coupling the protamine to the surface, might reduce the non-specific adsorption on the Ta_2O_5 surface and therefore reduce the offset and improve the detection limit. Another difference in comparison with the measurement of the heparin concentration in PBS is the slope of the linear curve fit corresponding with the relation between ΔA and the heparin concentration, which is significantly smaller in the case of measurements in plasma. A possible explanation would be a smaller amount of heparin bound to the protamine during the incubation time of 2 minutes and/or a partly compensation of the charge of the heparin molecules by heparin-binding proteins which are immobilized at the ISFET surface together with the heparin molecule. It is known that protamine is able to bind all possible active heparin molecules, and protamine has successfully been used to separate all active heparin from plasma samples [5]. The kinetics of heparin in plasma could be different due to binding to proteins, which might reduce the amount of bound heparin during the 2 min. incubation time. Further research is necessary to be able to understand the exact mechanism. This includes the observation that the slopes of the linear curve fit corresponding with the measurement in plasma are different for the three ISFETs, whereas the slopes of the linear fit of the measurements in PBS are almost alike.

The accuracy of the measured heparin concentration in plasma, according to the accuracy in ΔA, is 0.07 U/ml for ISFET A, presented in fig.6.3 and 0.08 U/ml for ISFET D, presented in fig.6.4. Also in these cases, an extra inaccuracy might be caused by the procedure as explained earlier.

The measurements of the heparin concentration in the patient plasma samples, as shown in table 6.2, show that in 9 out of 13 samples the added amount of 0.5 U/ml was correctly measured within the accuracy of the used ISFET ($\pm$0.08 U/ml). In these cases the calibration curve, which was recorded in normal plasma, could be used to determine the concentration in the individual plasma samples. The measured increase in the concentration in the four other samples was smaller than 0.5 U/ml. Apparently the calibration curve obtained from measurements in normal plasma cannot be used in these cases. It is unclear which effects cause this difference and more specific experiments will be needed to investigate these effects.

From fig.6.5 it is obvious that there is no direct relation between the heparin

concentration and the APTT. This finding is not unexpected because the APTT is dependent on several other parameters (e.g. the concentration of AtIII and other clotting factors) which may vary from one patient to another. The therapeutic range for the APTT as used in the MST hospital has been defined as 70-120 sec (normal values 25-35 sec). From the figure it can be seen that some of the plasma samples show clotting times within the therapeutic range, whereas the heparin concentration appears to be >1.0 U/ml. In another case the APTT clearly exceeds the therapeutic range (156 sec) whereas the heparin concentration appears to be only 0.85 U/ml. These results support the statement that the APTT is not a suitable assay to monitor heparin concentrations. Jaques and co-workers also determined absolute heparin concentrations in patient plasma samples and plotted the APTT as function of the heparin concentration resulting in a similar figure as fig.6.5 in which no relation could be determined [6]. The heparin concentration was determined by first separating the heparin from the plasma followed by microelectrophoresis to determine the absolute amount. In this context, it would be interesting to compare the heparin concentration as measured with the heparin sensor system described in this chapter, with the result of a specific chromogenic substrate test which uses additional AtIII and gives a result which is related to the concentration of active heparin molecules.

In this chapter a heparin sensor system has been described which can determine absolute heparin concentrations in blood plasma in the range 0.25-2.0 U/ml with an accuracy of ±0.08 U/ml. With respect to the heparin sensor which uses a porous membrane on top of the ISFET, as described in chapter 4 [7], the non-specific interactions with other plasma components is significantly reduced. The incubation time is also reduced from 15 to 2 minutes. More experiments are needed to study the behaviour of the sensor in individual plasma samples. The specifications of the sensor system can still be optimized by establishing a higher degree of coverage of the Ta_2O_5 surface with protamine, which might reduce the non-specific interactions of other plasma components and increase the sensitivity to heparin. The procedure can be optimized by a more accurate timing of the incubation time and by stirring the sample during incubation.

References

[1] R.E.G. van Hal, J.C.T. Eijkel, & P. Bergveld, The pH sensitivity of ISFETs described in terms of buffer capacity and double layer capacitance. Technical digest of the fifth international meeting on Chemical Sensors, Rome, 11-14 July, 1994.

[2] J.C. van Kerkhof, J.C.T. Eijkel, & P. Bergveld, ISFET responses on a stepwise change in electrolyte concentration at constant pH, Sensors and Actuators B, 18 (1994), p.56-59.

[3] A.J. Bard, and L.R. Faulkner, Electrochemical methods, fundamentals and applications, John Wiley & Sons, New York (1980).

[4] R.B. Cundall, G.R. Jones, & D. Murray, Polyelectrolyte complexes, 3. The interaction between heparin and protamine. Makromol. Chem., 183 (1982), p.849-861.

[5] J. Kim, A.J. Yang, & V.C. Yang, Protamine immobilization and heparin adsorption on the protamine-bound cellulose fiber membrane. Biotechnology and Bioengineering, 39 (1992), p.450-456.

[6] L.B. Jaques, S.M. Wice, & L.M. Hiebert, Determination of absolute amounts of heparin and of dextran sulfate in plasma in microgram quantities. J. Lab. Clin. Med., 115 (1990), p.422-432.

[7] J.C. van Kerkhof, P. Bergveld, & R.B.M. Schasfoort, Development of an ISFET based heparin sensor using the ion-step measuring method. Biosensors and Bioelectronics, 8 (1993), p.463-472.

Final conclusions and suggestions for future developments

7

7.1 Conclusions

In this thesis the development of an ISFET-based heparin sensor is described, with the ion-step measuring method as a starting point. Apart from the development of the first application of the ion-step measuring method, the research project described in this thesis has also contributed to a better understanding of the mechanism behind the ion-step measuring method. This has resulted in an optimal use of the specific features of the ISFET and the measuring method in the final design of the heparin sensor. The conclusions following from this thesis are summarized below.

- From the review given in chapter 2 regarding the clinical use of heparin as an anticoagulant, it can be concluded that there is no real consensus of opinion about what should be monitored for the optimal control of a heparin treatment. Nevertheless, a simple sensor system measuring absolute heparin concentrations, might be a useful device, because besides the biological activity of heparin, the absolute concentration of heparin seems to be an important parameter.

- In chapter 3, where a detailed description of the ion-step measuring method is given, it is shown that the ISFET itself (without membrane) also responds to an ion-step. This means that the ISFET can not be regarded as an ideal transducer for measuring the ion-step response of a membrane deposited on top of the ISFET. The ion-step response of the 'bare' ISFET is dependent on the surface charge density of the ISFET gate oxide and the change in the double-layer capacitance resulting from the ion-step. The time constant of the response is determined by the proton flux in the stagnant layer in front of the ISFET. At the point of zero charge, the ISFET does not respond to an ion-step. This means that the ion-step measuring method is a very direct method to determine the point of zero charge of an ISFET gate oxide.

- In combination with a porous membrane of polystyrene beads, the ISFET response can interfere with the membrane response. This interference is larger in the case of very porous membranes with low buffer capacity than in the case of dense membranes with high buffer capacity. In the latter case, the membrane will respond to an ion-step with a large proton release or uptake, which in most cases will diminish the effect of the proton release or uptake from the oxide surface.

- Using membranes of polystyrene beads with immobilized protamine, it is possible to determine heparin concentrations in buffer solutions, despite the interfering ISFET responses to an ion-step. For every measured concentration, another device has to be used. Depending on the incubation time and the porosity of the membranes, the slope of the linear curve, representing the change in the amplitude of the ion-step response as function of the heparin concentration, varies from 26 $mV/Unit.ml^{-1}$ to 3 $mV/Unit.ml^{-1}$. The detection limit, after 15 minutes of incubation, has been calculated as $5.3*10^{-8}$ mol/l. Covalent coupling of protamine to the beads, using a small spacer, results in larger slopes than physical adsorption. The used incubation times vary from 40 hours to 15 minutes. Incubation in blood plasma causes a significant non-specific adsorption of plasma components. This might be reduced by blocking redundant adsorption sites by albumin or small polypeptides after the immobilization of protamine.

- By a treatment with an amino-functionalized silane, it is possible to modify the surface of a Ta_2O_5-ISFET in such a way that the point of zero charge, as determined by the ion-step response, can be shifted. If the pH_{pzc} is adjusted to the pH of the ion-step solutions, the ion-step response of a membrane of polystyrene beads can independently be determined, without an interfering ISFET response.

- The fact that 'bare' ISFETs do respond to an ion-step, creating an artefact in the measurement with membranes of polystyrene beads, can be seen as a disadvantage. On the other hand, this effect can also directly be used as a sensing principle. The introduction of amino-groups at the surface as binding sites, results in a sensitivity towards heparin. It is possible to determine heparin concentrations in PBS after an incubation time of 10 minutes. However, it seems that the interaction of heparin with the silane leads to a less strong binding than the interaction of heparin with protamine. The results from the experiments in blood plasma are poor, probably due to non-specific binding of plasma components. A significant problem is the poor stability of the silane layers with respect to hydrolysis, which seems to be the major factor restricting the possibilities of using the amino-groups for additional chemistry (e.g. covalent coupling of protamine).

- The best results are obtained with Ta_2O_5-ISFETs with a layer of protamine, immobilized by physical adsorption. The ion-step responses can be described as responses of 'bare' ISFETs with a modified surface charge density, even after binding of heparin to the surface. With these devices it is possible to determine heparin concentrations in PBS as well as in blood plasma after an incubation time of only 2 minutes with a detection limit of 0.1 U/ml in PBS and 0.25 U/ml in plasma. These values correspond with $5.3*10^{-8}$ and $13.3*10^{-8}$ mol/l respectively, assuming an average molecular weight of 15000 and a value of 8 microgram per unit. Since the devices can be regenerated after incubation in a heparin solution, the calibration curves can be recorded with only one device. The accuracy of the measured heparin concentrations in plasma is 0.08 U/ml. It is suggested that the accuracy can be improved by adjustments in the procedure (stirring, more accurate timing). There is some non-specific adsorption of plasma components, but the results with the plasma samples of the different heparinized patients show that in most cases (9 out of 13) this non-specific binding results in a constant offset. Calculations indicate that the coverage with protamine is not maximal, which means that there are still adsorption sites available at the Ta_2O_5-surface. These sites could be responsible for the non-specific adsorption. In the next section a suggestion is given to improve the coverage of the surface with protamine.

- One of the parameters used to qualify measuring principles or methods is the detection limit. In the work described in this thesis a detection limit of $5.3*10^{-8}$ mol/l heparin is measured, but this value is empirically obtained with a system which was not optimized. The question then arises: what is the theoretical detection limit of the ion-step measuring method in general? To be able to answer this question, two main processes in the ion-step measuring method are distinguished. The first process is the transport of the analyte from the sample solution to the sensor surface and the subsequent binding of the analyte to the affinity ligand. The second process is the change in charge density at the sensor surface as a result of bound analyte at the surface and the resulting change in ion-step response. The first process determines the amount of analyte that will bind to the surface during a certain incubation time. The parameters for this process are the diffusion coefficient of the analyte, the binding constant of the interaction of the analyte with the affinity ligand, the 'adsorption isotherm' of the analyte to the affinity ligand and the concentration of the analyte. This process is independent of the sensor or measurement method which is used. It may be clear that it is very difficult to make a general model of the amount of analyte molecules that binds to the surface as a function of the incubation time and the

analyte concentration.
The second process is the change in surface charge density resulting from bound analyte molecules and the subsequent change in the ion-step response. For determining the theoretical detection limit, we can calculate the minimum change in charge density that can be detected by the change in ion-step response. The theoretical maximum amplitude of an ion-step response is given in chapter 3 by eq. 3.25 with the subscript 1 referring to the situation at 10 mM KCl and subscript 2 to the situation at 100 mM KCl:

$$\Delta\psi_{max} = \psi_{0,1}\left(\frac{C_{dl1}}{C_{dl2}} - 1\right) \tag{7.1}$$

It is assumed that the smallest significant change in ion-step response which can be detected, is 0.1 mV. Because of the small change in surface potential ψ_0, the quotient C_{dl1}/C_{dl2} can be considered as constant which yields for the change in ion-step response after incubation:

$$\Delta\psi_{max,a} - \Delta\psi_{max,b} = (\psi_{0,1,a} - \psi_{0,1,b})\left(\frac{C_{dl1}}{C_{dl2}} - 1\right) \tag{7.2}$$

with the subscripts b and a referring to the situation before and after incubation. As an example the situation of a surface potential $\psi_{0,1,b}$ of -236 mV is taken which gives a value of 12.7 μF/cm^2 for $C_{dl,1}$ and 16.1 μF/cm^2 for $C_{dl,2}$ according to fig.6.6. A change in the theoretical ion-step response of 0.1 mV ($\Delta\psi_{max,a}$-$\Delta\psi_{max,b}$=0.1) then results according to eq.7.2 in a value for $\psi_{0,1,a}$ of -236.5 mV, and thus in a change of only 0.5 mV. This change in surface potential, resulting from bound analyte molecules, corresponds with a change in surface charge density of $6.35*10^{-9}$ C/cm^2 or $4*10^{10}$ charged groups per cm^2. To illustrate this value it is assumed that this change in surface charge density is caused by the binding of albumin molecules. At pH 7.4, albumin molecules have a net charge of -20 [1]. The value of $4*10^{10}$ charged groups therefore corresponds with $2*10^9$ albumin molecules per cm^2. From literature it is known that a monolayer of albumin, which is the maximum amount that can be bound to a surface, corresponds with 0.9 μg/cm^2, which corresponds with $8.2*10^{12}$ molecules/cm^2 [2]. This means that the theoretical detection limit of $2*10^9$ albumin molecules per cm^2 is 0.024% of the maximum amount of albumin molecules that can be bound to the surface.

7.2 Suggestions for further research

In this section a number of suggestions for further research will be given, which may direct the continuation of the research project described in this thesis. First, some suggestions are given referring to the heparin sensor with the immobilized protamine layer as described in chapter 6

- A better coverage of the Ta_2O_5-surface with protamine might reduce the non-specific adsorption of plasma components to the ISFET surface, as described in chapter 6. This can be achieved by adjusting the pH of the buffer, from which the protamine is adsorbed to the Ta_2O_5 surface, to the iso-electric point (i.e.p.) of protamine. It is known that at the i.e.p. of a protein the adsorption is maximal. However, in this case the pH should be in the range 10-12 which means that also the surface charge of the Ta_2O_5 increases which might reduce the amount of adsorbed protamine. Most likely there will be an optimum which can only be determined empirically.

- It would be interesting to compare the results of measurements with the heparin sensor as described in chapter 6 with results of chromogenic substrate tests, as described in chapter 2. These tests give a parameter related to the concentration of heparin molecules with high affinity to antithrombin III (AtIII). It can be expected that the correlation between these results is much better than between the measured heparin concentration with the sensor and the APTT, as shown in fig.6.5.

- The ion-step measuring method can in principle also be used to determine a parameter directly related to the biological activity of heparin. If thrombin or factor Xa is immobilized at the ISFET surface, AtIII from the blood sample in which the device is incubated, will bind to the thrombin or factor Xa. The amount of AtIII which will bind during the incubation time, is determined by the biological activity of heparin, which acts as a catalyst for this reaction as described in chapter 2. In this way a parameter is determined related to the biological activity of heparin.
  Since the ion-step measuring method is based on measuring changes in charge density at a surface or in a membrane, it has to be examined whether binding of AtIII to thrombin or factor Xa results in a measurable change in charge density. The i.e.p. of all three molecules, thrombin, factor Xa and AtIII lies around pH 5, which means that at pH 7 these molecules probably all have a comparable negative charge. The effect of a bound AtIII molecule is therefore much smaller

then for instance the effect of the binding of a negatively charged heparin molecule to a layer of positively charged protamine. However, it has been shown in the previous section that the theoretical detection limit for albumin, which has a comparable charge at pH 7.4, is 0.024% of the maximum amount, which means that the theoretical detection limit will not be a limitation for a successful application.
Another point to mention is the immobilization of thrombin or factor Xa to the ISFET surface or to polystyrene beads. The interaction of thrombin or factor Xa with AtIII consists of binding by a specific binding site. After immobilization, this binding site must still be accessible for AtIII. This is important for the first process which has been distinguished in the ion-step response in the previous section. This process determines the amount of analyte (AtIII) which is bound to the surface after a certain incubation time.

- Another alternative possibility to use the ion-step measuring method for heparin monitoring, is using the principle of a chromogenic substrate test. In these tests a fixed quantity of factor Xa or thrombin is added to the heparinized plasma sample. After a certain incubation time, residual factor Xa or thrombin is determined either by addition of a specific peptide substrate to the mixture or subsampling a sample from the reaction mixture into the specific substrate solution. As a result of the reaction with factor Xa or thrombin, a chromophore is released from the substrate which can be measured by monitoring the optical density at a certain wavelength. If the substrate is immobilized to the ISFET surface, the release of the chromophore will change the charge density at the surface, which can be measured by the ion-step response. To amplify the change in surface charge density, a charge label can be added to that part of the substrate that is released after the enzymatic reaction. An advantage of this method would be that the results can directly be compared with the results of the 'normal' chromogenic substrate tests which will improve the acceptability of such a device. A disadvantage is that a fixed quantity of thrombin or factor Xa has to be added to the plasma sample as a reagent, which will make the procedure of using the sensor more complicated.
  The principle of immobilizing a standard substrate to an electrode has already been examined by Arwin [3], who immobilized a commercially available substrate to a platinum electrode and measured the rate of electrode capacitance change that resulted from the release of the polypeptide. Unfortunately, the procedure which had to be followed was still rather complicated and the results were not really convincing.

The following suggestions for further research refer to the ion-step measuring method in general.

- If membranes are used of polystyrene beads in an agarose gel, a new method has to be developed to ensure a reproducible thickness of the membranes. Spin-coating in combination with lift-off techniques seems a good possibility to achieve a constant thickness [4].

- Silanes that contain no charged functional groups (e.g. dichlorodimethylsilane), yield a more hydrophobic surface which might improve the stability with respect to hydrolysis and will result in a larger amount of adsorbed proteins to the surface.

- Because in some cases the process of applying the ion-step and the following re-establishment of the equilibrium partly coincide, it is important that the ion-step is applied in a reproducible way. A constant flow in the flow through system is a condition that certainly has to be fulfilled. Another important parameter is the position of the gate area of the ISFET in the measurement cell. Since the devices are manually prepared at this moment, the position of the gate in the area of the chip that is exposed to the solution, can be different from device to device.

7.3 Future developments

For a practical application of the ion-step measuring method, it will be necessary to have a simple measurement system in which the ion-step is applied to the ISFET, the transient ISFET response is recorded and the data is processed. It has been suggested to apply the ion-step by a solid state actuator integrated on the ISFET chip [4], but it has to be proven whether such an actuator has the capacity to adequately change the ion concentration in front of the ISFET or in a membrane on top of the ISFET. The increase in the concentration as function of time is also important; a rise time of less than 200 ms has to be achieved.

A straight forward application would be the incorporation of the heparin sensor in a wall jet cell in an existing flow injection analysis (FIA) system. These systems are nowadays commercially available, even with incorporated ion-selective electrodes and several (amperometric) biosensors. FIA systems are usually equipped with powerful soft- and hardware to direct the different liquid flows and acquire the data from the sensor. However, because of the high costs and complexity of these systems, FIA systems are only suitable for laboratory testing.

In the research project described in this thesis, a very simple configuration of a measurement system has been developed, based on applying the ion-step by

subsequently inserting the device in two different solutions. Basically the system consists of two cylindrical containers, holding the two ion-step solutions which are separated by a thin (0.25 μm) polyethene membrane as schematically shown in fig.7.1. The ISFET with integrated reference electrode is mounted in the tip of a perspex needle. For applying the ion-step, the needle is placed in the upper container until the ISFET is in equilibrium with the first solution. Then the needle is pressed through the polyethene membrane, thereby initiating a liquid flow through the groove in the needle in which the ISFET is located. The flexible polyethene film prevents the two solutions to mix.

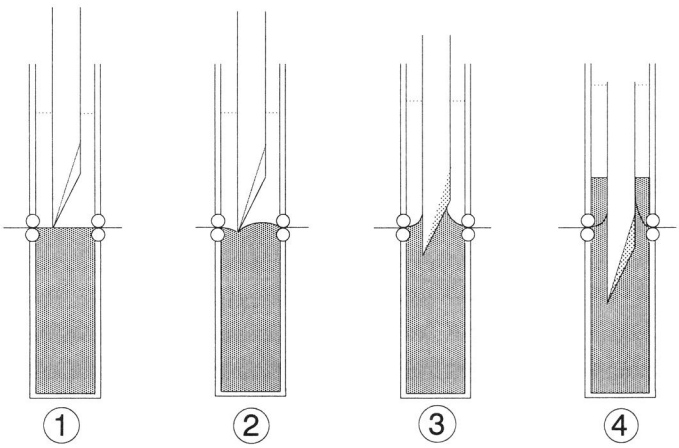

Fig.7.1 A simple configuration of the ion-step measurement set-up.

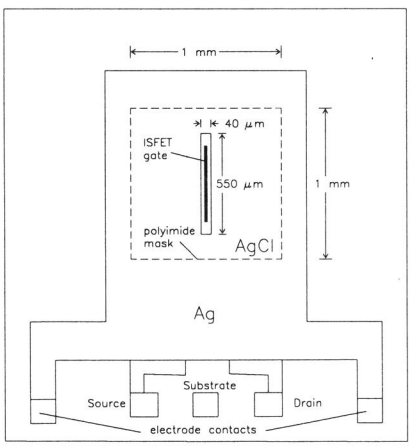

Fig.7.2 A top view of the ISFET with integrated Ag/AgCl reference electrode.

A top view of the ISFET with integrated reference electrode is given in fig.7.2. A silver layer was deposited around the gate area as shown in the figure. The silver electrode was electrochemically chlorinated by leading a current of 4 $\mu A/mm^2$ through the electrode in a solution of 0.1 M HCl, for 6 minutes [5]. After preparation the electrodes were stored in demi-water for 1-2 days. Because a Ag/AgCl electrode was used as reference electrode, the Cl^- activity had to be kept constant during the ion-step. Therefore, the ion-step was performed with KNO_3 solutions with a constant Cl^- activity.

A more detailed view of the perspex needle is given in fig.7.3. The ISFET is located in a groove which improves the flow across the surface after the needle is pressed through the membrane. To evaluate the ion-step applied in this simple system, two perspex needles as shown in fig.7.3 were equipped with planar conductance cells which are schematically shown in fig.7.4. The conductance cells consist of two interdigitated platinum electrodes, each with 50 fingers with a width of 7 μm and a length of 1 mm. The distance between the fingers is 3 μm. The ion-step can be monitored by an AC measurement of the conductance of the solution during the perforation of the membrane. Before use, the conductance cells were characterized by measuring the impedance as a function of the electrolyte concentration and the measuring frequency. The ion-step was performed with solutions of 0.5 and 5 mM KCl and the impedance was measured at 520 kHz. The measured changes in the impedance were characterized by the rise time of the response, defined as the time between 10 and 90% of the final response.

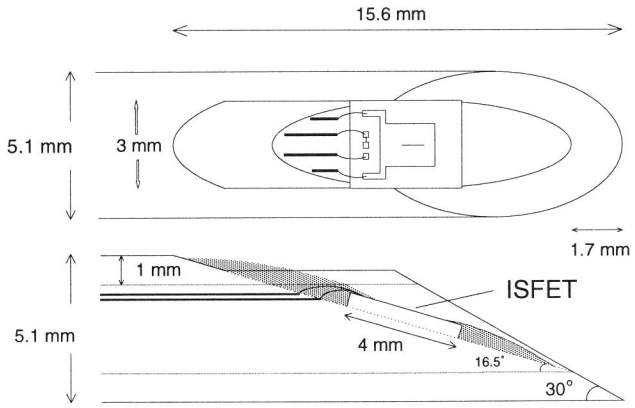

Fig.7.3 The perspex needle with incorporated ISFET. The ISFET is located in a groove.

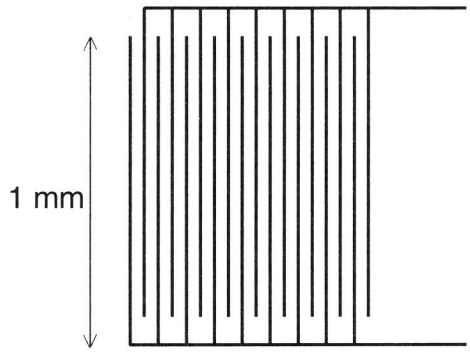

Fig.7.4 A top view of the conductance cell.

Both needles with the conductance cells showed reproducible and very fast responses with a rise time of 11.9 ± 0.7 ms. The speed with which the needles were pressed through the membrane did not have a significant influence on the results. These preliminary results show that it is possible to apply a very fast change in electrolyte concentration in a reproducible and very simple way.

Unfortunately, the ISFET needles have not been provided yet with a layer of protamine as affinity ligand for heparin, to repeat the experiments as described in chapter 6, with this alternative ion-step system. The incubation in blood plasma can then be accomplished by adding a drop of plasma on top of the ISFET.

A recent development that may be of interest for the future evolvement of the ion-step measuring method, is the multi-channel clinical sensor, mounted in a disposable cartridge as developed by i-STAT corporation, Princeton (NJ), USA. This cartridge contains a sensor array for the determination of Cl^-, K^+, Na^+, Urea, Glucose and Haematocrit, a pouch containing a calibrant solution, a sample chamber and a fluid channel to conduct the calibrant and the sample over the sensor array. Two drops of whole blood are placed into the sample port and the cartridge is inserted into a portable clinical analyzer for processing. When the cartridge is inserted in the analyzer, a test cycle is started. During the test cycle, the analyzer presses the front of the cartridge, causing a barb to puncture the calibrant pouch. The calibrant fluid is released over the sensor array for measurement. When calibration is completed, the analyzer presses the cartridge air bladder which pushes the calibrant solution into the waste reservoir and sends the blood sample over the sensor array for measurement. This principle of a sensor cartridge with one or more fluid channels and several pouches containing the solutions, might be an interesting alternative for the ion-step measuring system.

Another recent field of research which is of interest regarding the ion-step

measuring method, is the development of so-called μ-TAS: micro total analysis systems. The principle is the same as that of the sensor cartridge described before, but in a μ-TAS all different components are integrated in silicon. This includes micro pumps, fluid channels and sensors. Because of the small dimensions of the ISFET and the compatibility towards integration in silicon, the ion-step measuring method is very eligible to implement in a μ-TAS.

References

[1] C. Tanford, S.A Swanson, W.S. Shore, Hydrogen ion equilibria of bovine serum albumin, J. Am. Chem. Soc., 77 (1955), p.6414

[2] H.G.W. Lensen, Concurrerende adsorptie van plasma eiwitten aan vast/vloeistof grensvlakken, Thesis University of Twente, Enschede, The Netherlands (1985)

[3] H.R. Arwin, The electrode adsorption method, a new way to measure enzymatic activity, Linköping Studies in Science and Technology, Dissertations, No. 49 (1980)

[4] R.B.M. Schasfoort, A new approach to immunoFET operation, Thesis University of Twente, Enschede, the Netherlands, ISBN 90-9003145-6 (1989)

[5] D.J.G. Ives, G.J. Janz, Reference electrodes Theory and Practice, Academic Press (1961)

Summary

In this thesis the development of a heparin sensor is described as the first practical application of the ion-step measuring method. Heparin was chosen because of its high charge density per molecule, which is favourable for detection with the ion-step measuring method, and because of the presumption that there is a need and a significant clinical market for a simple sensor system determining heparin concentrations in blood. In the first chapter the ISFET is introduced and its role as transducing element in several chemical sensors is briefly depicted. It is shown that when using the ISFET in combination with a protein membrane on top of the gate area, the membrane does not influence the static gate-source potential of the ISFET. However, the charge density in the protein membrane can be determined when the dynamical ion-step measuring method is used.

Chapter 2 is devoted to the description of the clinical use of heparin as anticoagulant. The bloodclotting process is described together with the mechanism by which heparin retards this process. The anticoagulant activity of heparin is mainly based on its ability to increase the inhibitory effect of antithrombin III which is a normal component of blood that can inactivate some of the enzymes involved in coagulation. Because the dose-response relation of heparin is not exactly known and differs per patient, it is necessary to monitor a heparin treatment. Most of the current methods for monitoring are relatively complicated and the results are influenced by variations in concentrations of certain enzymes involved in coagulation. A simple sensor system that specifically measures heparin concentration in blood, might therefore be a useful device for monitoring heparin treatments.

In chapter 3 the ion-step measuring method is described in more detail. An ISFET with a protein membrane is exposed to a step-wise change in electrolyte concentration (an ion-step) at a constant pH and the ISFET responds with a transient change in the gate-source potential. In the new equilibrium situation after the ion-step, the gate-source potential has returned to the same value as before the ion-step. The amplitude of the transient response is a function of the charge density in the membrane. The origin of the ion-step response is a change in the Donnan potential at the membrane-solution interface and a release or uptake of protons by the proteins in the membrane resulting in a temporary pH change in the membrane which is detected by the underlying ISFET. It appears that the ISFET cannot simply be considered as an ideal transducer for detecting the ion-step response of the membrane, but the ISFET itself (without membrane) also shows a response to an ion-step. Due to a change in the double-layer capacitance, the surface potential of the ISFET gate oxide temporarily changes until the surface charge is adapted by dissociating surface OH-sites. This means that the ISFET also responds to an ion-

step with a transient potential. The amplitude of this transient response is a function of the surface charge density of the ISFET gate oxide which is determined by the pH of the solution and the point of zero charge of the gate oxide.

In chapter 4 the first experiments are presented concerning the measurement of heparin. The protein protamine is used as an affinity ligand for heparin and immobilized in membranes of polystyrene beads in an agarose gel. In the clinical situation, protamine sulphate is used as an antidote for heparin to neutralize excessive heparin in the blood. The interaction between protamine and heparin is purely electrostatic but very strong. It is shown that heparin concentrations in buffer solutions can be determined in this way. The results in blood plasma show a significant amount of non-specifically bound plasma proteins and no clear relation between the heparin concentration and the change in the ion-step response is observed.

In chapter 5 ion-step responses of surface modified ISFETs are presented and discussed. The amino-functionalized silane aminopropyltriethoxysilane (APS) is used as surface modifier of Ta_2O_5 ISFETs. Several methods of applying APS are investigated and in some cases the amino groups of the APS can directly be used to bind heparin to the surface resulting in a change in ion-step response. The results in blood plasma are however again disappointing. Surface modification by silylating ISFETs with APS is also used to 'tune' the point of zero charge of Ta_2O_5 ISFETs to pH 7. In this way the modified ISFET does not respond to an ion-step and the ion-step response of a membrane of polystyrene beads deposited on top of an ISFET can be measured without an interfering ISFET response.

In chapter 6 the results are presented of ISFETs with a monolayer of protamine as affinity ligand for heparin. Protamine is immobilized by physical adsorption directly at the Ta_2O_5 surface. After heparin has bound to the immobilized protamine, it can be removed by rinsing in 4 M NaCl. This treatment only removes the bound heparin from the protamine and not the immobilized protamine from the Ta_2O_5 surface. This makes it possible to incubate one device subsequently in different heparin solutions. With these devices it is possible to measure heparin concentrations in buffer solutions as well as in blood plasma and the results show a linear relation between the heparin concentration and the change in ion-step response.

The last chapter is the concluding chapter which contains the final conclusions and some suggestions for further research. These include some suggestions for determining other parameters which are related to the overall clotting time of blood. In this chapter also a new and simple way of applying the ion-step is presented which for practical applications can be an alternative for the laboratory set-up as used for obtaining the results presented in this thesis.

Samenvatting

In dit proefschrift wordt de ontwikkeling van een heparinesensor beschreven als de eerste praktische toepassing van de ion-stap meetmethode. Er is voor heparine gekozen omdat heparine een hoge ladingsdichtheid per molekuul heeft, wat gunstig is voor detectie met de ion-stap meetmethode en omdat er een behoefte en een significante klinische markt veronderstelt wordt voor een simpel sensorsysteem dat heparineconcentraties in bloed kan bepalen.

In het eerste hoofdstuk wordt de ISFET geïntroduceerd en vervolgens de rol van de ISFET als transducent in verschillende chemische sensoren. Het blijkt dat een eiwitmembraan op de gate van een ISFET geen invloed heeft op de statische gate-sourcespanning van de ISFET. De ladingsdichtheid in een eiwitmembraan kan echter wel worden bepaald als de dynamische ion-stap meetmethode gebruikt wordt.

Hoofdstuk 2 is gewijd aan de beschrijving van het klinische gebruik van heparine als antistollingsmiddel. Het bloedstollingsproces wordt beschreven en de manier waarop heparine dit proces vertraagt. De antistollingsaktiviteit van heparine wordt voornamelijk bepaald door het vermogen om de remmende werking van antithrombine III (AtIII) te vergroten. AtIII is een component van bloed die de aktiviteit remt van sommige enzymen die bij de stolling betrokken zijn. Omdat de verhouding tussen de dosis en de responsie niet precies bekend is en bovendien verschilt per patient, is het noodzakelijk om een heparinebehandeling te controleren. De huidige heparinetesten zijn relatief ingewikkeld en de resultaten worden beïnvloed door variaties in de concentraties van verschillende bij de stolling betrokken enzymen. Een eenvoudig sensorsysteem dat de heparineconcentratie in bloed specifiek kan meten, lijkt daarom een bruikbaar instrument voor de controle van heparinebehandelingen.

In hoofdstuk 3 wordt de ion-stap meetmethode in detail besproken. Een ISFET met een eiwitmembraan wordt blootgesteld aan een stapsgewijze verandering van de elektrolietconcentratie (een ion-stap) bij een constante pH. De ISFET responsie is een tijdelijke verandering van de gate-sourcespanning. In de nieuwe evenwichtssituatie na de ion-stap, heeft de gate-sourcespanning dezelfde waarde als voor de ion-stap. De amplitude van de potentiaalpiek is een functie van de ladingsdichtheid in het membraan. De ion-stap responsie wordt veroorzaakt door een verandering in de Donnanpotentiaal aan het membraan-vloeistof grensvlak en door een opname of afgifte van protonen door de eiwitten wat een tijdelijke pH-verandering in het membraan veroorzaakt die door de ISFET gemeten wordt. Het blijkt dat de ISFET niet kan worden beschouwd als een ideale transducer om de ion-stap responsie van een membraan te detecteren, omdat de ISFET zelf (zonder membraan) ook een tijdelijke responsie na een ionstap vertoont. Als gevolg van de

verandering van de dubbellaagcapaciteit verandert de oppervlaktepotentiaal van het gate-oxyde totdat de oppervlaktelading zich aangepast heeft door OH-groepen te dissociëren. De amplitude van deze potentiaalpiek is een functie van de ladingsdichtheid van het gate-oxydeoppervlak van de ISFET.

In hoofdstuk 4 worden de eerste experimenten met betrekking tot de meting van heparine gepresenteerd. Het eiwit protamine wordt als affiniteitsligand gebruikt en wordt geïmmobiliseerd in een membraan van polystyreen bolletjes in een agarose gel. Protaminesulfaat wordt in de klinische situatie gebruikt als een antistof om overvloedig heparine in de bloedsomloop te neutraliseren. De binding tussen heparine en protamine is puur elektrostatisch maar erg sterk. Het is mogelijk om op deze manier heparine-concentraties in bufferoplossingen te bepalen. Uit de resultaten in bloedplasma blijkt dat er sprake is van een aanzienlijke hoeveelheid a-specifieke binding van plasma-eiwitten en dat er geen duidelijk verband bestaat tussen de heparineconcentratie en de verandering van de ion-stap responsie.

In hoofdstuk 5 worden ion-stap responsies gepresenteerd van ISFETs waarvan het oppervlak is gemodificeerd. De silaanverbinding aminopropyltriethoxysilaan (APS) is gebruikt om Ta_2O_5-ISFETs te modificeren. Verschillende methodes zijn gebruikt om APS aan te brengen en in sommige gevallen kunnen de aminogroepen van het APS direct gebruikt worden om heparine aan het oppervlak te binden. De resultaten in bloedplasma zijn echter teleurstellend. Oppervlakte-modificatie met APS is ook gebruikt om het 'point of zero charge' van Ta_2O_5-ISFETs af te regelen op pH 7. Op deze manier is het mogelijk om de ion-stap-responsie van een eiwitmembraan te bepalen zonder een artefact van de onderliggende ISFET.

In hoofdstuk 6 worden de resultaten gepresenteerd van ISFETs met een monolaag protamine als affiniteitsligand voor heparine. Protamine wordt geïmmobiliseerd door fysische adsorptie direct aan het Ta_2O_5 oppervlak. Nadat heparine aan het protamine gebonden is, kan het worden verwijderd door te spoelen in 4M NaCl. Deze behandeling verwijdert alleen het gebonden heparine en niet het geadsorbeerde protamine van het Ta_2O_5-oppervlak. Het is nu mogelijk om steeds dezelfde ISFET te incuberen in verschillende heparineconcentraties. Met deze ISFETs is het mogelijk om heparineconcentraties te meten in zowel buffer-oplossingen als in bloedplasma. Er bestaat een lineaire relatie tussen de heparineconcentratie en de verandering in de ion-stap responsie.

Het laatste hoofdstuk bevat de algemene conclusies en enkele aanbevelingen voor verder onderzoek. Een aantal van deze aanbevelingen heeft betrekking op de bepaling van andere parameters die gerelateerd zijn aan de totale stollingstijd van bloed. In dit hoofdstuk wordt tevens een nieuwe en eenvoudige manier gepresenteerd om een ion-stap te bewerkstelligen als alternatief voor de huidige laboratorium opstellling voor praktische toepassingen.

List of publications

related to the work described in this thesis

Chapter 3:

J.C. van Kerkhof, J.C.T. Eijkel, P. Bergveld. ISFET responses on a stepwise change in electrolyte concentration at constant pH, Sensors and Actuators B, 18 (1994), 56-59.

Chapter 4:

J.C. van Kerkhof, P. Bergveld, R.B.M. Schasfoort. Determination of heparin concentrations with the ion-step measuring method. Technical digest of the fourth international meeting on chemical sensors, september 1992, Tokyo, Japan, 370-373.

J.C. van Kerkhof, P. Bergveld, R.B.M. Schasfoort. Development of an ISFET based heparin sensor using the ion-step measuring method. Biosensors and Bioelectronics, 8 (1993), 463-472.

Chapter 5:

J.C. van Kerkhof, P. Bergveld, R.B.M. Schasfoort. A heparin sensor based on a modified Ta_2O_5-ISFET and the ion-step measuring method. Proceedings of the Dutch conference on Sensor Technology 1994, University of Twente, Enschede, The Netherlands, Feb. 17-18, 1994, Ed. P.V. Lambeck, ISBN 90-73461-06-5, p.p.281-285.

J.C. van Kerkhof, P. Bergveld. Characterization of silylated ISFETs by the ion-step measuring method. To be submitted.

Chapter 6:

J.C. van Kerkhof, P. Bergveld, P. R.B.M. Schasfoort. The ISFET-based heparin sensor with a monolayer of protamine as affinity ligand. Biosensors and Bioelectronics, in press.

Dankwoord

Tenslotte is het moment aangebroken om de mensen te bedanken die op een of andere manier een bijdrage hebben geleverd aan de totstandkoming van dit proefschrift.

Op de eerste plaats is dat mijn promotor Piet Bergveld die altijd zeer snel en zorgvuldig werkrapporten of conceptversies van commentaar voorzien heeft en vervolgens ook tijd maakte om deze te bespreken. Richard Schasfoort die het project vanuit TNO begeleid heeft, bedank ik voor het vinden van het benodigde draagvlak binnen TNO om het project te financieren en voor zijn veelal creatieve inbreng tijdens de besprekingen in Zeist en Enschede.

Aan Jan Eijkel ben ik bijzondere dank verschuldigd vanwege zijn theoretische beschrijving van de ion-stap meetmethode waardoor de meetmethode is uitgegroeid van een empirische methode tot een methode die (bijna) volledig beschrijfbaar blijkt te zijn. Hierdoor kon ik meer gerichte experimenten doen en ben ik er tenslotte in geslaagd om een werkende heparinesensor te maken. Ik bedank Jan voor zijn functie als aanspreekpunt om (vreemde) resultaten te bespreken en wens hem veel succes met de afronding van zijn proefschrift. In dit kader wil ik ook Ronald van Hal bedanken die via zijn bijdrage aan de 'nieuwe' ISFET-theorie voor mij een aanspreekpunt was voor lastige ISFET-vragen.

De bijdrage van Johan Bomer is van onschatbare waarde geweest voor dit project. Hij was verantwoordelijk voor de vervaardiging (inclusief afmonteren!!) van de naar schatting enkele honderden ISFET's die ik in de afgelopen vier jaar gebruikt heb. Daarnaast wil ik hem bedanken voor zijn bijdrage bij de optimalisering van de meetopstelling. Ton Verloop bedank ik voor zijn technologische ondersteuning bij verschillende stadia van het project. Sjouke Hornstra wil ik bedanken voor zijn veelzijdige ondersteunig in het lab.

Henk-Jan Bergveld, Bram Roukema en Ronald de Vries hebben in hun opdrachten een bijdrage geleverd aan het onderzoek, waarvoor mijn dank. Special thanks to Bruno Chiodi who worked for three months in our laboratory and assisted with some of the experiments. Ad Shatat heeft in een doktoraalopdracht een belangrijke bijdrage geleverd aan het nieuwe ion-stapsysteem dat in hoofdstuk 7 beschreven is.

Jans Kruise bedank ik voor zijn kritische beschouwing van het manuscript en omdat hij de rol van paranimf op zich wilde nemen samen met Kees den Besten die ik hiervoor ook wil bedanken.

Wouter Olthuis is de afgelopen vier jaar de perfecte kamergenoot voor mij geweest van wie ik het nodige heb geleerd en afgeleerd, waarvoor ik hem zeer erkentelijk ben.

Stellingen behorende bij het proefschrift

The development of an ISFET-based heparin sensor

1. Het probleem van a-specifieke adsorptie bij affiniteitssensoren kan niet worden opgelost d.m.v. *differentieel* meten met twee sensoren waarbij slechts één van beide sensoren voorzien is van het affiniteitsligand.
   J.-S. Kim et al., Biotechnology and Bioengineering, 39 (1992), p.450

2. Het karakteriseren van ISFETs met de pH-gevoeligheid (mV/pH) veronderstelt vaak ten onrechte dat er een lineair verband bestaat tussen de pH en de oppervlakte spanning van het gate-oxyde.
   K.-M. Chen et al., Sensors and Actuators B, 13-14 (1993), p.209

3. Het behandelen van een oxyde-oppervlak met een silaanverbinding om vervolgens via de functionele groepen eiwitten te binden, is een minder vanzelfsprekende procedure dan veelal wordt voorgesteld.
   Hoofdstuk 5 van dit proefschrift

4. Het overheidsbeleid betreffende studiefinanciering vertoont de laatste jaren grote overeenkomsten met de in dit proefschrift beschreven stimulus-respons metingen.

5. Zolang veel sprekers op wetenschappelijke conferenties de kwaliteit van hun presentatie ondergeschikt achten aan de inhoud, blijft deze vorm van informatieoverdracht inefficient.

6. De werkelijke bijdrage van een onderzoeker aan wetenschap en maatschappij is sterk gerelateerd aan zijn vermogen tot communiceren.

7. Het kunnen omgaan met de verschillende disciplines in biosensoronderzoek is vergelijkbaar met het bespelen van verschillende koperblaasinstrumenten.

8. Het voorkomen van roest en het laten functioneren van de verlichting zijn twee tegenstrijdige doelstellingen bij het traditionele ontwerp van een fiets.

9. Een goede planning is het halve werk.

Joost van Kerkhof
7 oktober 1994

ISBN 90-9007514-3